PhD degree in Molecular Medicine (curriculum in Molecular Oncology)

European School of Molecular Medicine (SEMM),

University of Milan and University of Naples "Federico II"

Settore disciplinare: Med/04

A ROLE FOR MYC IN THE SELF-RENEWAL OF MAMMARY STEM CELLS AND CANCER STEM CELLS

Angela Santoro

IEO, Milan

Matricola n. R09385

Supervisor: Prof. Pier Giuseppe Pelicci, M.D. Ph.D.

European Institute of Oncology IEO, Milan

Anno accademico 2014-2015

To my parents

Table of contents:

List of figures:

List of tables:

List of abbreviations

4-OHT	4- HydroxyTamoxifen
ACD	Asymmetric cell division
AML	Acute myeloid leukemia
CML	Chronic myeloid leukemia
CSC	Cancer Stem Cell
DAVID	The Database for Annotation, Visualization and Integrated Discovery
DEG	Differentially expressed gene

DIA	Digital image analysis
DMEM	Dulbecco's modified Eagle's medium
ELDA	Extreme Limiting dilution analysis
EMT	Epithelial to mesenchymal transition
ER	Estrogen receptor
ESC	Embryonic stem cell
FDR	False discovery rate
GBM	Glioblastoma
GFP	Green fluorescent protein
GO	Gene Ontology
GR	Growth rate
GSEA	Gene set enrichment analysis
HE	Hematoxylin - eosin
HSC	Hematopoietic stem cell
IHC	Immunohistochemistry
IP	Intra peritoneum
iPSC	Induced pluripotent stem cell
K14	Cytokeratin 14
K18	Cytokeratin 18
K5	Cytokeratin 5
K8	Cytokeratin 8
KEGG	Kyoto Encyclopedia of Genes and Genomes
LIF	Leukemia inhibitory factor
LSC	Leukemic stem cells
MaSC	Mammary stem cell
MEBM	Mammary epithelial basal medium
miRNA	micro RNA
MMTV	Mouse mammary tumor virus
MOI	Multiplicity of infection
MSigDB	Molecular signature database
NES	Normalized enriched score
OSKM	Oct4, Sox2, Klf4, Myc
PI	Propidium iodide

ProcR	Protein C receptor
SC	Stem Cell
TCGA	The Cancer Genome Atlas
TEB	Terminal end bud
TET	Tetra- cycline-responsive promoter element
TF	Transcription factor
TIC	Tumor initiating cell
UPS	Ubiquitin Proteasome System
UT	Untreated
WT	Wild type

1 Abstract

Cancer Stem Cells (CSCs) are a clinically relevant population at the apex of the inner hierarchical organization of many tumors. It was previously demonstrated by our group that loss of the p53 tumor suppressor leads to an increase in the mammary stem cell (MaSC) and breast CSC content, due to a switch of the mode of division from mainly asymmetric to symmetric. However, which of the many pathways instructed by p53 is directly involved in the execution of this biological phenotype remains to be determined.

Following a candidate gene approach, we investigated Myc as the putative key downstream effector of p53 in breast SCs and CSCs. The *Myc* oncogene is very often altered in cancer and has been clinically associated with poor differentiation and aggressiveness in breast cancer. We have found that Myc endogenous expression is de-regulated in our ErbB2 model of breast tumorigenesis, upon attenuation of p53 signaling. We also observed that de-regulated Myc extends the lifespan and proliferative potential of wild type mammospheres. This occurs by two distinct but cooperative mechanisms: the increase in the frequency of symmetric divisions of MaSCs and the reprogramming of progenitor cells. Importantly, in the ErbB2 model, de-regulated Myc levels are critical and sufficient to sustain the unlimited self-renewal of CSCs, independently of p53. Of note, the above described phenotype is characterized by the over expression of a mitotic gene signature which is dictated by the identified p53-Myc axis.

Taken together these results demonstrate that the loss of a tight control on Myc levels, which derives from the loss of p53 functionality, is responsible for the expansion of the SC and CSC pool by regulating modality of SC division and reprogramming of mammary progenitors. Finally, our data suggest that the p53-Myc axis exerts a putative tumor suppressor function in SCs through the coordinated regulation of a set of mitotic genes.

2 Introduction

2.1 The heterogeneous nature of cancer

Cancer is a very widespread disease and represents one of the leading causes of death in the modern era. Based on 2012 estimates the GLOBOCAN program predicted a considerable increase to 19.3 million new cancer cases per year by 2025, due to growth and ageing of the global population. Despite the many advances made in terms of therapeutic options for patients, which have led to a consistent increase in the "tumor free time window", cancer recurrence is still a very frequent event, often mortal.

It is becoming more and more clear that cancer cannot be considered a single disease, as it is extremely heterogeneous, from tissue to tissue and from patient to patient. Intra-tumor heterogeneity, in particular, is a key source of complexity that ultimately leads to tumor progression, therapy resistance and cancer recurrence. Tumors are increasingly seen as ecosystems containing both malignant cells and infiltrating endothelial, hematopoietic, stromal, and other cell types that all together go under the definition of "microenvironment" and can influence the function of the tumor as a whole (Junttila and de Sauvage 2013). As an ecosystem, the inner nature of tumors is to evolve in response to cell-autonomous and non cell-autonomous stimuli that aim at increasing its fitness and that eventually lead to variations in the cellular processes of growth, metabolism, apoptosis and other "hallmarks of cancer" (Hanahan and Weinberg 2011).

Two main models have been proposed to dissect the mechanisms by which tumors evolve: the first is the Cancer Stem Cells (CSCs) theory that predicts an inherent functional heterogeneity among tumor cells; the second is the clonal evolution model that is based mainly on the observed genetic heterogeneity within tumors. Both models harbor strengths and limitations which I will try to summarize in the following section.

2.1.1 The Cancer Stem Cell theory, past and present

The cancer stem cells model of tumor evolution predicts the existence, within a given tumor, of a cell population that is at the apex of a functional and developmental hierarchy, the so-called Cancer Stem Cells (CSCs). As the name implies, these cells are believed to share many properties with the stem cells (SCs) that compose normal tissues (normal SCs), above all, self-renewal ability (potential to generate new CSCs), multi-lineage capacity (ability to generate non-CSC) and quiescent nature. Therefore, the tumor is understood as a functionally organized entity with the CSC being the only population able to sustain tumor progression and, potentially, being responsible of relapse upon pharmacological therapies.
The existence of this hierarchy was first demonstrated in acute myeloid leukemia by the pioneering work of John Dick's lab (Lapidot, Sirard et al. 1994). In this study, the authors showed that only a rare population of leukemic cells, which were positive for the CD34 surface marker and negative for the CD38 antigen, was able to seed a tumor upon xenotransplantation in immuno-compromised hosts. Later on, many other works demonstrated the existence of such tumorigenic populations also in solid tumors, taking advantage of cell type specific surface markers. In particular, the validity of the CSC theory was reported first in human breast cancer (Al-Hajj, Wicha et al. 2003), and then in numerous other tumors, including glioblastoma (Singh, Hawkins et al. 2004), pancreatic

cancer (Hermann, Huber et al. 2007), lung cancer (Eramo, Lotti et al. 2008), prostate cancer (Patrawala, Calhoun et al. 2006), colorectal cancer (O'Brien, Pollett et al. 2007). All these works rely on the transplantation, in murine hosts, of isolated cell populations which are then proven tumorigenic (they are therefore also known as TICs, tumor initiating cells) and capable to give rise to a progeny of non-TICs, thus providing evidence for a hierarchical organization.

The CSCs theory has remarkable implications for therapeutic strategies aimed at curing cancer. Indeed, these cells seem to possess all the clinically relevant features that determine cancer maintenance, drive cancer heterogeneity, and cause resistance to conventional drug regimens. In line with this, gene expression signatures specific to CSCs and normal SCs are prognostic of patients' disease outcomes, regardless of their genetic landscape (Ben-Porath, Thomson et al. 2008, Eppert, Takenaka et al. 2011, Merlos-Suárez, Barriga et al. 2011). The work of Ben-Porath and colleagues was one of the first to explore this correlation. The study hypothesized that the un-differentiated stage of breast cancer could be driven by the combined expression of oncogenes and SC-associated genes; the authors showed that an embryonic stem cell (ESC) gene signature is enriched in human tumors, particularly in poorly differentiated (grade 3) breast tumors. The ESC gene signature included under-expression of Polycomb target gene sets and over-expression of ES-expressed sets, while the well differentiated grade 1 tumors displayed an opposite pattern (Ben-Porath, Thomson et al. 2008).

Not only gene signatures from ES cells, but also gene expression profiles of adult normal SCs and validated CSCs were proven to correlate with prognostic parameters. In the study of Eppert and colleagues, 16 primary human acute myeloid leukemia (AML) samples were tested for the presence of leukemic stem cell (LSCs) populations by the use of a classic combination of CD34 and CD38 surface markers (Bonnet and Dick 1997). Once found, the

putative LSCs were validated functionally in transplantation assay and their gene expression profile was assessed by microarray analysis, in parallel with normal human hematopoietic stem cells (HSCs). The expression profiles of the two populations resulted very similar and were shown to positively correlate with groups of patients expressing molecular markers of poor prognosis (like FLT3ITD) and to be highly expressed in high risk subjects (Eppert, Takenaka et al. 2011).

The same types of conclusions were also shown to be valid for solid cancers. For example, Merlos-Suarez et al. demonstrated that a gene signature specific for adult intestinal stem cells predicts disease relapse in colorectal cancer patients (Merlos-Suárez, Barriga et al. 2011).

All these findings demonstrate that "stemness" is a crucial biological property for cancer cells and their sustainment. Indeed, despite the fact that numbers of CSCs may vary greatly across different tumors, and that the identified markers cannot be universally applied, it appears clear that the content of CSCs and/or their associated expression program correlate with the aggressiveness of the disease. One study clearly shows the applicability of this concept to breast cancer (Pece, Tosoni et al. 2010): high grade estrogen receptor- negative tumors (G3/ER-) are enriched in CSCs, as demonstrated by mammosphere culture and tranplantation assays.

Furthermore, CSCs are also intrinsically resistant to therapies. In chronic myeloid leukemia (CML), LSCs are able to survive imatinib treatment independently of the presence of resistance-associated mutations in the BCR-ABL gene and of the selective inhibition of the fusion protein, suggesting that they are not oncogene-addicted like the non-LSC population (Corbin, Agarwal et al. 2011). A similar scenario also occurs with classic chemotherapy drugs: a clinical study in breast cancer showed that docetaxel or doxorubicin treatment leads to a significant increase in the percentage of CD44+/CD24-

cells (putative CSCs) (Al-Hajj, Wicha et al. 2003), from a mean of 4.7% at baseline to 13.6%, regardless of the molecular subtype (Li, Lewis et al. 2008). Furthermore, breast CSCs were also shown to be resistant to radiotherapy: murine models of spontaneous breast cancer (MMTV-Wnt1 mice) were treated with courses of ionizing radiation and the percentage of CSCs (defined in this model as Thy1+CD24+Lin- cells) was found to be consistently increased compared to the non-TIC fraction (Diehn, Cho et al. 2009).

Several molecular processes underlying differential sensitivities among hierarchically organized tumor cells have been proposed, including up-regulation of anti-apoptotic molecules and lower content of reactive oxygen species, with consequent less accumulation of DNA damage; however, a full understanding of CSC specific mechanisms is still lacking.

Taken together, all these finding demonstrate that CSCs are clinically relevant entities and that therapeutic strategies intended to kill them would be extremely beneficial for complete disease eradication. Nevertheless, the concept of a hierarchical structure inherent to tumors has been challenged in recent years by new experimental approaches that dissected other sources of tumor heterogeneity, such as genetic evolution, complexity of the microenvironment cross talks, and reversible changes in CSC properties.

2.1.2 The clonal evolution model

One major criticism towards the CSC theory regards the validity of the gold standard assay that defines CSC properties, that is, the transplantation procedure. The process of implanting cells in a host is, physiologically, a profound barrier to tumor development as it measures the tumorigenic potential on the base of a permissive environment. In order to avoid the xenogeneic immune response that would kill human cells in mice, mouse strains

with various degrees of immune dysfunction (immune-compromised mice) have been employed; notably, the frequency of CSCs varies a lot after transplantations in these mice, being much higher in more severely immunodeficient mice (Quintana, Shackleton et al. 2008, Ishizawa, Rasheed et al. 2010). Syngeneic transplantation of murine tumors has given support to the CSC theory, confirming their existence in the absence of an immunological barrier to engraftment.

Another limitation of the model is that it relies entirely on the presence/absence of surface markers both for defining the CSCs and for showing the generation of their heterogeneous progeny. This has two main implications: first, it does not take into consideration the variability among patients and, second, it does not prove that the genetic heterogeneity of the tumor is fully recapitulated by the SC progeny. Indeed, it was shown for some tumors that the identified markers are not predictive of CSC functions, while for others it is clear that they do not work for all patients and tumor subtypes (Meacham and Morrison 2013). For example, it is not true for all AML patients that the CD38-/CD34+ population is the most enriched in CSCs, as other fractions of cells were also shown to be tumorigenic (Eppert, Takenaka et al. 2011).

Indeed, tumor heterogeneity could also arise when the cells composing the tumor differ genetically. If this were the case, transformation could occur through the accumulation of multiple stochastic genetic mutations that are selected by tumor evolution because they provide a survival advantage to the cell. The result is the generation of a heterogeneous population of cancer cells within the same tumor: this model has been named the clonal evolution model.

Recent works of genome sequencing have confirmed this concept. Indeed, it was recently demonstrated that, within a single patient, a cancer is composed of genetically distinct sub-clones that arise through branching evolution and that possess different mutations which,

in turn, can differently contribute to cancer development and, so, give rise to functional heterogeneity (Kreso and Dick 2014). New sub-clones survive if they are fit enough for the tumor environment, otherwise they can be completely lost, dominated by the fittest clone; some minor sub-clones, though, can persist alongside the dominant one, supporting its growth or acting as a reservoir of genetic diversity from which evolution can continue (Kreso and Dick 2014).

In this context, the anti-cancer therapy could represent an external stimulus for the selection of mutations that confer resistance on the tumor clone, thus ensuring its survival.

Therefore, the clonal evolution model can explain several features of cancer, including its morphological and functional heterogeneity, tumor progression and recurrence. Nevertheless, a recent study demonstrated that even within a single genetic clone, cancer cells retain functional heterogeneity (Kreso, O'Brien et al. 2013). In this work, the authors isolated individual subclones from patients' colorectal cancer and propagated them in xenografts, creating monogenetic cancer lineages. The tumor cells in each lineage, marked by a lentiviral system, exhibited a very wide spectrum of behaviors in terms of proliferative potential and ability to survive to serial passages. Furthermore, upon treatment of the mice with conventional chemotherapy, the authors observed that only cells with a low proliferative index (*i.e.*, quiescent) were able to survive and contribute to tumor regrowth, without selection of new genetic subclones (Kreso, O'Brien et al. 2013).

Thus, these results directly identify functional diversity among cells that are part of a single genetic clone and add a new layer of complexity to our attempts to dissect the heterogeneous nature of tumors (**Figure 2-1**).

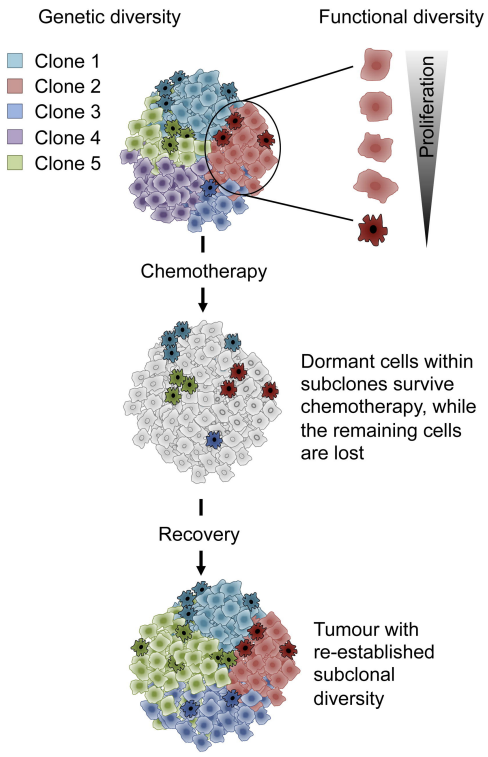

Figure 2-1: Functional heterogeneity within cancer genetic sub-clones (Kreso et al. 2014)

Given all the available knowledge about tumor evolution, it seems reasonable to hypothesize that hierarchical organization and clonal evolution coexist during tumor progression. Regardless of the type of evolution that tumors undergo, it appears that "stemness", intended as an undifferentiated state of cells which are capable of self-renewal and giving rise to long-lived clones of propagating cells, is a key property of cancer. Therefore, the dissection of self-renewal specific mechanisms (in SCs and in CSCs) might help us to understand the alterations that are at the basis of carcinogenesis and lead to more efficient anti-cancer therapies.

In the next section, we will examine the de-regulation of specific SC pathways in the mammary gland tissue and how much they are predictive of malignant transformation.

2.2 Mammary stem cells and breast cancer stem cells

2.2.1 Mammary gland physiology and mammary stem cells

The mammary gland is a very unique organ in the female body and undergoes complex morphological changes and re-arrangements in response to reproductive and hormonal stimuli for which it is required a high level of dynamicity. It is composed of two tissue compartments: the epithelium, made of ductal and alveolar cells, and the stroma, that mainly consists of adipocytes together with fibroblasts and infiltrating hematopoietic cells. The epithelium is organized in a system of branched ducts terminating in lobular structures or alveoli which represent the core of the secretive function. The ducts are composed of two cellular types: the luminal cells, which express the cytokeratins 8 and 18 (K8/K18), reside around the central lumen, and terminally specialize in the production of milk at pregnancy, and the outer basal-myoepithelial cells, which express the keratins 5 and 14 (K5/14) and are located in proximity of the basement membrane where they contract to facilitate milk release (**Figure 2-2**).

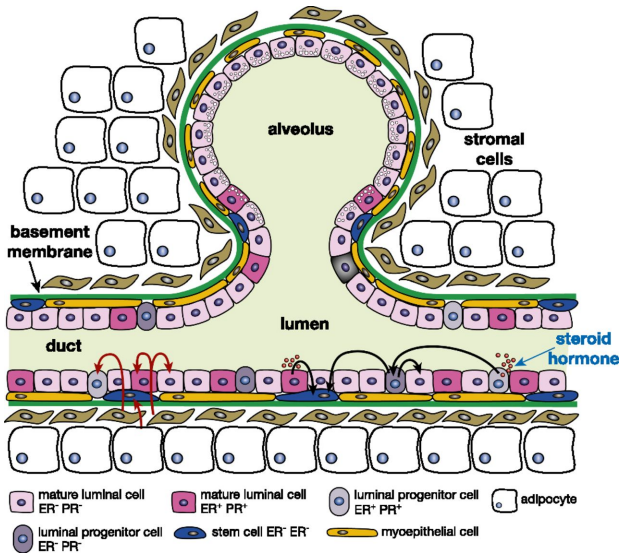

Figure 2-2: Composition of mammary gland epithelium. © 2014 Visvader and Stingl; Published by Cold Spring Harbor Laboratory Press

The epithelial branching of the mammary gland starts at puberty, when sex hormones signaling stimulate the elongation of terminal lobular units and end buds (TEBs) so that they can penetrate the fat pad. During pregnancy, the gland reaches its full differentiation capacity, with the expansion and maturation of the alveolar compartment that lead to the secretion of milk during lactation (**Figure 2-3**). Lactation is followed by an involution stage, during which the alveoli undergo apoptosis and remodeling to restore a simple ductal structure. This complex cycle of rearrangements is repeated at every new pregnancy, suggesting the existence of a cellular reservoir which sustains and regenerates the tissue and is able to self-renew and give rise to a multi-specialized progeny. Therefore, it seems reasonable to hypothesize a differentiation hierarchy within the mammary gland tissue, with mammary stem cells (MaSCs) at its apex.

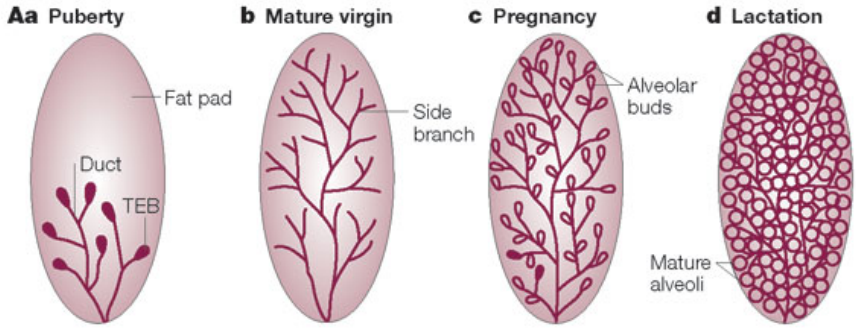

Figure 2-3: Series of re-arrangements through which the mammary gland tissue undergoes. (Hennighausen & Robinson 2005) Copyright © 2005 Nature Publishing Group

In 2006, two pioneering works led to the isolation of a population of cells enriched in MaSCs in the murine gland, as demonstrated by transplantation assays and by multi-lineage differentiation ability (Shackleton, Vaillant et al. 2006, Stingl, Eirew et al. 2006). This cell population was characterized by the expression of a combination of surface markers such as: low levels of Sca-1, CD24 (heat-stable antigen) and high levels of CD49f (α6 integrin) or CD29 (β1 integrin) (Sca-1^{neg}/ CD24$^{med/+}$CD49f^{hi}/CD29^{hi}) and was shown to be resident in the basal/myoepithelial layer on the epithelial ducts. Later works have shown that MaSCs can be preferentially enriched over other basal cells based on their higher expression levels of CD24 or CD61 (β3 integrin), and EpCAM (Visvader and Stingl 2014).

Recently, however, the concept of multi-potent SCs in the mammary gland has been challenged by one work in which the cell fate of basal and luminal cells was followed *in situ* in a so-called lineage tracing experiment. The study was based on basal (K14/K5) and luminal (K18/K8) keratins-inducible mouse models and demonstrated that both the myoepithelial and the luminal compartments contain long living unipotent SCs that sustain the development of the adult mammary gland during puberty and pregnancy, without any

evidence of the existence of rare multipotent SCs (Van Keymeulen, Rocha et al. 2011). These findings have been subjected to a long debate and were challenged by at least two independent works. These studies, while highlighting, with independent lineage-tracing approaches, the existence of MaSCs with multi-lineage capacity coordinating the homeostasis of the adult murine gland, conceded that unipotent long-lived progenitors might cooperate with SCs in the pubertal dynamics (van Amerongen, Bowman et al. 2012, Rios, Fu et al. 2014).

More recently, a study by Wang et al. (Wang, Cai et al. 2015) has identified the protein C receptor (ProcR) as a unique marker of MaSCs (assessed by both lineage tracing and transplantation assays). This marker characterizes a MaSC population that is at the top of the functional and developmental hierarchy, supporting a model in which unipotent and multipotent MaSCs could coexist in the adult mammary gland, thus reconciling the opposite views emerged from previous lineage tracing studies (**Figure 2-4**).

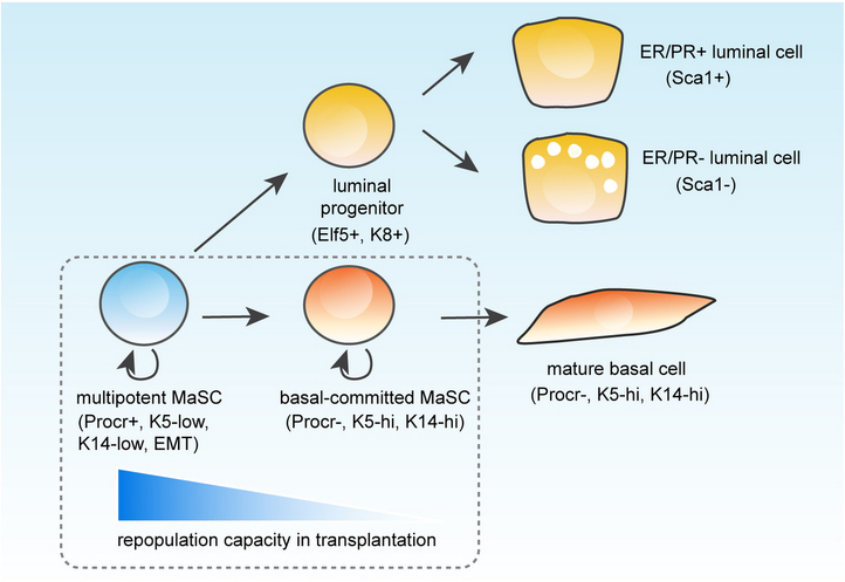

Figure 2-4: Hierarchical organization of the mammary epithelium. Wang et al. 2015 © 2014 Macmillan Publishers Limited. All Rights Reserved.

Another strategy which has been employed in the effort to isolate and characterize MaSCs is that of exploiting their quiescent or slowly proliferating nature. To this end, researches have taken advantage of a label-retaining assay based on the incorporation of a liphophilic fluorescent dye (PKH-26) which binds the cell membrane and whose fluorescent intensity gets diluted at every cell division. Therefore, actively cycling cells rapidly become negative for the dye, while slowly proliferating cells retain it. It was shown that, by this technique, it is possible to isolate a highly enriched population of MaSCs, as assessed by limiting dilution transplantation (SC frequency = 1:4) (Cicalese, Bonizzi et al. 2009, Pece, Tosoni et al. 2010).

The perspective isolation of *bona fide* MaSCs has important implications not only for the understanding of the complex developmental dynamics within the tissue, but also because de-regulation of SC specific processes is known to lead to malignant transformation (Visvader 2009).

2.2.2 Breast cancer stem cells

Since the 2008 estimates, breast cancer incidence has increased by more than 20%, while mortality has increased by 14%. Breast cancer is also the most common cause of cancer death among women (522,000 deaths in 2012) and the most frequently diagnosed cancer among women worldwide (Globocan, 2012).

Breast tumor is a highly heterogeneous disease that comprises many different pathological and molecular subtypes. Indeed, it is now categorized into at least five different subtypes based on distinct gene expression signatures that correlate with patient outcome (Reis-Filho and Pusztai 2011), representing a major challenge for the research of efficacious therapies. It is believed that the wide inter-tumor heterogeneity is a reflection of the

different "cells of origin" that drove the malignant transformation. This is why the dissection of the hierarchical structure of the normal epithelium is fundamental for understanding tumor development. In this context, SC defining properties of self-renewal and self-maintenance makes these cells prospective candidates in the search for the potential cells of origin of cancer, although there is also considerable evidence that progenitors too can be targets of the transformation process (Visvader and Stingl 2014).

The human breast cancer was the first solid malignancy for which the cancer stem model was described. Breast cancer SCs were isolated based on the expression of the cell surface markers ESA and CD44 and on the absence of CD24 (Al-Hajj, Wicha et al. 2003). Since then, other markers have been described to isolate human breast CSCs, as, for example, aldehyde dehydrogenase (ALDH) (Ginestier, Hur et al. 2007), whose expression correlated with aggressiveness and metastatic potential (Charafe-Jauffret, Ginestier et al. 2010). Furthermore, in transgenic models of spontaneous breast tumors, the same surface markers that were found to enrich for normal SCs, were also predictive of CSC functions. In details, CSC enrichment was reported: *i)* in the CD24posThy1pos (Cho, Wang et al. 2008) and in the CD29lowCD24posCD61pos (Vaillant, Asselin-Labat et al. 2008) breast cancer fractions derived from MMTV-Wnt-1 transgenic mice; *ii)* in the CD24highCD29high populations from p53-null mice (Zhang, Behbod et al. 2008). Perspective isolation of CSCs was also documented in a model of murine tumorigenesis driven by a mutated form of the ErbB2 gene (MMTV-NeuT), in which the positivity to the surface marker Sca1 (Sca1+) selects a tumorigenic population of cells over a non tumorigenic one (Grange, Lanzardo et al. 2008).

However, as we already discussed, surface markers have shown to be inadequate in light of the extreme heterogeneity that is found from patient to patient, and many of them have failed to recognize a CSC population in specific breast tumor subtypes (Visvader and

Lindeman 2008). Therefore, other methods that rely on the functional characterization of CSCs have been adopted.

Taking advantage of protocols that have been established for neural SCs, a population enriched in SCs was isolated from the normal mammary gland and propagated *in vitro* as non-adherent spheroids called mammospheres (Dontu, Abdallah et al. 2003). Briefly, mammospheres were shown to be: *i)* clonal in origin and able to self-renew, as they can form successive generations of spheroids upon dissociation and re-plating; *ii)* able to grow in anchorage independent conditions; *iii)* able to differentiate along the basal and luminal epithelial lineages and, in the presence of prolactin, generate acinar structures positive for β-casein. Furthermore, mammospheres were shown to contain cells that are slowly proliferating and endowed with higher self-renewal capacities than highly proliferating cells, and to be hierarchically organized according to each cell's replicative potential (Cicalese, Bonizzi et al. 2009, Pece, Tosoni et al. 2010).

Therefore, the mammosphere assay represents a useful tool to model self-renewal *in vitro* since it provides a measure of: *i)* the clonogenic and differentiating potential of a given population, and *ii)* its self-replating ability, as only SCs can be serially passaged. Indeed, mammosphere assays have been widely used to estimate SC and CSC contents in the mammary field. For example, mammospheres arising from primary human breast tumors are composed of cells that show a CD44+/ CD24- phenotype and are greatly enriched in tumor initiating cells, thus indicating that the mammosphere assay is indeed a good system to propagate cancer SCs (Ponti, Costa et al. 2005). Furthermore, as mentioned before, Pece and colleagues demonstrated that poorly differentiated (G3) breast cancers have higher mammosphere forming ability than well differentiated G1 tumors, as they possess higher content of CSCs (Pece, Tosoni et al. 2010).

This explains why the mammosphere assay has been so extensively used lately to study SC/CSC specific players and pathways, and how their manipulation impacts on their self-renewal ability. This assay also represents a valuable tool to test therapeutics and predict biological response in tumors organized according to the CSC model.

2.3 Cancer stem cell specific mechanisms

Up to now, we have described the CSCs as "caricatures" of the normal adult SCs, indeed many are the features that are shared between these two populations, and the normal SCs are thought to be the "cell of origin" of particular subtypes of cancers.

As successful therapeutic strategies should aim to minimize their impact on normal SCs while eradicating the malignant regenerative clones, understanding the mechanisms inherent to CSCs that distinguish them from their normal counterparts is a key issue in cancer biology. To this end, the dissection of SC de-regulated cell processes in the presence of an activated oncogene (or a de-activated tumor suppressor) is fundamental.

2.3.1 CSC specific pathways

Many pathways have been found to be essential regulators of self-renewal and proliferation in SCs and profoundly de-regulated in the oncogenic process. Among them, several ligand-dependent signaling pathways involved in normal self-renewal and development, such as Wnt, Notch and Hedgehog have raised the interest of many research groups. On the other hand, genes which regulate the apopototic and DNA damage response pathways, such as

p53, p21, pTEN, and negative regulators of the SC state like TGF-β are also considered for their role in inhibiting SC self-renewal (Visvader and Lindeman 2008) (**Figure 2-5**).

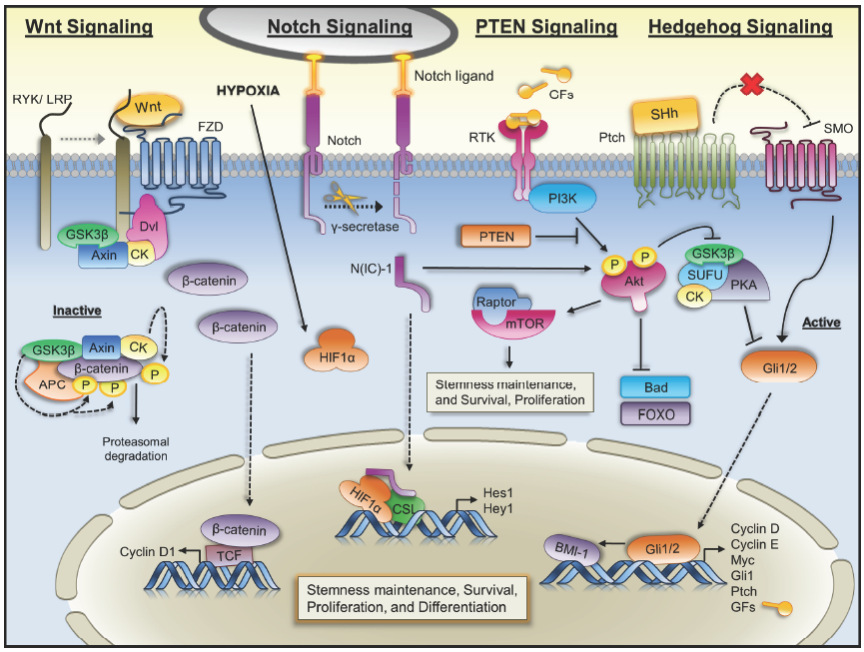

Figure 2-5: CSC specific signaling cascades: Notch, Wnt, PTEN, Hedgehog pathways are depicted. (Templeton, Miyamoto et al. 2014) ©Stem Cell Investigation.

The Notch receptor family is part of signaling pathways involved in the regulation of the fate of cells in a variety of tissues and is fundamental in the development of the embryo. In the mammary gland, while Notch1 and 3 are expressed in luminal committed progenitors, Notch4 expression is higher in bipotent MaSCs and significantly down-regulated upon differentiation along the luminal and myoepithelial lineages (Liu, Dontu et al. 2005). Transgenic mice harboring a constitutively active Notch4 (MMTV-Int3) exhibited impaired mammary gland development and grew poorly differentiated adenocarcinomas (Uyttendaele, Marazzi et al. 1996). The same tumorigenic effects on the mammary gland were also observed for over-activation of both Notch1 and Notch3 (Hu, Dievart et al. 2006). Furthermore, high levels of Notch1 and Notch3 were correlated with poor prognosis in breast cancer patients (Reedijk, Odorcic et al. 2005). All together these findings

highlight that abnormal Notch expression is linked to breast carcinogenesis through the deregulation of normal mammary stem cell self-renewal.

Wnt signaling is another very well studied pathway for its involvement in SCs, development and tumorigenesis. The canonical Wnt pathway has its main downstream effect in the stabilization of β-catenin in the nucleus, which, together with the transcription co-factors TCF/LEF, initiates the transcription of target genes essential for normal mammary gland development. Notably, it was shown that the adult mammary gland contain a Wnt-responsive cell population that is enriched for stem cells and that Wnt constitutive signaling expands this cell population (Zeng and Nusse 2010). The role of Wnt in tumorigenesis is being also widely studied in many different cancers. As regards breast carcinogenesis, the MMTV-Wnt1 mouse model develops tumors with 50% penetrance and 6 months latency (Li, Hively et al. 2000) and presents increased number of MaSCs, which were shown to be radio-resistant (Diehn, Cho et al. 2009). Furthermore, it was reported that the active form of β-catenin is over-expressed in breast cancer (Visvader and Lindeman 2008).

All together the above examples confirm that an aberrant regulation of SC self-renewal triggers tumor development and progression.

A way to avoid any potential toxicity to normal SCs, since the above-mentioned mechanisms are shared with them, is to target mutations that are active only in CSCs.

There have been several attempts to apply this concept, mainly in hematopoietic malignancies. For example, deletion of the PI-3 kinase pathway regulator Pten, combined with targeting of the mTOR pathway by rapamycin, led to the selective elimination of LSCs without affecting the survival and the function of normal HSC, which were instead impaired upon depletion of Pten alone (Yilmaz, Valdez et al. 2006). In addition, therapies against surface markers exclusively exhibited by CSCs have been tried. Monoclonal

antibodies against CD44, IL-3R, CD47 and the immunoglobulin mucin Tim-3 have been developed and utilized to specifically target LSCs in human AML (Chen, Huang et al. 2013). Targeting CD44, in particular, might be a good candidate therapy also for CSCs in solid cancers, as normal HSCs do not seem to use this molecule for their adhesion signaling (Jin, Hope et al. 2006).

These observations suggest that a CSC based anticancer approach should be selectively targeting mechanisms of tumor propagation.

2.3.2 P53 role in CSCs

The tumor suppressor p53 is unequivocally one of the most crucial genes for cancer. Inactivation of its function is a very common event as it happens in more than 50% of all sporadic human tumors (Vousden and Prives 2009). During tumor development, a mutational event in the p53 gene is usually followed by loss of heterozygosity, which results in the complete loss of p53 function. Depending on the tumor type, p53 deficiency is involved in the initiation or progression of cancer and it is frequently associated with higher tumor aggressiveness (Miller, Smeds et al. 2005). In breast cancer, inactivation of p53 is present in around 80% of basal-like tumors, the most malignant and undifferentiated subtype (Cancer Genome Atlas 2012, Curtis, Shah et al. 2012), and several reports indicate that p53 loss is correlated with the acquisition of a SC transcriptional signature and SC-like phenotypes (Spike and Wahl 2011).

The tumor suppressive function of p53 has been historically associated with its role in hindering the cell cycle, through induction of apoptosis and senescence in response to a plethora of diverse stresses: DNA damage, hyperproliferative signals, oxidative stress, hypoxia, just to mention a few. In the presence of these stimuli, p53 is stabilized by the

displacement from the E3-ubiquitin ligases that control its levels (Mdm2, mainly, and Mdm4) and consequently activated. However, more recently, p53 tumor suppressive role has been involved in many additional biological processes including SC-related functions (Vousden and Prives 2009) (**Figure 2-6**).

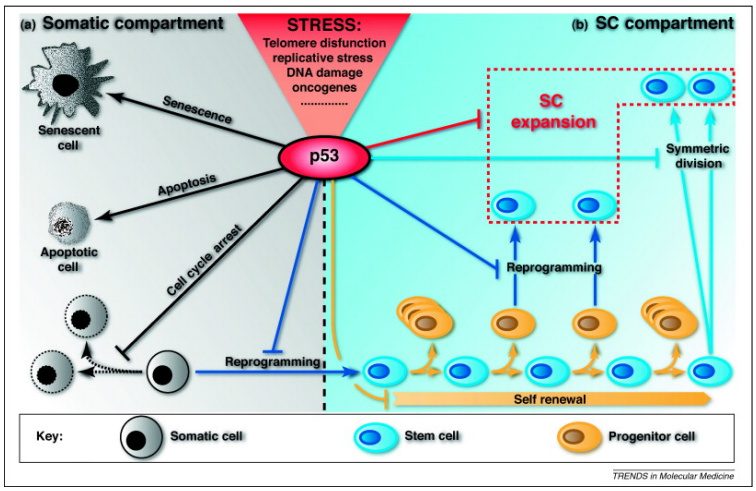

Figure 2-6: Pleiotropic nature of p53 functions in a) somatic and b) SC compartments. (Bonizzi, Cicalese et al. 2012) ©TRENDS in Molecular Medicine

P53, in fact, acts as a negative regulator of SC self-renewal at multiple levels. First of all, p53 maintains the quiescent pool of HSCs, preventing their exhaustion (Liu, Elf et al. 2009) and its loss has been shown to induce severe impairment of self-renewal in hematopoietic progenitors, thus facilitating AML development (Zhao, Zuber et al. 2010). Furthermore, a key evidence supporting this role comes from the fact that p53 can inhibit reprogramming of differentiated somatic cells into induced pluripotent stem cells (iPSCs) (Hong, Takahashi et al. 2009). This is achieved both through p21-dependent cell cycle arrest and through trans-activation of miR-34a and miR-145, which negatively regulate essential pluripotency genes (Bieging, Mello et al. 2014). Conversely, a recent study in liver cancer has shown that p53 loss contributes to tumorigenesis by favoring de-

differentiation of adult hepatocytes into early progenitor cells, endowed with CSCs potential to give rise to hepatocellular carcinomas (Tschaharganeh, Xue et al. 2014).

Indeed, it is becoming more and more evident that certain tumor cells have the ability to reversibly transit among states with different competence in tumor sustainment, a biological property that goes under the definition of cancer plasticity. In breast cancer, for example, tumor cells can switch from epithelial to mesenchymal functional specializations, a process called epithelial to mesenchymal transition (EMT) which also occurs physiologically during organism development or wound healing, with the cells in the mesenchymal state appearing more capable of forming tumors (Mani, Guo et al. 2008).

In details, the expression of a certain set of genes in epithelial cells promotes the disassembling of cell-to-cell junctions and endows them with a mesenchymal, migratory phenotype. Many transcription factors promote EMT, among them the Snail, Twist and Zeb families, and, importantly, their activity seems to be orchestrated by p53. For example, p53 indirectly inhibits the expression of Snail, Zeb1 and Bmi1 by trans activating regulatory miRNAs (Bieging, Mello et al. 2014). In the work of Mani and colleagues, the induction of EMT in immortalized human mammary epithelial cells by the ectopic expression of *snail* or *twist* leads to the formation of cells with CSC characteristics. Also, markers of EMT were found to be expressed by CD24-/CD44+ cells in human breast cancer (Mani, Guo et al. 2008). Thus, there is increasing evidence that more differentiated cells can undergo phenotypical changes that allow them to acquire CSC specific features. This process has the direct consequence of expanding the pool of CSC.

Furthermore, a role for p53 in the regulation of the balance between SC symmetric and asymmetric division has been demonstrated. The mode of division of SCs is a key issue in SC biology and one of the critical features that allows them to sustain tissue homeostasis

and tissue specialization. Indeed, unlike more specialized cells, SCs have the ability to undergo both symmetric and asymmetric cell division, generating daughter cells that are either both endowed with the same properties of the mother or that are distinct in terms of their cell-fate. Under physiological conditions, the ratio between symmetric and asymmetric division is tightly regulated in order to maintain the balance between SC self-renewal and differentiation. When the choice between symmetry and asymmetry is uncontrolled, the consequences for development and disease are huge, inducing disruption of organ morphogenesis or leading to malignant transformation. This was demonstrated for the first time in *Drosophila* through genetic screens that showed how the mutagenesis of critical players of the asymmetric cell division (ACD), such as Brat, triggered the formation of brain tumors upon transplantation (Betschinger, Mechtler et al. 2006).

Our group showed that, in a murine model of breast cancer driven by the mutated form of the *erbB2* gene, the increased frequency of symmetric divisions in CSCs, compared to their normal counterparts, is the underlying mechanism of CSC expansion, as seen by sphere forming assay and *in vivo* sustainment of the cancer clone. In this work, Cicalese and colleagues reported that the switch towards symmetric self-renewal was instructed, at the molecular level, by p53 loss; indeed, by restoring p53 function, asymmetric cell division in the CSCs was re-established, leading to a reduced frequency of tumor formation (Cicalese, Bonizzi et al. 2009). Other reports confirmed the role of p53 (and its downstream effectors) in regulating asymmetry in neural progenitors (Sugiarto, Persson et al. 2011) and in colon cancer cultures, through the asymmetric segregation of miR-34a, a p53 target micro-RNA (miRNA), whose role is to promote differentiation in one of the daughter cells (Bu, Chen et al. 2013). Therefore, it appears clear that increased symmetric renewal could be the basis of the differentiation arrest and clone expansion that are inherent to cancer progression.

All together these findings highlight the importance of a negative regulation of "stemness" as part of the tumor suppressive program orchestrated by p53. Indeed the expansion of the CSC compartment could be one of the driving forces for tumor development and maintenance. Nevertheless, the downstream pathways and effectors that are crucial for the execution of this program remain largely unknown.

2.4 Myc at the crossroad of SC biology and cancer

The product of the oncogene *c-myc* belongs to Myc family of transcription factors, which also includes N-Myc and L-Myc. This family contains basic helix-loop-helix (bHLHZ) domains that mediate the interaction with target DNA. Endowed with a very pleiotropic nature, Myc coordinates an impressive number of biological functions due to its ability to act as a *i)* transcriptional activator through its hetero-dimerization with Max, *ii)* transcriptional repressor, through its interaction with Miz1, and *iii)* chromatin remodeler (Amati, Frank et al. 2001). Myc is at the center of an intricate network of growth-promoting signals and it is activated downstream of many different ligand-dependent stimuli. Its expression in normal cells is highly regulated by a number of mechanisms at the transcriptional and post-transcriptional level (Dang 2012). The transcriptional program instructed by Myc touches many biological processes, such as cell proliferation, DNA replication, metabolic shifts, stemness, differentiation, and apoptosis, which, once de-regulated, constitute many of the "hallmarks of cancer" (Hanahan and Weinberg 2011). Therefore, it is not surprising that Myc aberrant activity is often linked to malignant transformation.

2.4.1 Myc in the maintenance of SC self-renewal

Among its functions, the role of Myc in SC biology is one of the most intense areas of study, as it constitutes the paradigm for the multiple aspects of its biological activity.

Myc plays a critical role both at the stage of organism development and in adult tissues by regulating the cell fate of stem and progenitor cells. In *Drosophila* neuroblasts, cell cycle exit and subsequent differentiation of one of the daughter cells generated by ACD is mediated by the Brat gene, that exerts this function by negatively regulating *Drosophila* Myc (dMyc) (Betschinger, Mechtler et al. 2006).

Similar observations have also been made in mammalian SCs. Myc is required for embryogenesis as knock-out of both c-Myc and N-Myc results in early lethality of mice embryos, thus proving that Myc is essential in ESC pluripotency and self-renewal (Varlakhanova, Cotterman et al. 2010). Accordingly, it has been demonstrated that ectopic expression of Myc inhibits the differentiation of ESCs; indeed, constitutive expression of a mutant form of Myc (T58A, which is not degraded by Fbw7 ubiquitin ligase) maintains ESC self-renewal and pluripotency even in the absence of leukemia inhibitory factor (LIF) in the growing media. In contrast, inhibition of Myc induces ESC differentiation (Cartwright, McLean et al. 2005). Furthermore, it is possible to recognize a distinct signature of Myc-dependent targets within the set of genes expressed in ESCs (Kim, Chu et al. 2008); notably, this set of genes was found to correlate with human cancer signatures (Kim, Woo et al. 2010) (**Figure 2-7**).

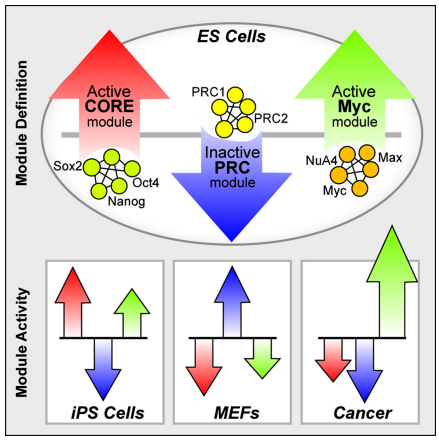

Figure 2-7: Myc-dependent network is a feature of ESCs and is highly activated in cancer. (Kim, Woo et al. 2010) Copyright © 2010 Elsevier Inc. All rights reserved.

These data are coherent with the fact that Myc has a fundamental role in somatic cell reprogramming together with other three transcription factors (TFs): Oct4, Sox2, Klf4 (all together under the name of OSKM) (Takahashi and Yamanaka 2006). Although several studies demonstrated that Myc is not absolutely required for iPSC generation, its presence increases the speed and the efficiency of the process. Indeed, for specific cell types harboring high levels of Myc expression (like neural progenitors and keratinocytes), Myc is completely dispensable from the "reprogramming cocktail" (Singh and Dalton 2009). It seems plausible that Myc aids reprogramming by maintaining the cells in a highly proliferative state, which is a characteristic of pluripotent cells (Singh and Dalton 2009). In addition, given that Myc-binding to promoter regions of target genes is associated with open chromatin marks and is correlated with the amount of RNA polymerase recruited, recent reports suggest that OSK factors might act as "pioneers" to enable binding of Myc to regions of inaccessible chromatin. At the same time, Myc might facilitate the initial binding of OSK factors to chromatin through a cooperative mechanism (Soufi, Donahue et al. 2012, Buganim, Faddah et al. 2013).

The role that Myc holds in ESC pluripotency and its effects on differentiation is maintained in adult SCs. The study of Myc in tissue SCs has revealed, however, a more blurred situation: depending on the cell context, Myc can enhance self-renewal and inhibit differentiation, or promote terminal commitment. For example, in the skin, ectopic expression of Myc, under the control of the SC-specific promoter K14, induces long-term depletion of SCs, due to increased rate of proliferation and accumulation of differentiated cells in the adjacent layers of the epidermis (Watt, Frye et al. 2008). In the hematopoietic system, depletion of Myc impedes the mobilization of HSCs from their niche causing their accumulation, an event that leads to concomitant loss of all the differentiated progeny. Interestingly, the depletion of Myc does not affect the dormant pool of HSCs, indicating that the dependence of cells on Myc varies according to the cell-cycle status (Wilson, Murphy et al. 2004, Laurenti, Varnum-Finney et al. 2008). As far as more differentiated progenitors are concerned, Myc overexpression confers on them higher self-renewal capacities; this is what happens, for example, in late-stage neural SCs, where this effect of Myc is exerted by its co-regulator Miz-1 (Kerosuo, Piltti et al. 2008). In line with this, it was reported that enforced Myc expression in an immortalized human breast line drives EMT through the induction of the GSK-3β/Snail signaling pathway (Cho, Cho et al. 2010), thus remarking the importance of Myc in reprogramming cell fates also in adult tissues.

The essential role of Myc in SCs was also characterized in the mammary gland. Conditional deletion of Myc in the basal compartment impairs SC self-renewal, as assessed by limiting dilution transplantation and mammosphere assays, and consequently disrupts differentiation into the luminal and myoepithelial lineages (Moumen, Chiche et al. 2012).

Taken together these data highlight the importance of Myc in cell fate determination as well as the strong dependency of its function on the cellular context. Therefore, it clearly emerges that a careful regulation of Myc levels is needed by each cell type to properly

function, according to its replicative potential and grade of specialization; however, additional studies are required to provide a richer mechanistic understanding.

2.4.2 Upstream of Myc

The regulation of Myc expression is a very complex area of study; indeed, many pathways and TFs converge into Myc signaling. The transcriptional regulation of the *c-myc* promoter itself is extremely challenging, with a lot of redundancy, many feedback loops, and several cross-regulatory circuits involved (Wierstra and Alves 2008). Indeed, besides the regulation acted by a number of TFs, it has been proposed that a number of unconventional DNA-binding proteins recognizing non–B DNAs structures, including single-stranded bubbles, G-quadruplexes, and Z-DNA, also regulate *c-myc* (Levens 2010).

As mentioned, numerous are the TFs that have the ability to bind and regulate the *c-myc* promoter and subsequently drive a plethora of different cell responses. Few examples include: TCF, whose role downstream of the Wnt pathway is important for embryonic development, proliferation and adult SC self-renewal (Dang 2012); TGF-β, one of the most important cytostatic stimulator that represses the *c-myc* promoter through its downstream effectors Smad3/4; STAT3, a mediator of cell proliferation and survival that participates in cellular transformation and tumorigenesis; the NF-κB/Rel family, that orchestrates inflammatory and immune responses and regulates cell proliferation, survival, and differentiation; AP-1 with c-Fos/Jun, E2F. Furthermore, Notch, Hedgehog and many other cell fate regulators pathways converge into Myc regulation (Wierstra and Alves 2008). Myc itself regulates its own expression at the transcriptional level in a concentration

dependent manner; this represents a fundamental homeostatic mechanism of protection for normal cells that is lost in many transformed cell lines (Wierstra and Alves 2008).

A fine control over Myc levels takes also place at the post-transcriptional level. For example, the Ras-driven pathway induces phosphorylation on Ser62, stabilizing the Myc protein, and at the same time inhibits the phosphorylation, by GSK-3β, of the Thr58 residue. This last modification is recognized by the Fbw7 E3 ubiquitin ligase that binds Myc for proteasomal degradation (Welcker and Clurman 2008). Furthermore, other ubiquitin ligases contribute to the regulation of Myc half-life; among them, the murine Brat orthologue Trim32 is asymmetrically distributed during the ACD of neural SCs and becomes up-regulated during neuronal differentiation, thus enhancing the ubiquitin-mediated degradation of Myc in the differentiating cells (Schwamborn, Berezikov et al. 2009, Izumi and Kaneko 2014). The ubiquitin-proteasome system (UPS) is not the only mechanism involved as many miRNAs, such as let-7, miR-34, and miR45, are known to target and degrade Myc transcripts (Dang 2012).

Therefore, it emerges that vigilant control of Myc levels is crucial for normal cells, as disruption of any of the regulatory mechanisms leads to pre-transformed phenotypes. Notably, most of the regulators of Myc activity are likely involved in the CSC specific mechanisms that we have described earlier.

Among the upstream regulator of Myc there is also p53: simultaneous inactivation of p53 and PTEN in neural SCs is accompanied by over-expression of Myc and its associated signature, and results in increased self-renewal and the promotion of an undifferentiated state that is one of the underlying traits of human glioblastoma (GBM) (Zheng, Ying et al. 2008). These findings are concordant with observations that describe a role for p53 in the repression of Myc expression and which is achieved by direct binding of p53 to the Myc

promoter (Ho, Ma et al. 2005), or to distal regulatory elements (Li, He et al. 2012), or by means of intermediate regulatory miRNAs (Sachdeva, Zhu et al. 2009).

2.4.3 Myc activation in cancer

Our brief overview emphasizes how the de-regulation of Myc in a permissive epigenetic and genetic cellular context allows overcoming the checkpoint mechanisms and leads to the establishment, in the cell, of many of the "hallmarks of cancer". A de-regulated Myc drives proliferation, high rate of DNA replication and transcription, altered cellular metabolism, increased protein synthesis, changes in the tissue microenvironment, supports stemness, and blocks senescence and differentiation. Each of these processes is associated with tumor growth and maintenance (Gabay, Li et al. 2014). The most common events that could results in Myc de-regulation are: genetic amplification, chromosomal translocation and constitutive activation/repression of the upstream regulatory signaling.

In breast cancer, Myc genetic amplification takes place in 22% of the cases reported in the Cancer Genome Atlas (TCGA) dataset (Cancer Genome Atlas 2012), while chromosomal translocation involving the *myc* locus has not been reported in breast cancer. Genetic amplification has been associated with higher risk of relapse and death by invasive metastasis and it seems to be an event correlated with other genetic predispositions: indeed, Myc amplification is found in 53% of tumors harboring Brca1 mutation (Xu, Chen et al. 2010).

Beside genetic amplification, the frequency of patients showing high levels of Myc, most likely due to the disruption of upstream regulatory mechanisms, is very high, but variable depending on the cancer subtype. Early studies on small cohorts of patients reported that Myc over-expression is associated with basal-like breast tumors (Sotiriou, Neo et al. 2003).

The basal-like breast cancer is the most challenging of the breast cancer subtypes: it histologically derives from the basal compartment of the normal mammary epithelia (the one that putatively contains SCs). It is negative for the expression of estrogen, progesterone and Her2 receptors; it shows an early stage onset and a strong tendency to metastasize, and currently there are no therapeutic options for targeted pharmacological treatment. In line with the data of over-expression, a Myc-dependent gene signature, which is included in a larger set of ESC specific genes, was reported to positively correlate with basal-like or ER negative breast tumors, with shorter interval to metastasis, and, generally, with poorer prognosis (Kim, Woo et al. 2010).

Therefore, like for the loss of p53, a role in the progression and sustainment of the less well-differentiated tumors, through the maintenance of a SC-like state, also emerges for Myc. In line with this, in Burkitt's lymphomas and hepatocellular carcinomas, it has been shown that inhibition of Myc causes tumor regression by restoring the physiological program of cellular differentiation (Karlsson, Giuriato et al. 2003, Shachaf, Kopelman et al. 2004), thus strengthening the concept that de-regulation of Myc favors tumor progression by enhancing self-renewal and inhibiting differentiation. Considering the role of both Myc and p53 in somatic cell reprogramming, it is plausible to hypothesize that they could be involved in tumor progression by promoting the formation of cancer cells that retain developmental plasticity.

3 Materials and Methods

3.1 Animal Manipulation

3.1.1 Animal Models

MMTV-ErbB2 transgenic mice were in the FVB background (Muller, Sinn et al. 1988). P53-/- and p53+/- mice were in the C57/BL6J background (back-crossed in our group starting from a 129sv background). Rosa26-MycER transgenic mice were in C57/BL6J background (Murphy, Junttila et al. 2008), kindly provided by B. Amati's group (Department of Experimental Oncology, European Institute of Oncology). As controls we used mice of the same strain, negative for the presence of the transgene (called wild type (WT) Rosa26-MycER). Transgenic mice expressing the green fluorescent protein (GFP) (Hadjantonakis, Gertsenstein et al. 1998), employed for serial transplantation experiments were in FVB background. All the experiments with WT mammospheres were carried out in samples derived from FVB WT mice.

3.1.2 4-Hydroxy-Tamoxifen (4-OHT) administration *in vivo*

WT C57/BL6J mice were tested for tolerability of long-term administration of 4-OHT and its effects on the mammary gland tissue. 3 week-old and 8 week-old mice were fed with Tamoxifen- containing diet or standard diet for 14 days, then they were sacrificed and their

mammary glands digested and analyzed at FACS for the expression of epithelial SC markers. Tamoxifen- containing food was purchased from Harlan (TD. 130859) and, according to manufacturer instructions, provided ~40 mg tamoxifen per kg body weight per day assuming 20-25 g body weight and 3-4 g intake.

3.1.3 Nutlin-3 treatment *in vivo*

Nutlin-3 for *in vivo* studies was purchased from Sigma Aldrich. FVB mice transplanted with tumor cells infected with either empty vector or MycER vector were treated with Nutlin-3 (20 mg/kg body weight) or DMSO (both diluted 1:1 with PBS) for two weeks by intra-peritoneal (IP) injection once every two days. Mice were sacrificed immediately after treatment to evaluate the effect o Nutlin-3 on tumor growth.

3.1.4 Transplantation Experiments

For mammary gland reconstitution assays, the sample material to be injected (dissociated mammospheres, PKHneg cell subset) was collected; cells were counted and resuspended in PBS at the appropriate cell density in 25 µL of final volume per injection. 3 week-old female FVB mice were anaesthetized with 2.5% Avertin in PBS (100% avertin: 10 g of tribromoethanol, Sigma, in 10 ml of tertamyl alcohol, Sigma) and the fat-pad of their inguinal mammary gland was depleted of the endogenous epithelium. At 3 weeks of age the mammary epithelial tree has not undergone the puberty-driven development that results in the penetration of the fat pad, and can be easily removed by surgical cut of the area

spanning from the nipple to the lymph node, leaving the fat-pad clear for the injection of exogenous cells.

For the injection of tumor cells (infected *in vitro* with MycER or the corresponding empty vector) we used 8 week-old virgin mice and no clearing of the fat pad was performed. 200,000 cells were injected orthotopically in one inguinal mammary gland per mouse and almost 100% of mice developed secondary tumors with a latency of 40-50 days.

3.1.5 Carmine Alum Whole Mount staining

Transplanted mammary glands were stretched out onto slides and fixed overnight in 4% formaldehyde. Slides were washed twice in distilled water for 10 minutes and then stained overnight at room temperature with Carmine Alum solution (0.2% carmine, 0.5% aluminium potassium sulfate in water, Sigma). De-staining was performed in 70% ethanol for 30 minutes, followed by two 30 minutes washes in 95% and 100% ethanol. Finally, samples were soaked in a 1:2 solution of benzylalcohol/benzylbenzoate (Sigma) until the fat pad color clarified. For immunohistochemistry (IHC) analyses, glands were re-hydrated through alcohol gradient (100% - 95% - 70%) and stored for paraffin embedding.

3.1.6 Evaluation of positive transplants and statistical analysis

For the evaluation of positive outgrowths, the fat pads were collected ~12 weeks after transplantation, stained with Carmine Alum and analyzed as previously reported (DeOme, Faulkin et al. 1959). Briefly, fat pads were scored as negative for outgrowths if no epithelial structures could be observed. In some cases, endogenous epithelial re-growth

was scored. This is defined as an epithelial ductal network in which the majority of ductal branching had the same direction and had grown in from the cut edge of the cleared fat pad; in those cases the transplants were excluded from the statistics. The outgrowths were scored as positive if the ductal branching had originated from a central region of the cleared fad pad and the directionality of the ductal branching was variable in different parts of the fat pad. The presence of TEBs in the outgrowths was also a hallmark of exogenous epithelial growth.

Limiting dilution analysis was performed using the Extreme Limiting Dilution Analysis (ELDA) web tool (http://bioinf.wehi.edu.au/software/elda/) (Hu and Smyth 2009). ELDA computes a 95% confidence interval for the active cell frequency in each population group. One-sided confidence intervals are developed for stem cell frequency for subpopulations that produce 0% or 100% positive outgrowths. Furthermore, ELDA implements a likelihood ratio test for the acceptance of the single-hit hypothesis, which guarantees greater power and much improved performance in small samples as compared to a t-statistic approach. ELDA also computes an overall test for differences between the population groups, analogous to a one-way ANOVA test.

3.1.7 Preparation of paraffin sections

For the preparation of paraffin-embedded sections: hydrated whole- mounted tissues were sequentially treated for 1 hour at room temperature with 70%, 80%, 95% ethanol, three times with 100% ethanol, twice with xylene and twice for two hours at 58°C with paraffin. The specimens were then embedded in paraffin and sectioned with a microtome at 5µm thickness. Slides were stained with haematoxylin-eosin for histological analysis or stained by IHC.

3.1.8 Immunohistochemistry

Paraffin sections were de-paraffinized with histolemon (Carlo Erba) for 10 minutes twice and hydrated through graded alcohol series (100%, 95%, 70% ethanol and water) for 5 minutes each. Antigen unmasking was performed in boiling citrate buffer (10mM sodium citrate, 0.05% tween20, pH 6.0) for 30 to 50 minutes, followed by incubation with 3% hydrogen peroxide in distilled water for 10 minutes at room temperature. Slides were subsequently pre-incubated with an antibody mixture (2% BSA, 5% FBS, 0.02% Tween20 in TBS) for 20 minutes at room temperature and then stained with primary antibody overnight at 4°C. After two washes with TBS slides were incubated with a secondary antibody (DAKO Envision system HRP rabbit or mouse) for 30 minutes at room temperature and washed twice again in TBS. The sections were subsequently incubated in peroxidase substrate solution (DAB DAKO) for 2 to 10 minutes, rinsed in water, counterstained with hematoxylin for 30 seconds, dehydrated through graded alcohol series (water and 70%, 95%, 100% ethanol) for 5 minutes each and ultimately mounted with Eukitt (Kindler GmbH). All primary antibodies and their relative concentrations used in this study are listed in **Table 3-1**.

Antibody	Clone	Company	Concentration
Rabbit anti-Cytokeratin 14 (K14)		Covance; PRB-155P	1:500
Mouse anti-Cytokeratin 18 (K18)	Ks18.04	Progen; 61424	1:20
Rabbit anti-KI67		Thermo Scientific; RM-9106-S	1:200
Rabbit anti-βcasein		Santa Cruz Biotech.; sc30042	1:500
Rabbit anti-GFP		Abcam; ab6556-25	1:500

Table 3-1: List of antibodies and conditions used for IHC analysis.

A subset of samples was examined for detailed histopathological analysis. To assess the extent of the mammary epithelium in each examined sample, the area (μm^2) occupied by mammary epithelium and the % Area = area occupied by epithelium/total area of field at 100x * 100) were evaluated in hematoxylin-eosin (HE) stained sections using the ImageJ 1.47v analysis program (imagej.nih.gov/ij/) in 4 100x microscopic fields selected in the areas with the highest amount of mammary epithelium (hot spots).

To assess the extent of the proliferative activity, the number of Ki67-positive and Ki67-negative cells were counted using the ImageJ analysis program in 400x microscopic fields centered on mammary epithelial structures. The Ki67 index was then calculated as: nr. of positive cells divided by nr. of total cells.

3.2 Cell culture

3.2.1 Isolation of mouse mammary epithelial cells

The inguinal and axillar normal mammary glands were collected from 6-10 week-old virgin WT, Rosa26-MycER transgenic heterozygous mice, or p53-/- and p53+/- mice. Tumors derived from MMTV-ErbB2 transgenic mice were collected at the time of their appearance (tumor latency: 12 to 16 weeks after birth). Mammary tissues were mechanically dissected into small pieces with scissors, and enzymatically digested with the following digestion mixture: Dulbecco's modified Eagle's medium (DMEM, BioWhittaker), 2 mM glutamine, 100 U/ml penicillin and 100 µg/ml streptomycin, supplemented with 200 U/ml collagenase (Sigma) and 100 U/ml hyaluronidase (Sigma) on rotating wheel for 2-3 hours at 37°C in a humid atmosphere containing 5% CO_2. When the digestion was complete, the cell suspensions were centrifuged at 600 rpm for 5 minutes

and then resuspendend in PBS and filtered through 100, 70 and 40 μm cell strainers to eliminate cell aggregates. Red blood cells were lysed with ACK lysis buffer (Lonza) for 2 minutes in ice. Cell suspension depleted of red blood cells was washed in cold PBS and plated to obtain mammospheres, stained with the PKH26 fluorescent dye or used for growth assays.

3.2.2 FACS analysis of epithelial cell sub-populations

Single cells isolated from the mammary tissue were mixed with digested organoids. Organoids were derived from the collection of aggregates that did not pass through each of the cell strainer used. This material was further digested with trypsin/EDTA (Lonza), dispase (5U/mL, Stem Cell Technologies) and DNase (1mg/ml, Stem Cell Technologies). Inactivation of the enzymes was performed with cold PBS supplemented with 2% FBS. The cell suspension of single cells and digested organoids was blocked in BSA 10% and then stained for mammary stem cell markers as listed below:

- Lineage cocktail (Lin-): anti-CD45 (eBioscience, clone RA3-6B2); ant-Ter119 (eBioscience, clone Ter119); anti-CD31 (eBioscience, clone 390); all PE-Cy7 conjugated (1:300)
- Anti-CD49f (eBioscience, clone GoH3) eFluor®450 conjugated (1:100)
- Anti-CD61 (eBioscience, clone 2C9.C3) PE conjugated (1:40)
- Anti-EpCAm (eBioscience, clone G8.8) APC conjugated (1:200).

In selected experiments, Lin- cells were isolated by column-based negative selection that was performed through the EasySep™ Mouse Epithelial Cell Enrichment Kit (Stem Cell Technologies).

Samples were acquired at FACS Canto II (BD bioscience) and analyzed with FlowJo 9.3-2 analysis software.

3.2.3 Mammosphere culture

Primary mammary cells were plated onto ultralow attachment 6-well plates (Falcon) at a density of 200,000 viable cell/mL (to obtain primary mammospheres) in a serum-free mammary epithelial basal medium (MEBM, BioWhittaker), supplemented with 2 mM glutamine, 100 U/ml penicillin and 100 µg/ml streptomycin, 5 µg/ml insulin, 0.5 µg/ml hydrocortisone, 2% B27 (Invitrogen), 20 ng/ml EGF and βFGF (Peprotech), and 4 µg/ml heparin (Sigma) and cultured at 37°C in 5% CO_2. In these conditions mammary epithelial cells grow as clonal colonies called mammospheres (Dontu, Abdallah et al. 2003) that reach their maximum size in 5-6 days. After 7 days of culture, primary mammospheres (obtained from freshly isolated mammary cells) were dissociated mechanically using a Gilson® pipette with filtered tips and re-plated to obtain secondary mammospheres at a density of 20,000 cells/ml in 6-well low-adhesion plates. The same procedure was repeated at each passage.

3.2.4 Mammosphere growth curves

For the modelling of mammosphere growth curves, primary mammospheres were dissociated mechanically and re-plated (at 20,000 cells/ml) to obtain secondary mammospheres in 6-well low-adhesion plates coated with poly-HEMA (Sigma). After 7 days, the newly formed mammospheres were counted, collected and manually dissociated

by pipetting. At each passage, the number of retrieved mammospheres reflects the number of mammosphere initiating cells present in the original culture and the number of cells counted after dissociation allows for the evaluation of the number of cells per sphere that was formed. At each passage spheres were enumerated using digital image analysis (Imagej; object threshold 100 microns). Cumulative sphere and cell curves were calculated based on the ratio between plated spheres and obtained spheres and cells respectively. The number of plated spheres was derived from the total number of cells divided by the size of the mammospheres (nr. of cells / nr. of spheres) over the passages, under the assumption that the average mammosphere size in a culture does not change (Cicalese, Bonizzi et al. 2009).

The cumulative curves were plotted in a semi-logarithmic scale and they approximated an exponential curve, as expected for a cell population that grows or dies with a constant rate during the time. Growth rates (GRs) were evaluated as the slope of the trend-line of the exponential curves. The exponential regression of the data resulted in the value of the coefficients of determination (R^2), which approximate 1 in each of the measured curve, thus indicating the goodness of the fitting model.

3.2.5 PKH26 assay

Primary Rosa26-MycER heterozygous and WT FVB mammary cells were resuspended at the concentration of 10 million cells/ml and stained for 5 minutes at room temperature by adding an equal volume of a PKH26 mix (1:2500 PKH-26 in PBS) (Sigma, PKH26- GL), light protected. The cells were then washed twice with culture medium and plated to obtain primary mammospheres. PKH-labeled mammospheres were collected after 7 days, and mechanically dissociated to obtain single cell suspension. After a filtering step with a 40

μm cell strainer cells were subjected to FACS sorting (Influx cell sorter equipped with a 488 nm laser and with a band pass 575/26 nm optical filter for PKH26 fluorescence detection, BD). The gate for PKH negative population was selected according to the basal fluorescence of unstained cells and usually included the 25% of the live cells. The obtained PKHneg cells were cultured as mammospheres, plated for growth curves in presence or absence of 4-OHT or infected with lentiviral vectors and used in transplantation assays.

3.2.6 Viral Infections

293-T and Phoenix-ECO packaging cells were cultured in DMEM supplemented with 10% FBS, 2 mM glutamine, 100 U/ml penicillin and 100 μg/ml streptomycin. For lentiviral production 293-T cells were transfected with the calcium-phosphate procedure with a mixture of: 2,5 μg of pRSV (Rev), 5 μg of pMDL/pRRE (gag&pol), 3 μg of pENV (VSV-G), and 10 μg of the lentiviral vector per plate. The same procedure was applied for transfection of Phoenix-ECO cells for retroviral production, which were transfected with: 5 μg of PKAT2, 10 μg of retroviral vector. 62.5 μl of 2M $CaCl_2$ were added to the DNA mix and brought to a total volume of 500 μl with water. The mix was added drop-wise to 500 μl of 2X HBS (HEPES buffered saline: 250mM HEPES pH 7.0, 250mM NaCl and 150mM Na2HPO4) by bubbling. After 15 minutes of incubation, the precipitate was distributed on 70% confluent exponentially growing cells. The medium was replaced 12-16 hours later with mammosphere medium deprived of EGF and FGF. Viral supernatant was collected 24 and 48 hours after and filtered through a 0.45 μm syringe-filter. Cells from dissociated primary mammospheres were resuspended in viral supernatants supplemented with growth factors and Polybrene (4 μg/mL) to a final concentration of 50,000 cell/ml and subjected to

two cycles of infection in suspension (overnight and 6h). Then, the cells were plated in fresh mammosphere medium to obtain secondary mammospheres.

In selected experiments, the viral supernatant was concentrated by ultra-centrifugation for 2h at 20,000 rpm at 4°C and the viral pellet obtained was resuspended in PBS at 1000X concentration. The viral stock was frozen (-80°C) and subsequently used to infect target cells in order to achieve high multiplicity of infection (MOI). The concentrated virus was employed for the infection of ErbB2 primary tumor cells in adhesion prior to the injection in congenic recipient mice. This alternative protocol allows for shorter culture periods compared to the mammosphere assay.

In this study we employed the following viral vectors (**Table 3-2**):

Lenti/Retro virus	Backbone	Insert	Reference
Lentivirus	pWPI (Addgene #12254)	MycER	(Littlewood, Hancock et al. 1995)
Lentivirus	pTRIPZ	Omomyc	(Annibali, Whitfield et al. 2014)
Retrovirus	pBABE-puro (Addgene #1764)	p53ER	(Vater, Bartle et al. 1996)

Table 3-2: List of viral vectors used in this study for stable transduction.

3.2.7 Cell Cycle Analysis

Clik-iT® Plus EdU kit for flow cytometry assay was purchased from Life Technologies. WT FVB and MMTV-ErbB2 mammospheres were labelled each day of the culture (from day 1 to day 5) for 1.5 hours and stained according to the manufacturer protocol. Cells were then fixed in ethanol 100% for 1 hour on ice and stained with propidum iodide (PI) solution (final 2.5µg/mL). Cells were then incubated with RNaseA (final 0.25mg/mL) at 4°C for a minimum of 3 hours; then, the fluorescence signal was acquired at FACS Canto II (BD Bioscience) and files analyzed with the FlowJo 9.3-2 analysis software.

3.3 Expression Analyses

3.3.1 Quantitative PCR (qPCR)

Total RNA from mammospheres was isolated using Maxwell® 16 LEV simplyRNA cells kit (Promega), and reverse transcribed using random primers and ImProm-II™ reverse transcriptase (Promega), following manufacturer instructions. Real-time RT-PCR analyses were done in triplicate on the Applied Biosystems 7500 Fast Real-Time PCR System with the fast-SYBR Green PCR kit as instructed by the manufacturer (Applied Biosystems). The amount of each mRNA was normalized to the amount of GusB mRNA. The genes whose expression was under analysis in this study and the relative primers used for their amplification are listed in **Table 3-3**:

Gene name	Primer FW	Primer RV
GusB	GTGGGCATTGTGCTACCTC	ATTTTTGTCCCGGCGAAC
c-Myc	TTTGTCTATTTGGGGACAGTGTT	CATCGTCGTGGCTGTCTG
Ncl	CATGGTGAAGCTCGCAAAG	TCACTATCCTCTTCCACCTCCTT
Odc1	GCTAAGTCGACCTTGTGAGGA	AGCTGCTCATGGTTCTCGAT
Cad	GATCATCATGGGGGAGAAAG	CCAAGCGTGAGAAGGAGAAC
P21	TCCACAGCGATATCCAGACA	GGACATCACCAGGATTGGAC
Noxa	CAGAGCTACCACCTGAGTTCG	TACACTTTGTCTCCGATCTTCCT
Bax	AAGCTGAGCGAGTGTCTC	CCTTGAGCACCAGTTTGC

Table 3-3: **List of genes and corresponding primers used for quantitative PCR analysis.**

3.3.2 RNAseq and statistical analysis

A total amount of 300,000 cells were collected for each experimental group in biological triplicates and RNA was extracted as described in previous section. Libraries of template RNA molecules suitable for subsequent sequencing were prepared from 0.5 to 2 µg high quality input RNA using the Illumina® TruSeq® RNA Sample Preparation Kit v2 and following the manufacturer instructions. Sequencing was performed on Illumina HiSeq 2000 sequencer, read length was 50 base pairs and sequencing depth was 35 million reads per sample.

FastQ files were filtered discarding low quality reads (threshold on the quality score across all bases= 28). Alignment of the reads was performed with TopHat 2.0.8 and HTseq-count algorithm was used to annotate the reads to the Mm10 reference genome (NCBI reference sequence database annotation) and to calculate the *per* gene raw counts (http://www-huber.embl.de/users/anders/HTSeq/doc/count.html) (Anders, Pyl et al. 2015). The read count was normalized via Loess normalization by the DESeq2 algorithm (Anders and Huber 2010). DESeq is an R package to analyze count data from high-throughput sequencing assays such as RNASeq to test for differential expression. In details, DESeq2 calculates the total counts in each condition, and then it performs test statistics under the assumption of negative binomial distribution from which it calculates the pvalue. The statistics is then adjusted for benjamini-hochberg correction to calculate the False Discovery Rate (FDR or qvalue). The final step of the DESeq algorithm calculates the log2 fold change between the two samples under comparison. Additionally a filter on the average low represented genes in terms of read count (cutoff = 10) is applied. The differentially expressed genes (DEGs) were obtained, as such, from pairwise confrontation of the selected sample and its relative control.

For the Gene Set Enrichment Analysis (GSEA, http://www.broadinstitute.org/gsea/index.jsp) we applied a filter on the q value setting the threshold as lower or equal to 0.01. The analysis was performed on GSEA v2.2.0 platform running the 5,618 ranked DEGs of the MycER list on the GSEA pre-ranked tool. As gene sets to overlap and calculate the normalized enrichment score (NES) we used the DEGs of selected experimental groups (ErbB2, p53-/- and ErbB2+Nutlin) subdivided in UP and DOWN regulated lists. P-values of GSEA were calculated by performing 1.000 random permutations of gene labels to create ES null distribution.

Pathway and Gene Ontology analyses were performed by overlap of our gene set with the Molecular signature database (MSigDB v5.0) on the GSEA website (www.broadinstitute.org/gsea).

3.3.3 Immunofluorescence

Cells from dissociated mammospheres were fixed in suspension with 2% formaldehyde for 5 minutes at room temperature, washed three times in PBS and plated onto poly-lysinated coverslips, where they were let adhere O/N at 4°C. Cells were then permeabilized for 10 minutes with 0.1% Triton-X100 in PBS at room temperature, washed three times in PBS and blocked with donkey serum (blocking solution) for 45 minutes. Staining with primary antibodies was performed in a humid chamber for 1 hour at room temperature and followed by three washes in PBS. Coverslips were then stained with secondary antibodies for 30 minutes at room temperature, washed three times in PBS, counterstained with DAPI and mounted with mowiol. Samples were analysed under an UpRight BX61 (Olympus) fluorescence microscope with a 60X/1.35 oil objective (Olympus). Acquired images were analyzed through MetaMorph® Microscopy Automation & Image Analysis Software

(Molecular Devices). In this work we used a rabbit monoclonal c-Myc antibody (1:250 in blocking solution, clone Y69, ab32072 Abcam) followed by an anti-rabbit A647-conjugated antibody (1:400 in blocking solution).

3.3.4 Western Blot Analysis

100,000 to 500,000 cells from dissociated mammosphere were collected, washed in PBS and lysed in 50 to 100 µl of RIPA buffer (Tris-HCl 50mM; NaCl 150mM; 1% NP-40; EDTA 1mM; 0.5% Sodium Deoxylcholate; 0.1% SDS) supplemented with protease inhibitors (Roche). Proteins were quantified with the use of the DC™ Protein Assay (Biorad) in a 96-well format and the absorbance was measured at 750 nm with the GloMax® 96 Microplate Luminometer (Promega). SDS-PAGE was performed using the NuPage® Novex® Gel System apparatus (Invitrogen) at a constant current of 120 V for approximately 2 hours. Samples were loaded on precast gels Nupage Novex 4-12% Bis-Tris (Invitrogen) and the 1X NuPAGE® MOPS SDS was used as running buffer (Invitrogen). Following SDS-PAGE electrophoresis, proteins were transferred to nitrocellulose membranes (Protan; Schleicher & Schuell) by electroblotting for 1.5 hours at 100 V and then were stained with Ponceau S to verify the efficiency of the transfer. Membranes were blocked for 1 hour in blocking solution: 10% low fat milk in TBS-T (Tris Buffered Saline, 0.1% Tween 20) for all the antibodies used except for anti-phospho-S15 p53, which was in 5% BSA (Bovine serum albumin). The detailed conditions used for each antibody employed in this study are listed in **Table 3-4**:

Antibody	Clone	Company	Concentration	Antibody Mix
Mouse anti-Vinculin		Sigma	1:10,000	1% milk in TBS-T
Rabbit anti-c-Myc		Cell Signaling cat.nr. 9402	1:500	1% milk in TBS-T
Mouse anti-p53	AI25	In house	1:5	1% milk in TBS-T
Rabbit anti-phosphoS15 p53		Cell Signaling cat.nr. 9284	1:500	1% BSA in TBS-T
Mouse anti-p21	F-5	Santa Cruz Biotechnology cat.nr. sc6246	1:500	1% milk in TBS-T

Table 3-4: List of the antibodies used for western blot analysis and relative conditions.

The membranes were washed three times in TBS-T (10 minutes each) and incubated with a secondary antibody linked to horseradish peroxidase for 1 hour at room temperature. After three washes in TBS-T, the proteins were visualized using enhanced Clarity™ Western ECL Blotting Substrate (Biorad) and the ChemiDoc™ MP System (Biorad).

4 Results

4.1 Myc is a downstream target of p53

Our group has contributed to elucidate one of the CSC specific mechanisms for breast cancer progression: the role of p53 in governing the SCs mode of division, favoring asymmetric segregation. Loss of function of p53 was shown to lead to unlimited expansion of a population enriched in CSCs, as assessed by mammosphere assay and limiting dilution transplantation (Cicalese, Bonizzi et al. 2009). Nevertheless p53 is implicated in a plethora of pathways involving responses to stress and cell cycle arrest. Therefore, the role of p53 in the regulation of SC divisions requires further analyses to understand the mechanisms with which this function is carried out. Following a candidate gene approach and based on the available knowledge that places Myc as a target of p53 (Ho, Ma et al. 2005, Sachdeva, Zhu et al. 2009, Li, He et al. 2012), we decided to evaluate the role of the *myc* oncogene as the key downstream effector of p53 loss in breast cancer.

4.1.1 Myc is over-expressed in ErbB2 mammary tumors

As a first step we investigated whether Myc is overexpressed in our murine model of spontaneous breast tumorigenesis, driven by the ErbB2 oncogene. This model consists of a transgenic mouse carrying a constitutively active form of the ErbB2 oncogene (with the activating mutation Val664 to Glu664) under the control of the Mouse Mammary Tumor

Virus (MMTV) promoter (Muller, Sinn et al. 1988). It is characterized by attenuated p53 signaling and enhanced self-renewal potential, as assessed by mammospheres re-plating ability compared to non-tumor mammary cells (Cicalese, Bonizzi et al. 2009). Furthermore, it was demonstrated that tumors that are formed in the MMTV-ErbB2 mouse follow a CSC model, as it was possible to isolate a tumorigenic population, marked by the expression of Sca1, from a non-tumorigenic one (Grange, Lanzardo et al. 2008).

To evaluate levels of Myc protein, we collected three mammary tumors from independent MMTV-ErbB2 transgenic mice and mammary glands of WT FVB mice, as control. We purified the epithelial cells by column-based negative selection of cells carrying antigens specific for hematopoietic or endothelial tissues (Ter119, CD45, CD31) and prepared cell lysates for protein quantification. The western blot in **Figure 4-1** shows that Myc is overexepressed in ErbB2-tumors, as compared with the normal tissue, though protein levels vary significantly among different tumors.

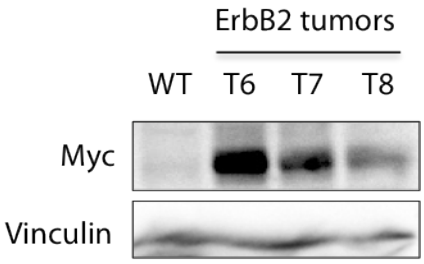

Figure 4-1: Myc expression in MMTV-ErbB2 tumors *ex vivo*.

Cells from three independent tumors arisen in 3 months old MMTV-ErbB2 mice and from adult WT mice were collected and CD31negTer119negCD45neg cells purified through column-based negative selection. Levels of Myc were analyszed by Western Blot using anti-Vinculin antibody as loading control.

To investigate whether over-expression also occurred in a population enriched in CSCs, we took advantage of the "mammospheres assay". Mammary cells endowed with self-renewal potential can be propagated in culture in anchorage-independent conditions, in the absence

of serum and in the presence of selected growth factors. Under those conditions, they expand clonally to form spheroids, which contain SCs and early progenitors (Dontu, Abdallah et al. 2003, Liao, Zhang et al. 2007), thus they represent a useful tool to study SC properties and functions.

Therefore, we analyzed levels of Myc (mRNA and protein) in mammospheres derived from either WT or MMTV-ErbB2 transgenic mice. The data in **Figure 4-2** indicate that Myc transcript expression is strongly up regulated in a CSC-enriched population of our tumor model. Equally, Myc protein levels were also increased in mammospheres obtained from two independent tumors, as compared to WT mammospheres (**Figure 4-3**).

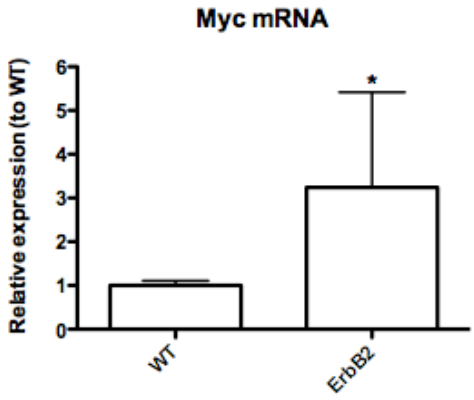

Figure 4-2: Myc mRNA is over-expressed in tumor mammospheres

Myc expression was assessed in WT (n=7) and MMTV-ErbB2 tumor (n=5) derived mammospheres by qPCR analysis of Myc mRNA (means ± standard deviation). Values are expressed as fold change relative to WT samples. Myc expression was normalized against the GusB housekeeping gene. Significance of differences between the two samples was calculated by t-test (*pvalue<0.05).

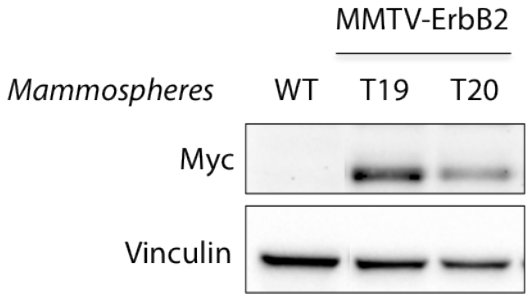

Figure 4-3: Myc protein is over-expressed in tumor mammospheres

Western blot analysis of the expression of Myc in WT mammospheres and in 2 independent MMTV-ErbB2 tumor cultures. Vinculin used as loading control.

4.1.2 Myc over-expression is the consequence of p53 loss of function

P53 is not mutated in our tumor model, nevertheless its signaling is attenuated, as shown by its blunted response upon DNA damage (Cicalese, Bonizzi et al. 2009). To investigate whether the up-regulation of Myc in ErbB2-tumor cells is a consequence of reduced p53 activity, we decided to analyze the effect of p53 reactivation on Myc levels, by *in vitro* administration of Nutlin-3. Nutlin-3 is a small molecule antagonist of Mdm2-p53 binding, that, preventing its degradation, stabilizes p53 and restores its levels in the cells (Vassilev 2004).

We first investigated the effective restoration of p53 function in Nutlin-treated tumor mammospheres, by measuring p53 response after Adriamycin administration, a known DNA damage agent inducing p53-dependent apoptosis (Wang, Konorev et al. 2004). The result confirms that when p53 is stabilized by Nutlin administration (2.5 or 10 μM) it re-gains its functional competences, as established by the increase in the levels of its phosphorylated and active form (phospho-S15) and up-regulation of its target p21 during the 4 to 8 hours exposure to doxorubicin (**Figure 4-4**).

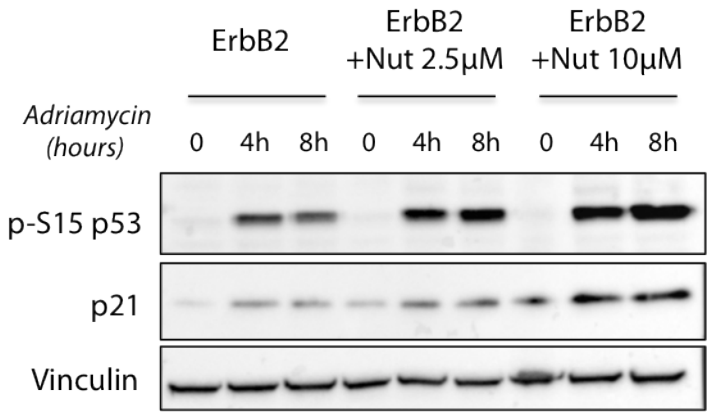

Figure 4-4: Nutlin-3 restores functional p53 signaling

ErbB2 tumor cells were plated and treated with Nutlin 2.5 or 10 μM for 16 hours and then administered with Adriamycin (0.5μM) for 4 or 8 hours, as indicated. Western blot analysis of the expression of phosphorylated form of p53 (phospho Serine 15) and p21. Vinculin used as loading control.

We then analyzed the levels of Myc in the ErbB2 tumor mammospheres, untreated or treated with Nutlin-3 for 72h. The results are reported in **Figure 4-5** and show that Myc mRNA is severely down-regulated, and its expression is brought back to the levels of WT mammospheres. Accordingly, Myc protein expression decreases upon Nutlin treatment of ~20%-30% of its levels, depending on the tumor under analysis (**Figure 4-6**).

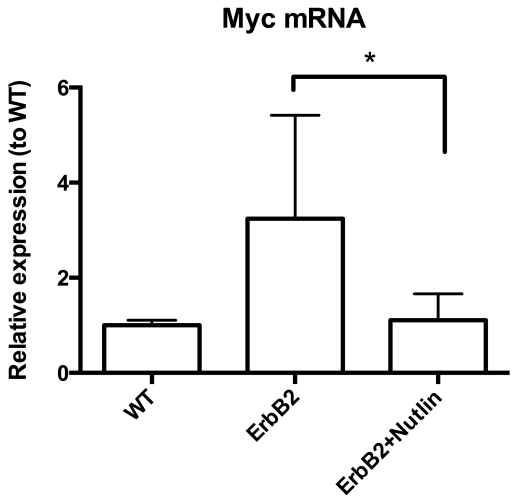

Figure 4-5: Effects of p53 restoration on Myc mRNA levels

Myc expression was assessed in WT (n=7), MMTV-ErbB2 tumor (n=3) and 3 corresponding ErbB2 tumors treated with Nutlin-3 (2.5µM) for 72h by qPCR analysis of Myc mRNA (means ± standard deviation). Values are expressed as fold change relative to WT samples. Myc expression was normalized against the GusB housekeeping gene. Significance of differences between treated and not-treated samples was calculated by paired t-test (*pvalue<0.05).

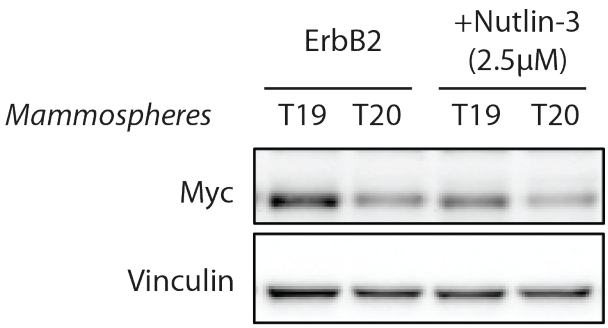

Figure 4-6: Effects of p53 restoration on Myc protein levels

Western blot analysis of the expression of Myc in two ErbB2 tumors grown as mammospheres. Cells were untreated or treated with Nutlin-3 (2.5µM) for 72h. Vinculin used as loading control.

To exclude p53-independent effects of Nutlin, we administered Nutlin to p53-/- derived mammospheres. No down regulation of Myc could be observed at any of the indicated timepoints after compound administration (**Figure 4-7**).

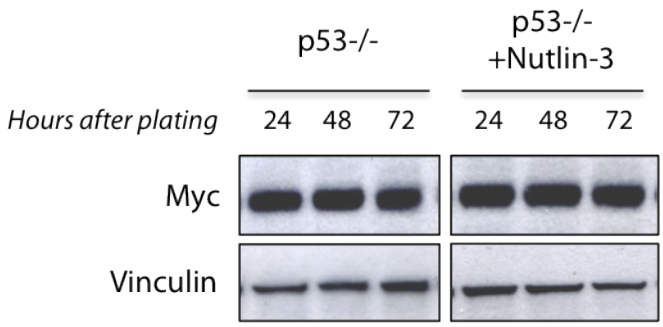

Figure 4-7: Nutlin administration has no effect on myc regulation in the absence of p53

P53-/- cells were plated as mammospheres in the presence or absence of Nutlin-3 (2.5μM). Cells were collected 24, 48 and 72 hours after plating and levels of Myc were evaluated by western blot analysis. Vinculin used as loading control.

4.1.3 Myc is a target of p53 also in non tumor contexts

To investigate whether p53 and Myc are epistatically linked independently of the tumor context, we analyzed levels of Myc expression in normal mammary cells, as a function of p53 expression and activation (p53+/- and -/- cells, Adriamycin treated WT cells, p53ER expression in p53-/- cells).

a) First, we evaluated Myc mRNA and protein levels in mammospheres derived from the mammary gland of p53+/- or p53-/- mice against levels in mammospheres from WT glands. Interestingly, while we observed a marked over-expression of Myc protein levels in the p53-/- mammospheres, levels in the p53+/- mammospheres

were approximately midway between those in p53 null and in WT spheres, suggesting that Myc abundance is strongly dependent on the levels of p53 (**Figure 4-8, right**). Again, Myc mRNA expression mirrored the protein levels (**Figure 4-8**, **left**).

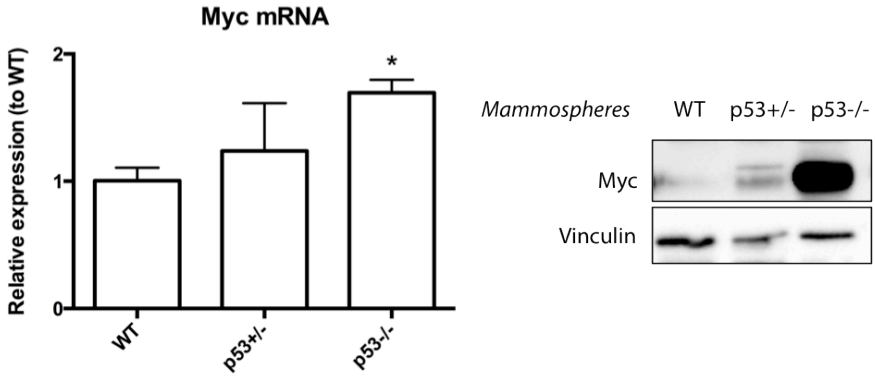

Figure 4-8: Myc levels depend on p53 abundance in normal mammary stem and progenitor cells

LEFT: Myc expression was assessed in WT (n=7), p53+/- (n=3) and p53-/- (n=4) mammospheres by qPCR analysis of Myc mRNA (means ± standard deviation). Values are expressed as fold change relative to WT samples. Myc expression was normalized against the GusB housekeeping gene. Significance of differences between samples and WT was calculated by t-test (*pvalue<0.05). RIGHT: representative western blot analysis of Myc protein in WT, p53+/- and p53-/- mammospheres. Vinculin used as loading control.

b) To exclude an indirect effect of p53 on Myc levels, possibly mediated by the high proliferating rate of p53-/- cells, we "acutely" activated p53 by DNA damage and evaluated the effect on Myc expression. WT, p53+/- and p53-/- mammospheres were treated with Adriamycin (0.5 μM) and cells were collected after 2, 4, 6 and 8 hours. The histogram in **Figure 4-9** depicts the levels of Myc expression as measured by qPCR. Myc mRNA appears progressively down-regulated in the presence of a functional p53 (both in WT and in p53+/- mammospheres), while in the p53-/- mammospheres it is not perturbed at any of the timepoints. The western blot in **Figure 4-10**, however, shows that, levels of the Myc protein in WT

mammospheres are only slightly down-regulated, despite strong p53 activation and up-regulation of p53-transcriptional targets (**Figure 4-10**, right).

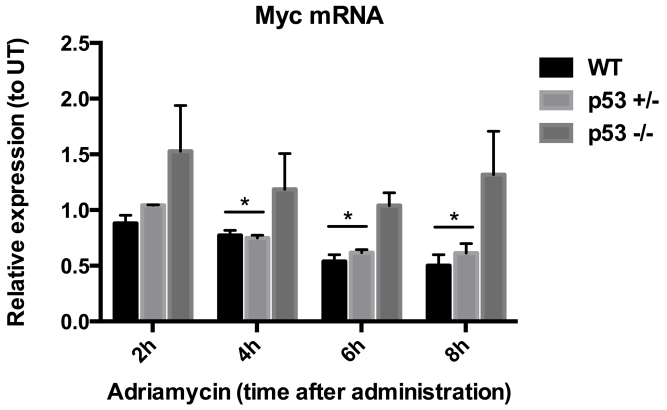

Figure 4-9: Effects of p53 acute stimulation on Myc mRNA levels

Myc expression was assessed by qPCR analysis of Myc mRNA in WT, p53+/- and p53-/- mammospheres treated with Adriamycin (0.5μM) for the indicated time points (means ± standard deviation of three independent experiments). Values are expressed as fold change relative to untreated (UT) samples of each cell-type. Myc expression was normalized against the GusB housekeeping gene. Significance of differences between treated and not-treated samples was calculated by t-test (*pvalue<0.05).

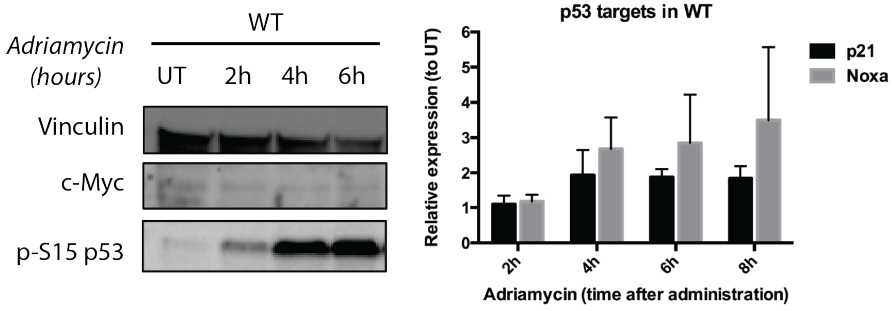

Figure 4-10: Effects of acute stimulation of p53 on Myc protein expression

LEFT: Western blot analysis of the expression of Myc and the phosphorylated form of p53 (phospho Serine 15) in WT mammospheres upon Adriamycin treatment (0.5μM) for the indicated times. Vinculin used as loading control. RIGHT: qPCR analysis of selected targets of p53 activation (p21 and Noxa genes). Values are expressed as average fold change relative to untreated (UT) sample, error bars indicate standard deviation of three biological replica.

Likely, the degree of down-regulation of Myc is not fully appreciable given the basal low levels of the Myc protein in WT cells. However, when we performed the same experiment in p53+/- mammospheres, which harbor one functional allele of p53 and higher basal levels of Myc, we observed a more evident down-regulation of Myc upon DNA damage, as opposed to the absent regulation of Myc levels in the p53-/- cells (**Figure 4-11**). As further evidence, we performed the same Adriamycin treatment on NMuMG cells, a murine breast immortalized line, and again we noticed a striking down-regulation of Myc expression in response to p53 acute activation (**Figure 4-12**).

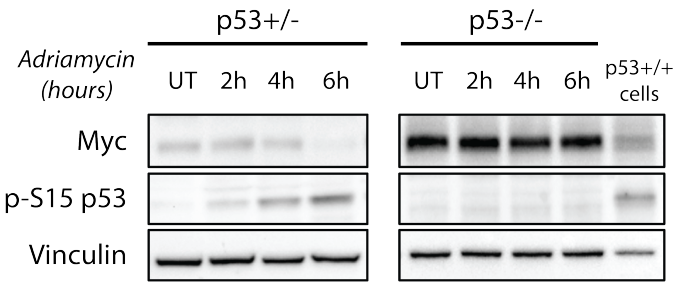

Figure 4-11: Effects of acute stimulation of p53 by DNA damage in p53+/- and p53-/- mammospheres

Western blot analysis of the expression of Myc and the phosphorylated form of p53 (phospho Serine 15) in p53+/- and p53-/- mammospheres upon Adriamycin treatment (0.5μM) for the indicated times. Vinculin used as loading control. P53+/+ ESCs are loaded as positive control for the p53 band.

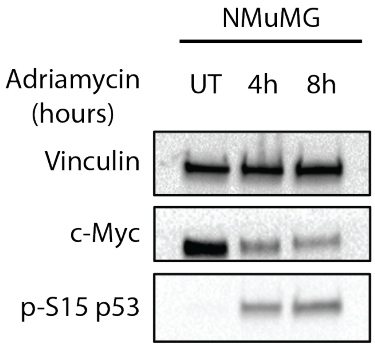

Figure 4-12: Effects of acute stimulation of p53 by DNA damage in NMUMG cells.

Western blot analysis of the expression of Myc and phosphorylated form of p53 (phospho Serine 15) in NMUMG cell line upon Adriamycin treatment (0.5μM) for the indicated times. Vinculin used as loading control.

c) Finally, taking advantage of a retroviral expression vector (pBABE-puro) harboring an inducible p53-ER sequence, we re-expressed p53 in p53-/- mammospheres by 4-OHT administration (200nM). The effectiveness of restoration is demonstrated by the up-regulation of p53 transcriptional targets p21 and Bax as shown in the qPCR in **Figure 4-13**, left. Through this last approach, we could also observe acute down-regulation of both Myc protein and RNA levels at all of the time-points following 4-OHT treatment (**Figure 4-13**, left and right).

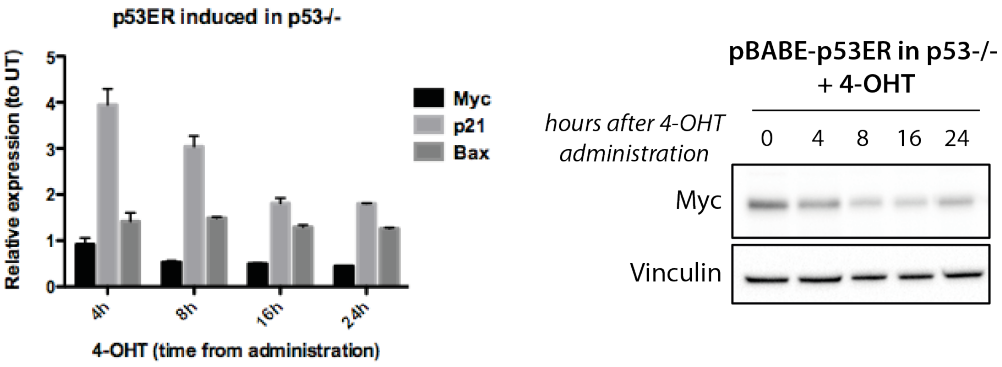

Figure 4-13: Effects of re-expression of p53 in p53-/- mammospheres

LEFT: qPCR analysis of Myc mRNA in p53-/- cells transduced with pBABE-puro-p53ER vector and treated with 4-OHT (200μM) for the indicated times. Values are expressed as average fold change relative to untreated (UT) sample, bars indicate standard deviation of three biological replica. RIGHT: Western blot analysis of the expression of Myc in WT mammospheres upon 4-OHT treatment at the indicated time points. Vinculin used as loading control.

All together these data suggest that a functional p53, either directly or indirectly, imposes a control over the levels of Myc mRNA and protein. When p53 is absent, as in the knock-out murine model, or dysfunctional, as in our ErbB2 tumour model, this control is lost and Myc levels are de-regulated, and this, in turn, could be the causative mechanism that leads to the unlimited growth described in the mammosphere assay (Cicalese, Bonizzi et al. 2009).

Notably, WT mammospheres down-regulate Myc during their growth (in a 5-days culture, from single cells to formed mammospheres), and exit the cell cycle (**Figure 4-14**). In the erbB2 tumor spheres, instead, Myc expression remains stable during the culture; cells do not exit the cell cycle and continue to proliferate (**Figure 4-14**). Therefore, the extended replicative potential of tumor spheres might be the consequence of both Myc over-expression and de-regulation.

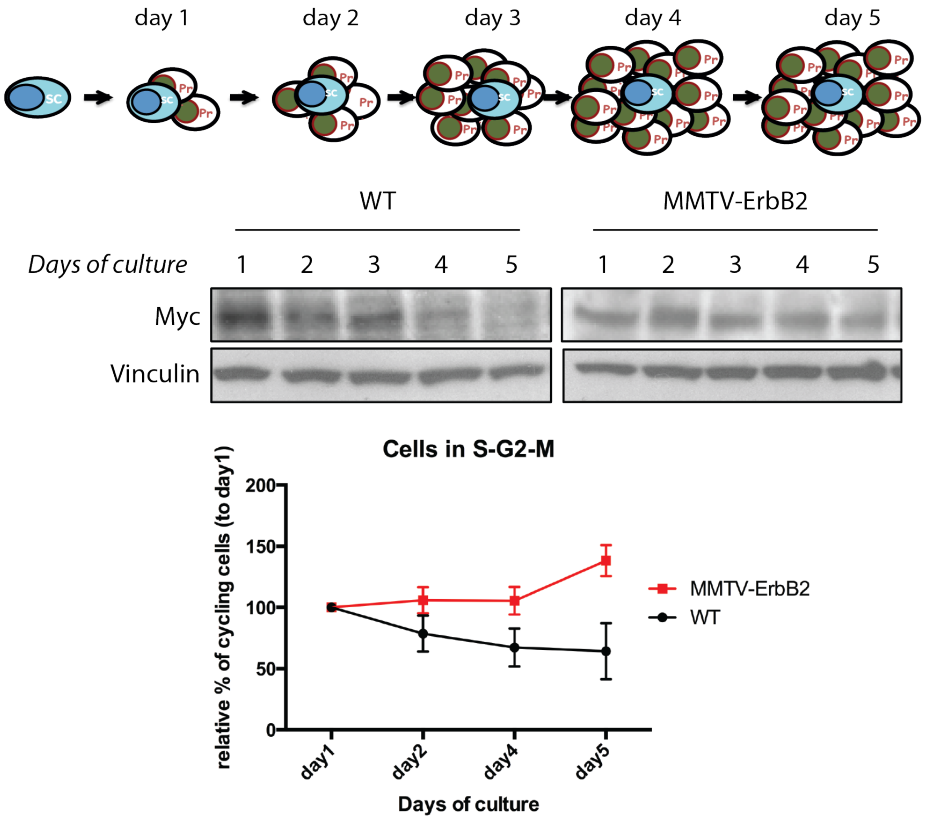

Figure 4-14: Myc is de-regulated in ErbB2 tumors

TOP: schematic representation of mammosphere growth over the days of culture. Mammospheres are used a surrogate of an organ development (the mammary gland) and originate from a single cell that gives rise to more differentiated progenitors. MIDDLE: Western blot analysis of the expression of Myc in WT and ErbB2 mammospheres during their formation. Vinculin used as loading control. BOTTOM: Cell cycle analysis of mammospheres at the indicated time points (BrDU coupled with PI staining). Cycling cells are defined as cells positive for BrDU (S-phase) and with 2n DNA content (G2/M). Values are calculated as percentage of cycling cells on day1 (mean ± standard deviation of three independent experiments).

4.1.4 The Myc transcriptional program is activated in ErbB2-tumor cells and depends on levels of p53

We then investigated whether Myc overexpression in ErbB2 mammary cells correlates with its transcriptional activity. Since the transcriptional program of Myc is cell-context and cell-state dependent (Littlewood, Kreuzaler et al. 2012, Tansey 2014), we first defined

the transcriptional effects of Myc in mammary epithelial cells. To this end, we performed RNAseq analyses of WT mammospheres transduced with a lentiviral vector expressing the inducible MycER fusion protein (fusion of human Myc with a modified version of the estrogen receptor), grown in the absence of the 4-OHT ligand (Littlewood, Hancock et al. 1995). Under these conditions, MycER is expressed at moderate levels in the nucleus of mammary cells and induces their immortalization [(Pasi, Dereli-Oz et al. 2011) and see next section].

Comparison of the normalized-reads-count *per* gene between MycER cells and control cells (transduced with the corresponding empty vector) led to the identification of 5,618 differentially regulated genes (cut-off on the q-value: lower or equal to 0.01) out of the around 13,000 genes expressed in our system. Of them, 3,023 genes are up-regulated compared to the empty vector-expressing cells and 2,595 genes result down-regulated.

To investigate whether the Myc transcriptional-program is activated in the ErbB2 mammary cancer-cells, we performed Gene Set Enrichment Analysis (GSEA) (Subramanian, Tamayo et al. 2005) of the MycER dataset in ErbB2 cells.

We first generated RNAseq datasets of three independent ErbB2 tumors in mammosphere cultures, and calculated the ratio of the mean of their normalized reads to that of WT mammospheres (n=3). A total of 2,460 genes resulted differentially expressed in tumors compared to WT cells. We then created two separate lists for the up-regulated (ErbB2-UP 1,162 genes) and the down-regulated (ErbB2-DOWN 1,298 genes) and aligned those to the ranked list of Myc transcriptional targets.

In the Gene Set Enrichment analyses, each gene set is ordered according to the regulation of a query dataset from the most up-regulated to the most down-regulated genes. If the gene set under analysis is not correlated with the query dataset, genes will be distributed randomly in the query dataset. Conversely, if the two datasets are correlated (positively or

negatively), the distribution will be asymmetric. GSEA computes the overlap between the gene sets mathematically, returning a normalized enrichment score (NES), which expresses the overlap within the two signatures, and a FDR (or q-value) as measure of statistical significance. We performed the GSEA analysis distinguishing each cell-type specific signature in UP and DOWN regulated genes that were then ranked according to their regulation in the MycER dataset.

GSEA analysis of ErbB2 and MycER datasets showed impressive correlation between the up-regulated genes in ErbB2 tumors and the core of genes that are up-regulated in WT cells by the presence of MycER; a similar correlation is also observed between ErbB2 tumor down-regulated genes and the genes that localize towards the bottom side (more down-regulated) of the ranked MycER list of target genes (Normalized Enrichment Score, NES = 4.9 and -4.6, respectively) (**Figure 4-15**).

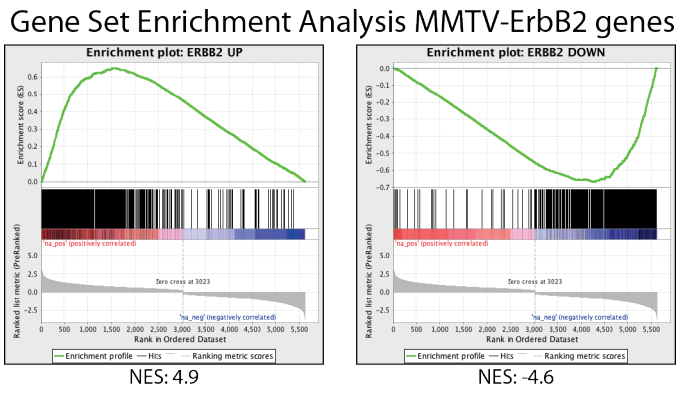

Figure 4-15: MycER signature in MMTV-ErbB2 tumors

Gene set enrichment analysis was performed to correlate the tumor (ErbB2-driven) transcriptional program with gene expression changes upon MycER infection (5,618 genes). The normalized enrichment score (NES) is shown and significance (FDR, qvalue) was reported to be approximately equal to 0.

We then asked whether the Myc transcriptional-program is dependent on p53 function. To do so, we analyzed the enrichment of the MycER program in p53-/- mammospheres. We performed RNAseq analyses of WT (n=3) and p53-/- (n=3) mammospheres and generated lists of p53ko-UP and p53ko-DOWN using the same cut-off criteria described for the previous RNAseq datasets (5,192 differentially regulated genes: 2,462 UP; 2730 DOWN). Once run on the GSEA software, we observed high enrichment of the MycER signature in the p53null genetic context, similarly to that of our tumor model (**Figure 4-16**), suggesting that a vast part of Myc activity is enhanced in the absence or impairment of p53. These findings further confirm that Myc de-regulation in tumors can be widely attributed to the missing functionality of p53 signaling.

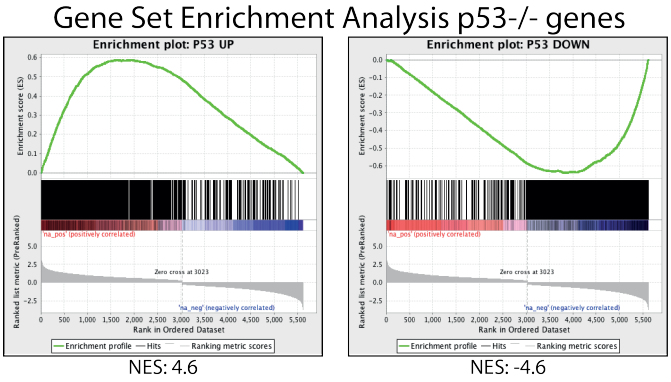

Figure 4-16: MycER signature in p53-/- cells

Gene set enrichment analysis was performed to correlate the p53-/- transcriptional program with gene expression changes upon MycER infection (5,618 genes). The normalized enrichment score (NES) is shown and significance (FDR qvalue) was reported to be approximately equal to 0

Finally, to address this point directly, we investigated whether the Myc-transcriptional program in the ErB2 cells depends on p53. To this end, we performed RNAseq analyses of ErbB2 cells treated, or not, with Nutlin-3 (n = 3 independent tumors). In this case, the UP

and DOWN lists of genes were obtained by calculating the paired ratio of gene expression and then the GSEA analysis was performed with the same cut-off criteria described earlier. Strikingly, when we ran the Nutlin-UP and DOWN lists on the GSEA software, we observed an enrichment curve profile completely opposite to that of the ErbB2 tumor. Indeed, the up-regulated side of the ranked list appears enriched for the "DOWN-list" and vice versa for the down-regulated side, thus demonstrating that the restoration of p53 induces a transcriptional response that completely reverts the MycER-dependent activity in ErbB2 tumors (**Figure 4-17**).

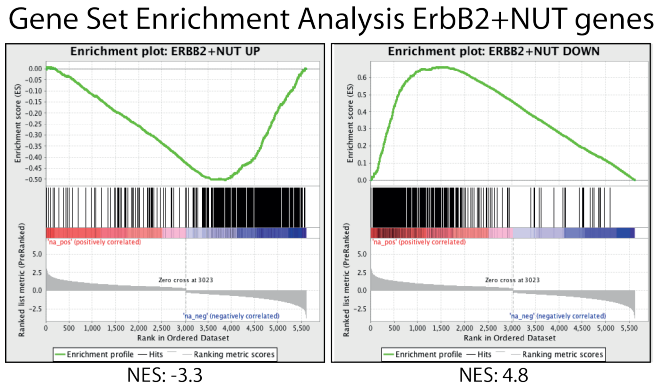

Figure 4-17: MycER signature in MMTV-ErbB2 tumors treated with Nutlin-3.

Gene set enrichment analysis was performed to correlate the transcriptional program of ErbB2 tumors treated with Nutlin-3 (2.5μM) with gene expression changes upon MycER infection (5,618 genes). The normalized enrichment score (NES) is shown and significance (FDR, qvalue) was reported to be approximately equal to 0.

Collectively these data demonstrate that Myc transcriptional activity is enhanced in the ErbB2 cancer cells, thus mirroring the data of its overexpression, and that, in mammary cells, it is strongly dependent on the levels of a functional p53.

All together, we have shown that p53 and Myc are epistatically related and that the loss of p53 has remarkable effects on the de-regulation of Myc levels in cell populations enriched for mammary SCs and breast CSC.

4.2 De-regulated Myc extends the life span and proliferative potential of mammary stem and progenitor cells

4.2.1 Transgenic R26-MycER mice as a tool to induce de-regulation of Myc levels

It emerges from our data that the de-regulation of Myc levels due to loss of p53 has important implications for mammosphere growth in culture. To define the effects of this de-regulation on mammary epithelial cells, we took advantage of a murine model harboring an inducible Myc-ER^{T2} allele within the *Rosa26* locus, whose translocation into the nucleus can be finely tuned by the administration of 4-OHT (Murphy, Junttila et al. 2008).

Mammary glands derived from these animals were collected and digested enzymatically in order to obtain single cell suspensions. Cells were then plated for mammosphere culture and dosage-dependent effects of 4-OHT evaluated in terms of proliferation potential and sphere forming ability. Specifically, the cells were plated at a clonal density of 20,000 cells/ml in 6 well plates and serially passaged in the presence or absence of 4-OHT. At each passage, we enumerated the spheres, disaggregated them, and counted the total number of cells, in order to measure their replicative potential (*i.e.*, cells/sphere). The data were then arranged into cumulative growth curves showing the variation in the number of mammospheres and cells during passages. As shown in **Figure 4-18** bulk mammospheres not treated with 4-OHT progressively decrease in number, exhaust in culture after 6-7 passages and cannot be further propagated, confirming that WT SCs have limited lifespan and self-renewing potential, as previously shown by our group (Cicalese, Bonizzi et al. 2009). Immunofluorescence analysis demonstrated that basal levels of nuclear Myc in

heterozygous Rosa26-MycER derived mammospheres were comparable to those of WT mammospheres, while when 4-OHT was administered, a bright nuclear signal could be detected, thus indicating that the fine-tuning of the inducible system is tightly controlled **Figure 4-19**. As previously observed in other cellular systems, different levels of Myc expression (e.g. different doses of 4-OHT) elicit different biological effects (Murphy, Junttila et al. 2008). When 500 nM or 1 μM 4-OHT was administered, mammospheres derived from heterozygous Rosa26-MycER mice rapidly faced self-exhaustion (**Figure 4-18**) due to Myc-dependent apoptotic cellular death (**Figure 4-20**). The same treatment did not induce cell death of spheres derived from mice of the same colony but negative for the presence of the transgene (from here on called Rosa26-MycER WT) (**Figure 4-20**). Intriguingly, when the sphere cultures were exposed to lower doses of 4-OHT (20 nM or 200 nM), they exhibited a remarkable increase in their self-renewing potential. Indeed, the cumulative sphere number approximated an exponential curve (R^2= 0.95 and 0.99 respectively) with a growth rate going from 121% for the 20 nM dose to 161% for the 200 nM (**Figure 4-18**), and the spheres could be passaged indefinitely (data not shown). Strikingly, this behavior of Myc-ER mammospheres was undistinguishable from that of p53 KO or ErbB2-tumor mammospheres (Cicalese, Bonizzi et al. 2009).

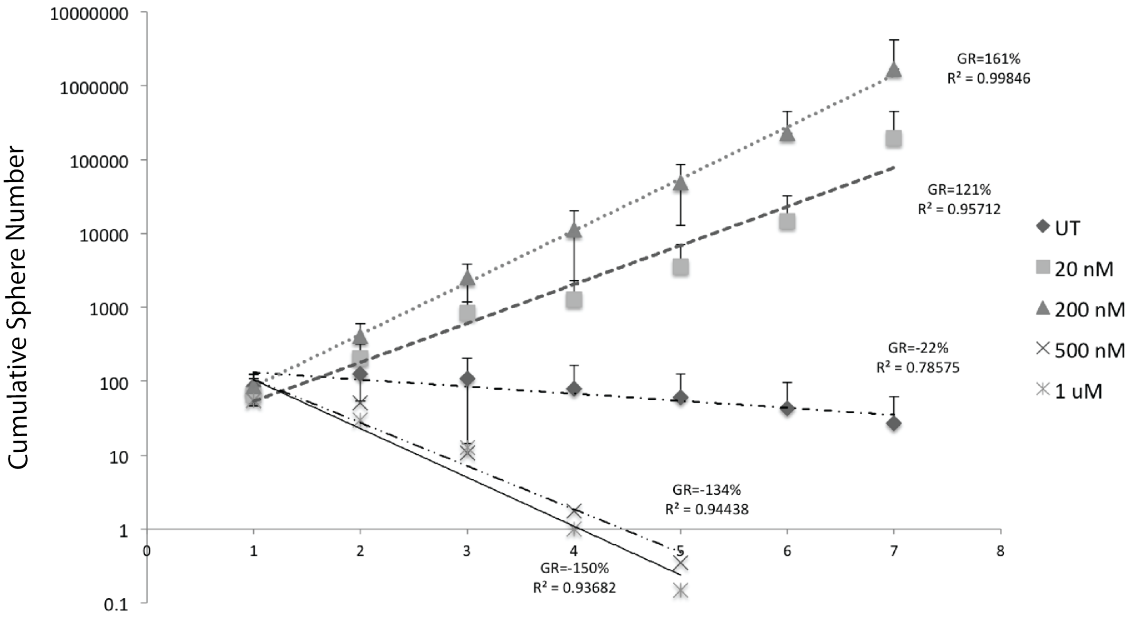

Figure 4-18: Growth curve of Rosa26-MycER mammospheres.

Semi-logarithmic plot of Cumulative Sphere numbers. Numbers were obtained from serial replating of Rosa26-MycER mammospheres in the absence or continuous presence of different concentrations of 4-OHT. Each dot in the curve represents the mean of six independent curves; error bars indicate the standard deviation. Regression analysis was performed to obtain trend lines (dashed lines) that best approximate the curves. Growth rates (GR) and coefficients of determination (R^2) for each trend line are reported inside the graph.

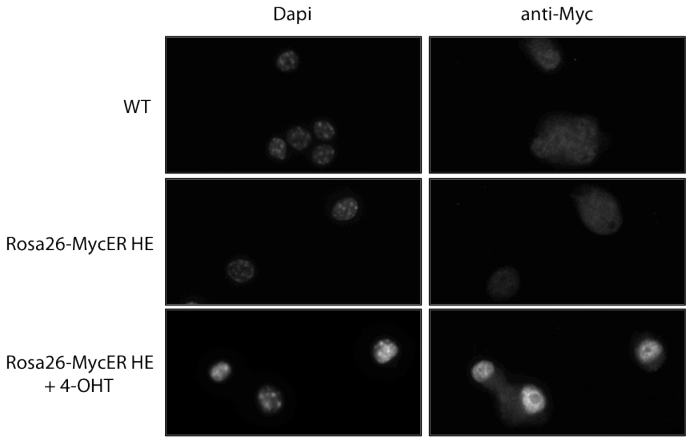

Figure 4-19: Myc translocation is inducible upon 4-OHT administration.

Immunofluorescence analysis of Myc expression with a Myc-specific antibody in WT and Rosa26-MycER heterozygous (HE) untreated or treated with 4-OHT (200 μM). Nuclei were counter-stained with Dapi (right panels).

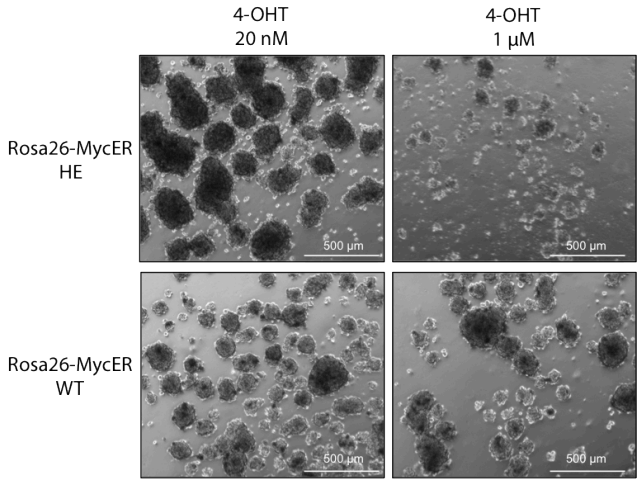

Figure 4-20: Morphology of mammospheres treated with different doses of 4-OHT.

Representative images of spheres derived from Rosa26-MycER mice heterozygous (top) or WT (bottom) for the transgenic allele. Both cultures were exposed to the lowest and highest dose of 4-OHT tested (20nM and 1µM) and pictures were taken at the third passage of the serial replating assay. Scale bar as represented.

Furthermore, compared to the untreated control, a dramatic increase in the total number of cells and in mammosphere size (number of cells per sphere) was observed upon low doses of 4-OHT, suggesting that treated Rosa26-MycER mammospheres also possess increased replicative potential (**Figure 4-20** and **Figure 4-21**). As shown in other systems (Reavie, Della Gatta et al. 2010), these observations indicate that tight regulation of Myc protein expression is critical in the control of numbers of mammary stem and progenitor cells.

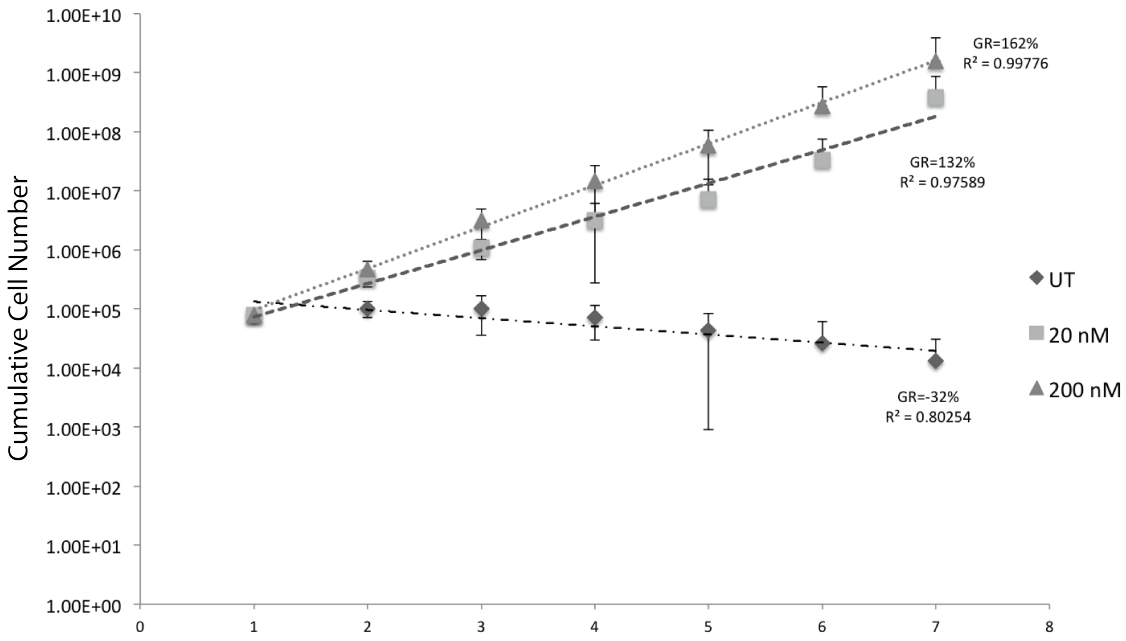

Figure 4-21: Growth curve of Rosa26-MycER cells grown as mammospheres.

Semi-logarithmic plot of Cumulative Cell number. Numbers were obtained from serial replating of Rosa26-MycER mammospheres in the absence or continuous presence of the two lowest doses of 4-OHT. Each dot in the curve represents the mean of six independent curves; error bars indicate the standard deviation. Regression analysis was performed to obtain trend lines (dashed lines) that best approximate the curves. Growth rates (GR) and coefficients of determination (R^2) for each trend line are reported inside the graph.

4.2.2 Low levels of Myc expand the mammary stem cell pool and are able to reconstitute the mammary gland in transplantation assays, without inducing transformation

The above results show that the continuous presence of low levels of myc is able to confer increased self-renewal and replicative potential to mammary stem cells and progenitors. We then decided to investigate the consequences of these effects on the development of the mammary gland *in vivo*. To this end, we planned transplantation experiments of our

Rosa26-MycER mammospheres in the cleared fat pad of recipient mice fed with a 4-OHT-containing diet.

Tamoxifen is an ER antagonist that is used in the treatment of ER positive breast cancer (Mouridsen, Palshof et al. 1978). Given that estrogen and its receptor have essential roles in mammary gland development, we first investigated the effects of continuous tamoxifen treatment on ductal development and function. Indeed, it was reported that acute doses of tamoxifen change the distribution of mammary epithelial populations (Shehata, van Amerongen et al. 2014), and severely affect mammary gland development when administered at puberty (3 administrations at 1.5mg; 1 administration at 2.5mg; (Rios, Fu et al. 2014)). We fed adult control mice (same genetic background of the Rosa26-MycER mice) with 4-OHT-containing food continuously for 2 weeks (40mg/kg, around 1mg per mouse every 3-4 days), and evaluated the distribution of mammary cell types using known surface markers (EpCAM; CD49f; CD61) (Guo, Keckesova et al. 2012). As shown in **Figure 4-22**, the effect of a Tamoxifen diet on the distribution of mammary progenitor populations is remarkable and leads to a significant decrease in the most differentiated population of luminal cells, and to a strong and unexpected increase in the percentage of basal (SC-enriched) cells, thus suggesting an impairment in the terminal differentiation of the treated glands. Also, when mice were treated at puberty (21 days after birth), we observed a dramatic decrease in the lin- EpCAM positive cells, hinting to potential disruption of mammary gland development, as previously shown (Rios, Fu et al. 2014).

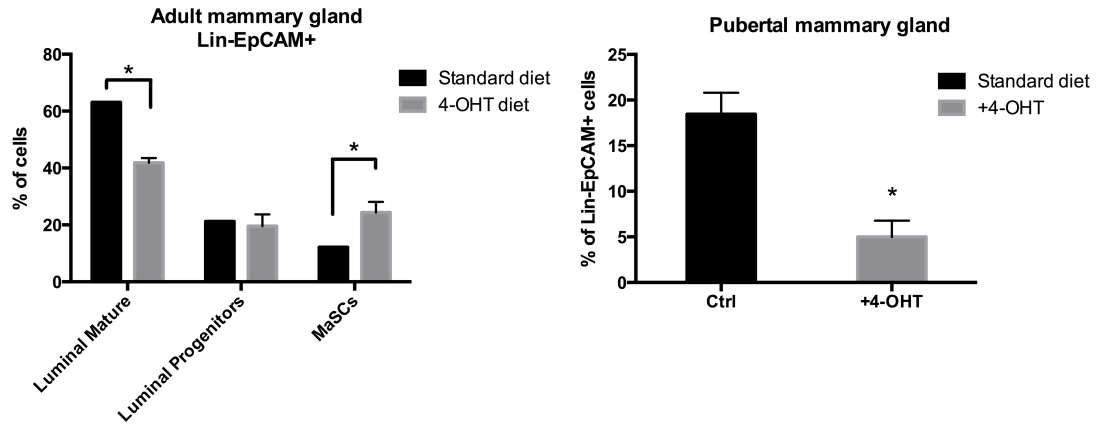

Figure 4-22: *In vivo* administration of 4-OHT in control adult or pubertal mice.

8 weeks or 3 weeks old mice were fed for two weeks with 4-OHT containing-food or with standard diet; mammary glands were then collected, single cells were stained for surface markers and their intensity was assessed by FACS. LEFT: percentage of Luminal Mature (EpCAM+/CD49f-/CD61-), Luminal Progenitor (EpCAM+/Cd49f-/CD61+) and Mammary stem cells (MaSC - EpCAM+/Cd49f+/CD61+) within the Lin-(CD31-/Ter119-/CD45-)/EpCAM+ cell population derived from the mammary glands of 8 week old mice. Values are shown as the mean of the relative percentage of each population from three independent mice treated with 4-OHT food and from two mice on standard diet; error bars indicate the standard deviation; significance of differences between the two experimental groups was calculated by t-test (*pvalue <0.05). RIGHT: percentage of Lin-/EpCAM+ cells in total mammary cell populations from 3-week-old mice. Values are shown as the mean of the relative percentage of each population from three independent mice treated with 4-OHT food and from two mice on standard diet; error bars represent the standard deviation; significance of differences between the two experimental groups was calculated by t-test (*pvalue <0.05).

As an alternative to the continuous administration of 4-OHT, we decided to use the lentiviral vector mentioned in section 4.1.4 (Littlewood, Hancock et al. 1995). Our group demonstrated that WT mammospheres transduced with the aforementioned vector undergo a severe p53-dependent apoptotic response upon induction with 4-OHT (Pasi, Dereli-Oz et al. 2011). Conversely, if cultured in the absence of 4-OHT, MycER infected cells become immortalized, expand unlimitedly in culture, and form larger mammospheres, suggesting that they possess increased self-renewal and replicative potential (Pasi, Dereli-Oz et al. 2011). This behavior is identical to that observed for the Rosa26-MycER spheres at low

doses of 4-OHT, suggesting that it could be due to a leakage in the Myc-ER infected cells of the ER conditional system. Immunofluorescence analysis of Myc nuclear translocation revealed, indeed, that while basal levels of Myc are almost undetectable, upon infection with the MycER vector a slightly higher nuclear signal could be detected also in the non-4-OHT treated mammospheres (**Figure 4-23**). Real time PCR (qPCR) of three Myc targets (Nucleolin; ODC1 and CAD) revealed upregulation of their expression upon MycER mammosphere infection, in the absence of 4-OHT induction, as compared to the control mammospheres transduced with the empty-vector (**Figure 4-24**). Likewise, qPCR showed that endogenous Myc expression is down regulated as expected by the auto regulatory loop that Myc exerts on its own promoter (**Figure 4-24**).

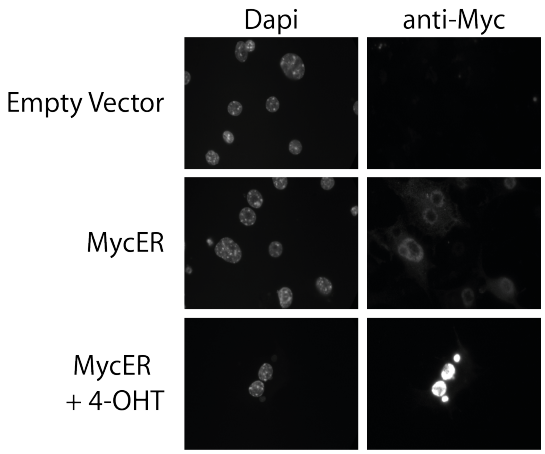

Figure 4-23: Immunofluorescence staining for Myc expression in control or 4-OHT untreated or treated MycER infected cells.

Staining of single cell suspensions from secondary WT mammospheres transduced with an empty vector (top) or MycER, in the absence (middle) or presence of 4-OHT (200 μM, bottom) for 72 hours, with a Myc specific antibody. Nuclei were counter-stained with Dapi (right panels).

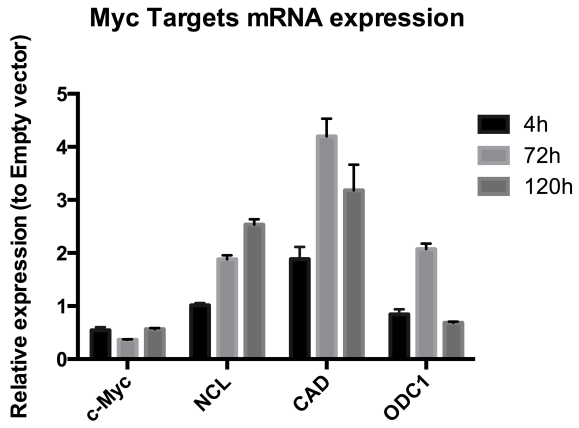

Figure 4-24: Myc targets are up-regulated in cells transduced with MycER in the absence of any 4-OHT stimulus.

RT qPCR of selected targets of Myc was performed in WT mammospheres transduced with Empty or MycER vectors and cultured for the indicated time points (means ± standard deviation of two biological replicas). Values are expressed as fold change relative to the empty vector expression (Empty vector = 1). Each gene expression was normalized against the GusB housekeeping gene.

Interestingly, the extent of regulation of the Myc targets was comparable to that observed in the Rosa26MER mammospheres upon 72h of low doses 4-OHT treatment (**Figure 4-25**). Therefore, we concluded that, prior to any 4-OHT induction, the lentiviral construct recapitulates what we saw in the inducible R26-MycER murine model, demonstrating that it represents a suitable system as a substitute for the Tamoxifen *in vivo* treatment experiments.

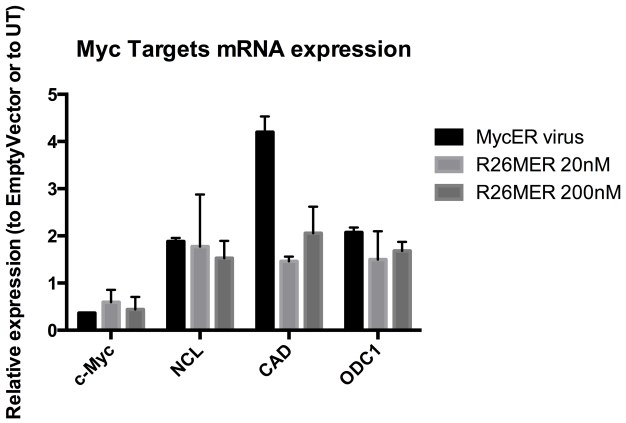

Figure 4-25: Myc transcriptional activity upon MycER infection is enhanced to the same extent to what observed for Rosa26-MycER mammospheres upon low doses of 4-OHT stimulation.

RT qPCR of selected targets of Myc was performed in WT mammospheres transduced with Empty or MycER vectors and cultured for 72 hours (means ± standard deviation of two biological replica) and in Rosa26-MycER mammospheres upon 72 hours induction by 4-OHT at the indicated doses (means ± standard deviation of five biological replica). Values are expressed as fold change relative to Empty vector expression or untreated cells (both = 1). Each gene expression was normalized against the GusB housekeeping gene.

Thus, we moved to an *in vivo* setting using Myc-ER infected mammospheres. To investigate whether continuous presence of low levels of Myc leads, *in vivo*, to an increase in mammary stem cell content, we performed limiting dilution transplantation experiments of the mammospheres transduced either with the MycER vector or with the corresponding empty vector in the cleared fat pad of three-weeks old virgin recipients. As shown in **Table 4-1**, MycER infected cells are able to give rise to positive outgrowths when as little as 100 cells were transplanted, unlike the empty vector transduced cells. These data suggest that low levels of Myc expression lead to an expansion of the pool of stem cells *in vivo*.

Cell Dose	**Empty Vector**	**MycER**
500	2/7	3/6
100	0/7	4/7
Frequency of repopulating units (95% confidence limit)	**1 : 1839 (7284-464)**	**1 : 368 (850-159)**
Overall test for differences in SC frequencies between the groups	**pvalue = 0.0273**	

Table 4-1: Limiting dilution transplantation experiment on mammospheres transduced with Empty vector or MycER.

Cells suspension from WT mammospheres infected with Empty or MycER vectors were inoculated in recipient mice in limiting dilution conditions (500 and 100 cells). Results show the number of positive outgrowths as defined by the presence of epithelial structures with radial organization in stained whole mounts 12 weeks after the injection. SC frequencies (estimates and upper/lower limits) were calculated by limiting dilution analysis, as described in the Materials and Methods section. The significance of the difference in SC frequency is indicated by the p-value (<0.05).

We then investigated whether low-levels of Myc expression initiates tumorigenesis in vivo. To address this question, we transplanted a total of 15 mice and kept them under observation for tumor formation for up to 1 year. Notably, no palpable masses could be detected in our cohort of mice and analysis of the outgrowths after whole mount staining showed that the morphology of the epithelial tree was not altered (**Figure 4-26)**. Taken together these data demonstrate that low levels of Myc expression induce expansion of SC numbers in vivo, without initiating the transformation process.

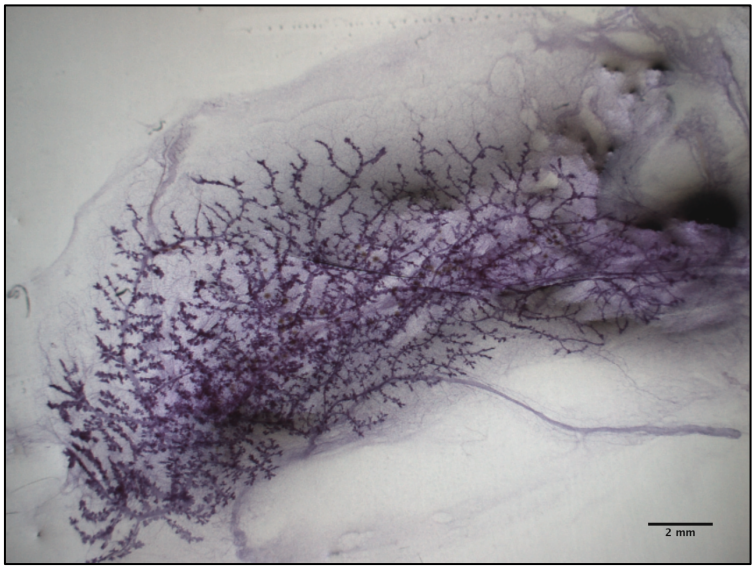

Figure 4-26: Whole mount staining of a positive outgrowth resulting from the injection of MycER expressing cells.

Representative image of carmine alum whole mount staining of a reconstituted gland after injection of 100 MycER transduced cells. Scale bar as indicated.

4.3 De-regulation of Myc expression increases numbers of mammary SCs by a dual mechanism

The results described in the previous chapters showed Myc to be a downstream target of p53 in mammary stem and progenitor cells: at the molecular level we observed a negative interplay that is dependent on p53 function, with Myc being constitutively expressed in the absence of p53. Accordingly, we saw that constitutive Myc expression phenocopies the biological effects of p53-loss, e.g. expansion in number of SCs, both in vitro and in vivo. We then investigated the biological mechanisms underlying the effects of Myc on SC numbers, starting from those documented for p53-loss.

It has been shown that p53 acts as a master regulator of homeostasis within several tissues, by controlling the size of the SC pool (Bieging, Mello et al. 2014). The effects of p53 on SCs are to ensure the correct balances between quiescence *versus* proliferation (Liu, Elf et al. 2009) and asymmetric *versus* symmetric self-renewing divisions (Cicalese, Bonizzi et al. 2009). Both functions are considered part of its well-known role as a tumor suppressor in cells, as the increase in the rate of SC symmetric division is thought to be one of the causes of the formation of a malignant clone (Morrison and Kimble 2006). P53 was also shown to affect numbers of SCs indirectly, by inhibiting reprogramming of more differentiated population into SCs. This was shown both in the context of iPS generation (Hong, Takahashi et al. 2009) and in physiological conditions (Tschaharganeh, Xue et al. 2014); our group's unpublished data). This is also very relevant for the tumor suppressive function of p53, as de-differentiation and developmental plasticity, particularly in epithelial tissues, were demonstrated to be key mechanisms supporting cancer growth (Mani, Guo et al. 2008).

Notably, we have previously reported that constitutive expression of low levels of Myc (those ensured through the "leaky" MycER vector) is able to skew the modality of division of mammary SCs towards symmetry, as demonstrated by the segregation of the cell-fate determinant Numb and time-lapse analysis of SC first mitotic events (Pasi et al. unpublished results). Furthermore, low levels of Myc also conferred mammosphere replating ability to progenitors in culture, suggesting that Myc confers self-renewal properties to progenitors (Pasi, Dereli-Oz et al. 2011). Thus, we investigated whether Myc induces reprogramming of mammary progenitors into SCs, using the Rosa26-MycER murine model (for *in vitro* assays) and the aforementioned MycER lentiviral construct (for *in vivo* assays).

4.3.1 Effect of Myc on the ability of mammary progenitors to form spheres

To separate the effects of enforced expression of Myc on SCs or progenitors, we purified these two populations, taking advantage of the PKH26 assay developed in our laboratory (Cicalese, Bonizzi et al. 2009, Pece, Tosoni et al. 2010). PKH26 is a lipophilic dye that binds the cell membrane and segregates in daughter cells after each cell division, such that the intensity of staining inversely correlates with the number of undergone cell divisions (Lanzkron, Collector et al. 1999). This method exploits one of the well-accepted properties of adult SCs, that is, their being mostly dormant (quiescence). By this assay, cell suspensions obtained from mammosphere cultures are separated in at least two subsets, among which only those retaining the dye (top 1.5% most brilliant; PKHhigh) contain SCs, while those where the intensity of the dye appears most diluted (bottom 25%; PKHneg) comprise lineage-restricted cells, as demonstrated by limiting dilution transplantation (Cicalese, Bonizzi et al. 2009).

PKH negative cells consist of a heterogeneous population of cells that has gone through multiple rounds of division. These actively cycling cells were previously characterized as mono-potent progenitors, able to give rise to either epithelial or, rarely, myoepithelial colonies, in 2D-differentiation matrigel assays and unable to form mammospheres upon serial replating (Pece, Tosoni et al. 2010) or a mammary gland upon transplantation (Cicalese, Bonizzi et al. 2009). Notably, PKHneg cells, as compared to PKHhigh, do not express many genes specific for the mammary SCs (Lim, Wu et al. 2010, Soady, Kendrick et al. 2015), including CD24, epcam, jag1, dll1, Apoe, Id4, Erg, Krt5, Krt14, grik3, Ift57, Ltbp2, Mllt3, Nfatc2, Ngfr, Ppp1r14a, scube3, Stk39, Tm6sf1, cdh5, Pdgfb, Ptprb, Ptprz1 (data not shown; obtained from RNAseq analyses of PKHhigh and PKHneg from WT mammosphere cultures).

To investigate if Myc can confer SC-like behavior onto more differentiated progenitors we employed the Rosa26-MycER transgenic model. Therefore, we sorted the population that had not retained the PKH26 dye after one week of labeling and plated the cells in anchorage independent conditions in order to favor mammosphere formation (**Figure 4-27**). As expected, PKHneg cells not treated with 4-OHT rapidly exhausted after few passages (GR=-73.7%), thus confirming that they consist of short living progenitors with limited self-renewal capacity. On the contrary, PKHneg cells treated with low-dose 4-OHT indefinitely extend their replating potential, thus implying the acquisition of unlimited self-renewal potential (**Figure 4-28**). This was mirrored, as previously observed for the bulk mammosphere culture, by an increase in the size and cumulative cell number of 4-OHT-treated spheres, as compared to the untreated cells (UT), which indicates acquisition of greater replicative potential (**Figure 4-29**).

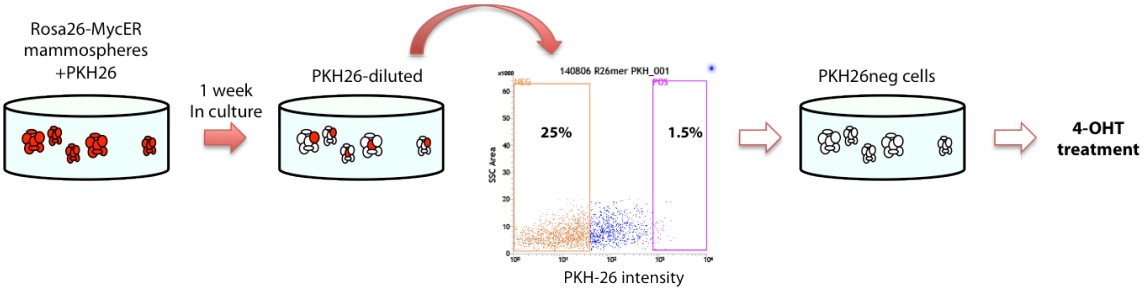

Figure 4-27: Schematic representation of the PKH-26 assay.

Rosa26-MycER HE cells were plated in mammosphere culture and labeled with PKH-26 dye for one week. Cells that did not retain the dye (PKHneg) were sorted at FACS and re-plated as mammospheres in the presence or absence of 4-OHT for the induction of Myc.

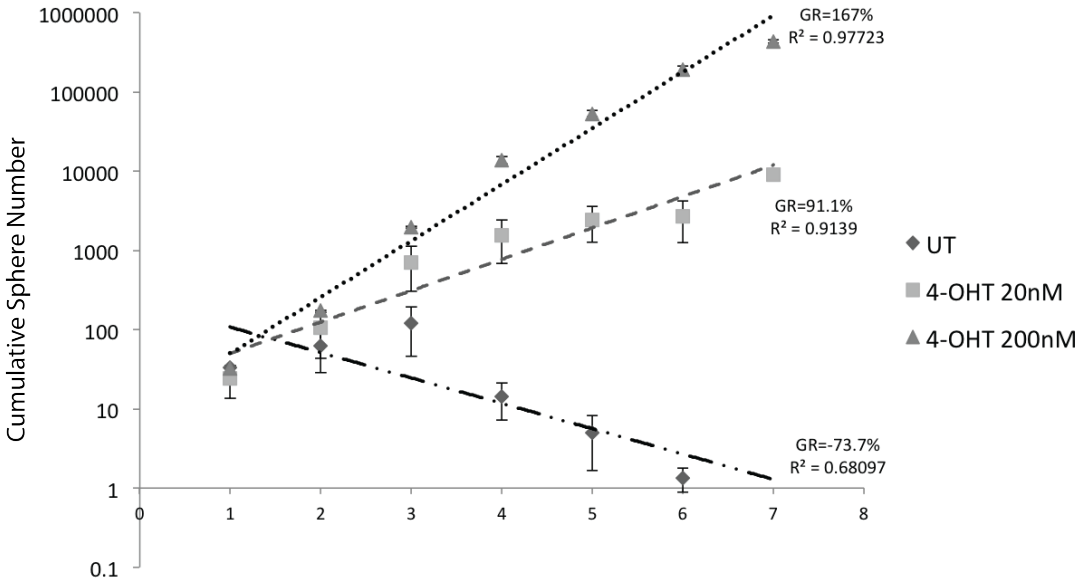

Figure 4-28: Growth curve of Rosa26-MycER progenitor spheres.

Semi-logarithmic plot of Cumulative Sphere numbers. Numbers were obtained from serial replating of PKHneg mammary progenitors derived from Rosa26-MycER mice in the absence or continuous presence of two different concentrations of 4-OHT. Each dot in the curve represents the mean of three independent curves; error bars indicate the standard deviation. Regression analysis was performed to obtain trend lines (dashed lines) that best approximate the curves. Growth rates (GR) and coefficients of determination (R^2) for each trend line are reported inside the graph.

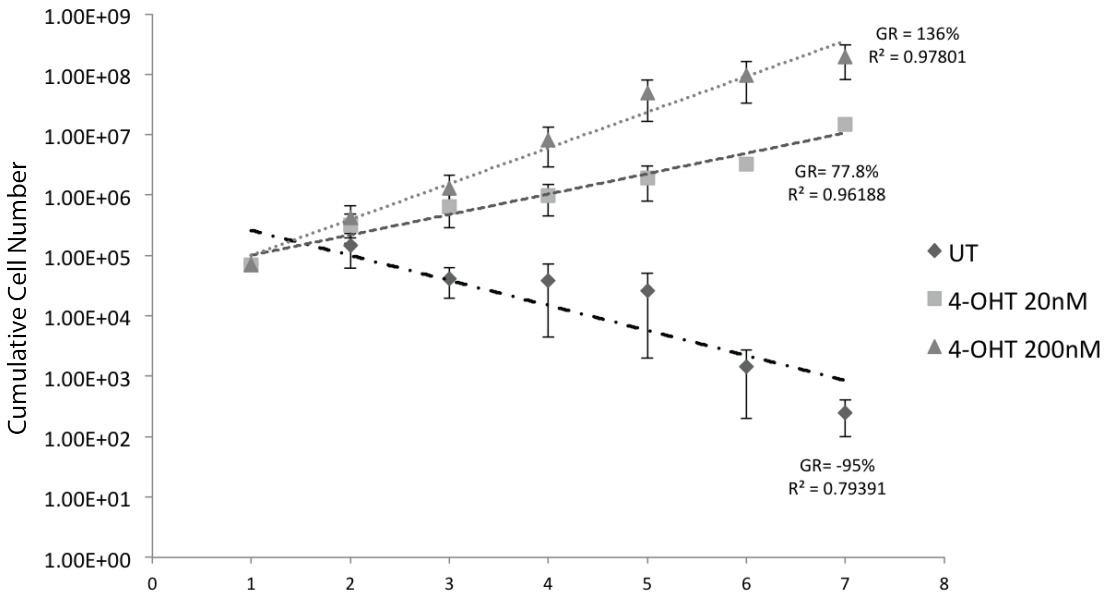

Figure 4-29: Growth curve of Rosa26-MycER progenitor cells.

Semi-logarithmic plot of Cumulative Cell numbers. Numbers were obtained from serial replating of PKHneg mammary progenitors derived from Rosa26-MycER mice in the absence or continuous presence of the two different concentrations of 4-OHT. Each dot in the curve represents the mean of three independent curves; error bars indicate the standard deviation. Regression analysis was performed to obtain trend lines (dashed lines) that best approximate the curves. Growth rates (GR) and coefficients of determination (R^2) for each trend line are reported inside the graph.

4.3.2 Effect of Myc on the ability of mammary progenitors to reconstitute a mammary gland tissue

To investigate whether Myc-expressing progenitors are able to differentiate into all the cell types that compose the mammary gland, we transduced PKHneg cells with the MycER vector and transplanted them under limiting dilution conditions into the cleared fat-pad of pre-pubertal recipient mice. The mice were sacrificed after 12 weeks and their inguinal mammary glands collected for whole mount staining to evaluate the presence of positive outgrowths (DeOme, Faulkin et al. 1959). Strikingly, PKHneg cells expressing MycER were able to give rise to complete outhgrowths with a calculated SC frequency of around

1:100,000 (**Table 4-2**, **Figure 4-30**), while PKHneg progenitors transduced with the empty vector never reconstituted the gland in the cleared fat pad. This suggests that low levels of Myc can reprogram progenitors into bona fide SCs, e.g. cells with repopulating ability, albeit at a low frequency.

Cell Dose	**PKHneg Empty Vector**	**PKHneg MycER**
100000	0/4	5/8
50000	0/10	5/12
10000	0/7	3/20
5000		0/18
Frequency of repopulating units (95% confidence limit)	**inf (inf-323794)**	**1 : 95864 (167263-54942)** *Slope* **1.02** *Fit* **0.94**

Table 4-2: Limiting dilution transplantation experiment of PKHneg progenitors transduced with Empty vector or MycER.

Cells suspension from PKHneg progenitors infected with Empty or MycER vector were inoculated in recipient mice in limiting dilution conditions (from 100,000 to 5,000 cells). Results show the number of positive outgrowths as defined by the presence of epithelial structures with radial organization in stained whole mounts 12 weeks after the injection. SC frequencies (estimates and upper/lower limits) were calculated by limiting dilution analysis, as described in the Materials and Methods section. Slope is a measure of the linearity of the limiting dilution test; its nominal value is equal to 1. Fitting to the single hit model is indicated by p-values >0.05.

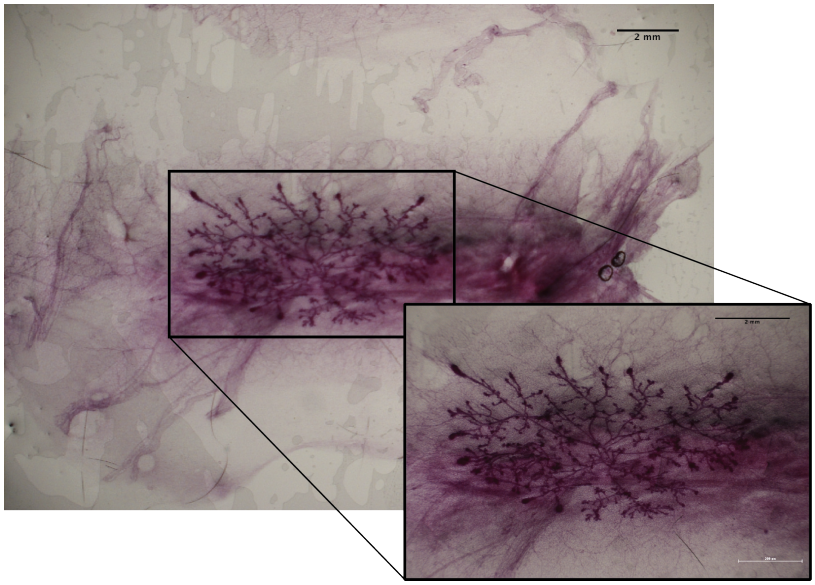

Figure 4-30: Whole mount staining of a positive outgrowth resulting from the injection of PKHneg-MycER cells.

Representative image of carmine alum whole mount staining of a reconstituted gland after injection of 50,000 MycER-transduced PKHneg progenitors. Scale bar as indicated.

To investigate whether PKHneg-MycER SCs are capable of normal physiological differentiation in vivo, we analyzed mammary glands from six outgrowths of 50,000 transplanted PKHneg-MycER cells, as compared to outgrowths derived from the transplantation of the same number of WT cells. We first tested the regenerative potential of PKHneg-MycER progenitors calculating the extent of mammary epithelium within the fat pad by digital image analysis (DIA). Results showed that the percentage of the area occupied by epithelial structures was around 2% in each acquired field and was in the same range of the value reported for outgrowths derived from WT mammospheres (**Table 4-3**). Staining for KI67, a nuclear marker of cycling cells, confirmed that the rate of proliferation was also comparable between the two experimental groups (**Table 4-3**). Analyses of histology of the mammary glands (on haematoxylin-eosin staining) showed some degree of

hyperplastic and dysplastic features in all mammary glands obtained from the PKHneg-MycER progenitors. (**Figure 4-31**, HE staining). Notably, however, when compared with those from four mammary-gland outgrowths arisen from WT control cells, we observed a similar degree of hyperplasia/dyspasia, suggesting that it is rather a consequence of active regeneration inherent to the transplantation procedure, not related to a process of transformation fired by Myc (**Table 4-3**). In line with this, a total of 6 mice were kept under observation for one year after the transplantation procedure and none of them displayed any palpable masses.

Transplants	Mean % Epithelial area	KI67 index	Hyperplasia/ Dysplasia
WT ctrl	1.64 ± 1.67	0.44 ± 0.29	+++
PKHneg-MycER	1.95 ± 1.29	0.43 ± 0.29	++

Table 4-3: Histological evaluation of the outgrowths resulting from "reprogrammed" progenitor and WT cells.

Outgrowths resulting from WT (n=4) and PKHneg-MycER (n=6) transplantations were stained for whole mount evaluation, paraffin embedded and sectioned for histopathological evaluation. To assess the extent of the mammary reconstitution in each examined sample, the area (μm^2) occupied by the mammary epithelium was calculated by DIA and it is shown as percentage of the total area (mean±sd) of the field under examination. Anti-KI67 staining was performed; KI67 index was calculated as the ratio between KI67 positive *vs.* negative cells (mean±sd) in 400X microscopic fields (four fields per sample). Histological grading of epithelial hyperplasia/dysplasia of ductular and alveolar epithelial structures was performed according to the following criteria: (++) = multifocal to diffuse moderate ductular and/or alveolar epithelial hypertrophy and hyperplasia, without relevant cell atypia; (+++) = focal to multifocal areas of mammary epithelial dysplasia with variable cell atypia

Differentiation capacity of the "reprogrammed" progenitors was analyzed on paraffin-embedded slides by immunohistochemical analysis for the terminal differentiation markers of the mammary gland epithelial structures. The results show that the PKHneg-MycER transplanted glands correctly express markers for basal (K14) and luminal (K18) development, thus demonstrating the ability of the "reprogrammed" cells to give rise to a normally differentiated gland (**Figure 4-31**).

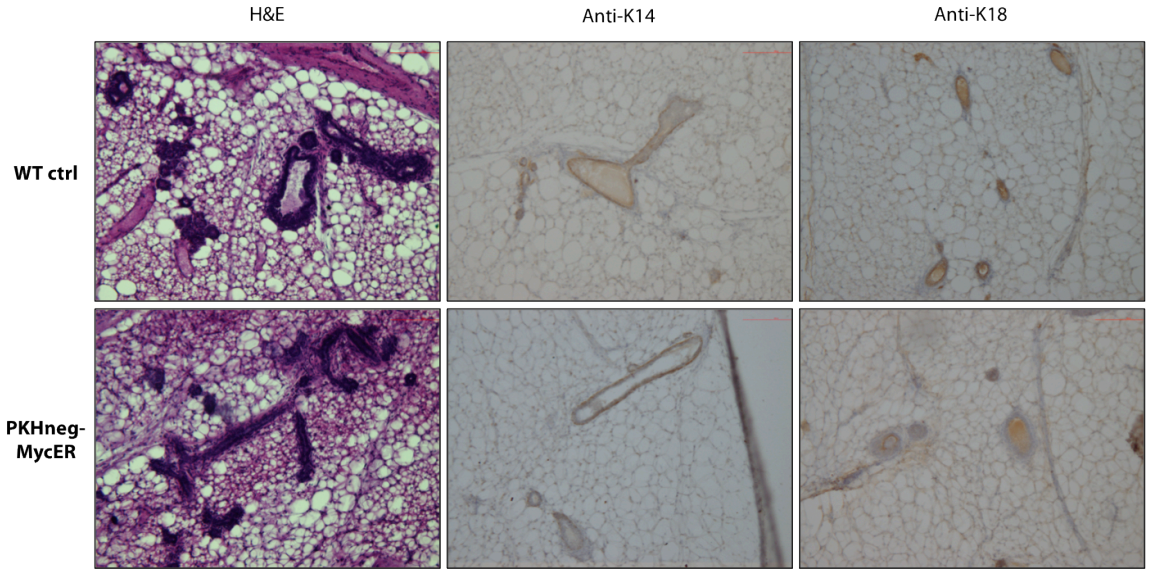

Figure 4-31: "Reprogrammed" progenitors form normal differentiating tissue upon transplantations *in vivo*.

Twelve weeks after transplant, whole mounts of outgrowths formed in the transplanted fat pads of injected mice were stained with carmine and then paraffin-embedded and sectioned for immuno-histochemical analysis. Tissue sections of samples from WT cells and PKHneg-MycER transplanted mice were then stained for HE evaluation of the epithelial structures (left); for basal epithelial marker K14 (middle) and for luminal epithelial marker K18 (right). All images were acquired with a 10X magnification objective.

Finally, to test the capacity of PKHneg-MycER progenitors to generate fully functional mammary glands, we analyzed mammary-gland changes during pregnancy. Therefore, 10 weeks after the injection of 50,000 PKHneg-MycER cells, we mated the transplanted mice

with control male mice and analyzed mammary glands at day 18.5 of pregnancy for the presence of milk, by staining whole mounts for beta-casein.

All the glands under analysis (n=5) resulted positive for beta-casein staining and to the same extent of not transplanted pregnant control animals **(Figure 4-32**), thus indicating that the transplanted glands are able to fully differentiate into a completely functional tissue.

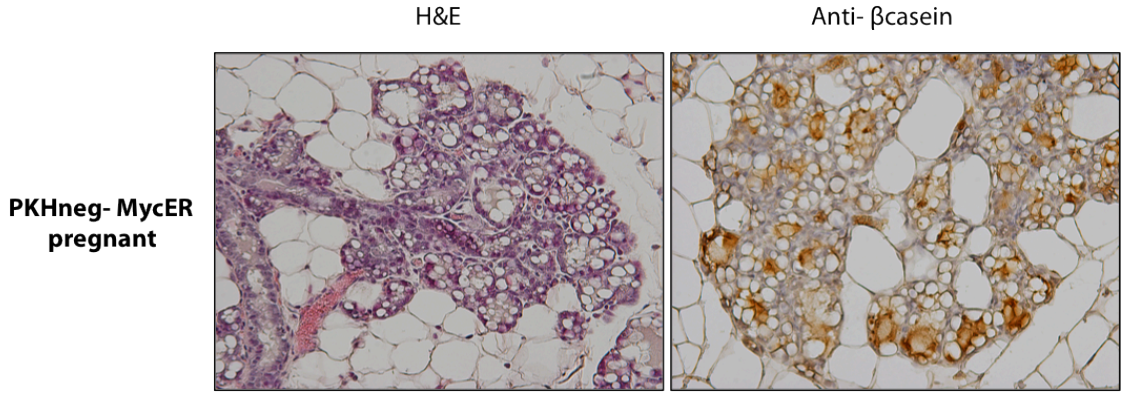

Figure 4-32: "Reprogrammed" progenitors form functional tissue upon transplantations *in vivo*.

Female mice were transplanted with PKHneg-MycER cells, successfully mated, and outgrowths collected at day 18.5 of pregnancy. The glands were stained with carmine for whole mount evaluation and then paraffin-embedded and sectioned for immuno-histochemical analysis. Tissue sections were stained for hematoxilin-eosin (H&E) evaluation of the epithelial structures (left) and for beta-casein as a marker of the presence of milk in the alveolar buds. All images were acquired with a 20X magnification objective.

4.3.3 Myc reprograms mammary progenitors into long living stem cells

Finally, we investigated the *in vivo* self-renewal properties of PKHneg-MycER progenitors, by the serial transplantation assay, which unequivocally proves the existence of long living SCs in a given population.

To perform serial transplantation assay of the PKHneg-MycER progenitors we took advantage of a GFP transgenic mouse model that allowed us to track the transplanted cells. We transduced with MycER vector the PKHneg cells derived from this model and we performed the first transplantation experiment (P1 in **Figure 4-33**). Twelve weeks later, we collected the glands and performed FACS-sorting of the GFP positive cells. These were then re-transplanted in the cleared fat pad of new recipients and positive outgrowths were scored 12 weeks later. As shown in **Table 4-4**, 2 out of 8 glands resulted positive to whole mount evaluation and, notably, their epithelial structures were positive to anti-GFP staining, thus confirming their derivation from the original "reprogrammed" population (P2, **Figure 4-33**). Furthermore, the predicted SC frequency of the secondary transplants (1:2607) is in line with the frequencies reported for total epithelial cell transplantations (Cicalese, Bonizzi et al. 2009), thus strengthening the concept of reconstitution of a completely normal gland upon transplantation of MycER transduced progenitors.

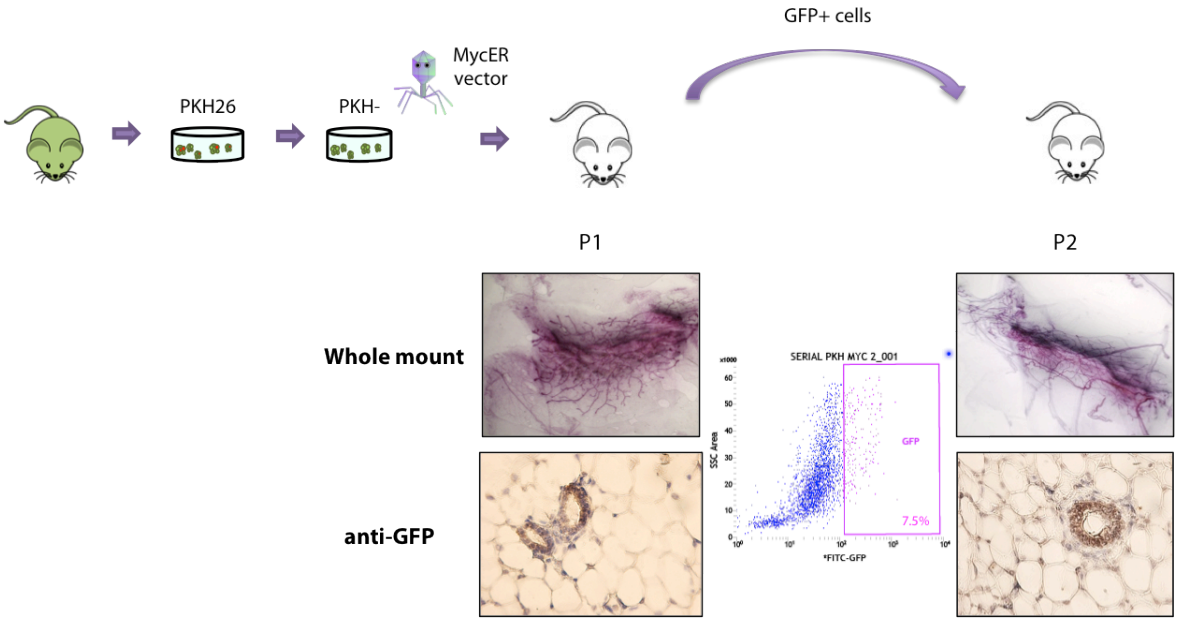

Figure 4-33: Serial transplantation of positive outgrowth.

TOP: Description of the experiment. Female mice were transplanted with 50,000 PKHneg-MycER cells derived from GFP-FVB mice, and glands collected 12 weeks after the injection (P1). The presence of positive outgrowths was scored with whole mount staining and IHC analysis of GFP expression (bottom). GFP positive cells from a pooled group of 8 glands were sorted by FACS and re-transplanted in 8 recipient mice. 12 weeks after, the presence of positive outgrowths was scored with whole mount staining and IHC analysis of GFP expression (P2, bottom).

P1 GFP+ cells (nr. transplanted cells)	**Positive Outgrowths**
750	2/8
Frequency of repopulating units (95% confidence limit)	**1 : 2607 (10474-649)**

Table 4-4: Efficiency of serial transplantation.

750 GFP+ total epithelial cells derived from P1 transplanted mice were re-transplanted into the cleared fat pad of 8 recipient mice. SC frequencies (estimates and upper/lower limits) were calculated by limiting dilution analysis, as described in the Materials and Methods section.

To summarize, we have shown that low levels of Myc expression in mammary progenitors: 1) confer on them mammosphere initiating potential; 2) endow them with reconstitution ability; 3) reconstitute a gland that is morphologically normal and fully functional; 4) generate true SCs able to survive upon serial transplantation. All together, these data demonstrate that Myc is able to reprogram a heterogeneous population of committed progenitors into *bona fide* SCs (albeit at low frequency).

Thus reprogramming might represent, together with the increased frequency of SC symmetric divisions (Pasi et al. unpublished results), one of the key mechanisms instructed by p53 loss and operated by Myc dysregulation that ultimately leads to the uncontrolled expansion of a SC-pool.

4.4 Myc expression alone is sufficient for the expansion of the SC pool

We next investigated whether constitutive Myc expression in ErbB2 tumors is the critical effector of p53-loss, by a reverse genetic approach.

4.4.1 Depletion of Myc impairs CSCs' unlimited expansion

First, we evaluated whether suppression of Myc activity, using a Myc-specific shRNA or a dominant-negative Myc mutant, leads to the disruption of the "p53-loss phenotype" of CSCs, e.g. immortality and exponential growth (Cicalese, Bonizzi et al. 2009). To this end, we infected ErbB2-tumor or WT mammospheres with a vector expressing Myc-specific shRNAs (pLKO-c-Myc-shRNA). Myc silencing, however, resulted in a rapid and complete cell growth arrest of both WT and ErbB2-tumor cells, likely due to a strict Myc-dependency of mammary epithelial cell proliferation (data not shown). As alternative approach, we expressed in ErbB2 mammospheres the dominant-negative mutant of Myc (Omomyc), which omo-dimerizes with endogenous Myc leading to its irreversible functional impairment (Soucek, Whitfield et al. 2008). The coding sequence for the Omomyc cDNA is downstream of a tetra- cycline-responsive promoter element (TRE) and was cloned in frame with a TurboRFP cassette in the pTRIPZ backbone, which harbors a TetO element ensuring Omomyc inducibility upon doxycycline administration. Once the tumor mammospheres had been transduced with the Omomyc construct, we induced its expression with two different concentrations of doxycycline (0.5 and 1 μM) and monitored sphere forming efficiency and replicative potential of our cells. In parallel, as a control, we

also induced cells transduced with the pTRIPZ empty vector. The results shown in **Figure 4-34** (right) depict the successful induction of the RFP-Omomyc fusion protein, as indicated by RFP positivity, and a significant drop in tumor sphere forming efficiency upon induction at both concentrations of doxycycline (**Figure 4-34**, left). This suggests that the presence of a functional Myc is a fundamental pre-requisite for CSC expansion in culture. Notably, Omomyc expression had little effect on the growth of WT mammospheres (data not shown).

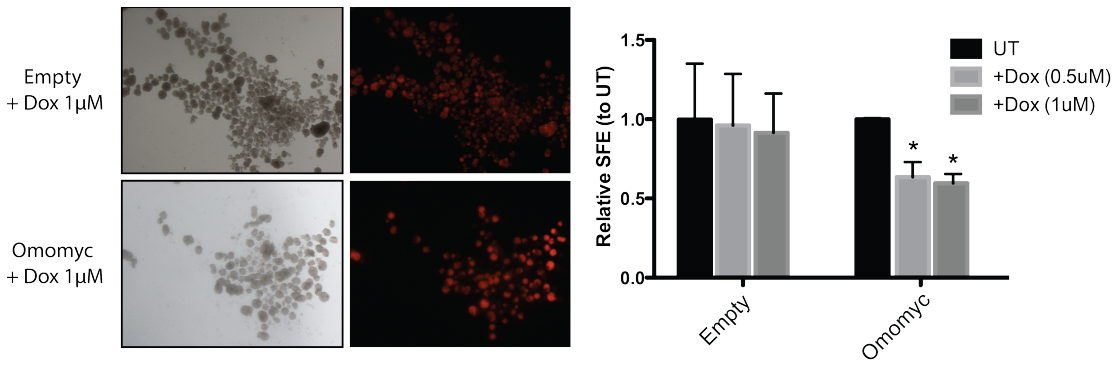

Figure 4-34: The expression of the pTRIPZ-Omomyc-TurboRFP vector impairs tumor sphere forming ability.

LEFT: ErbB2 mammospheres transduced with the Omomyc vector or the empty backbone and treated with doxycycline (1µM) for one week; the efficiency of induction is indicated by the RFP signal. Spheres pictures were acquired at a stereomicroscope with 0.8X magnification. RIGHT: Relative sphere forming efficiency (SFE) of cells transduced with the empty vector or the Omomyc vector and treated for one week with doxycycline at the indicated concentrations (untreated spheres of each group =1).

Additionally, qPCR of two known Myc targets (Nucleolin and ODC1) revealed a very modest effect of Omomyc expression on Myc transcriptional activity (**Figure 4-35**), suggesting that pTRIPZ-Omomyc vector does not allow high levels of expression of Omomyc in our cell system. Possibly this is why its expression is compatible with cell viability, in contrast with what we observed with Myc-shRNA.

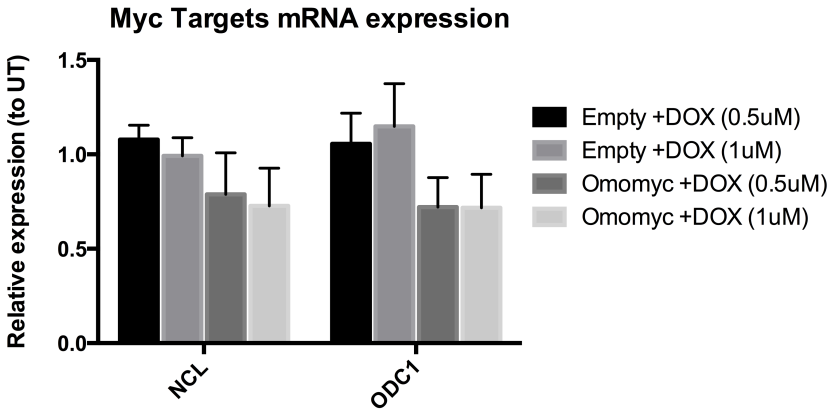

Figure 4-35: mRNA expression of Myc target genes upon Omomyc induction.

qPCR analysis of two known Myc target genes (NCL and ODC1) in empty vector or Omomyc transduced spheres. Induction was performed with two concentration of doxycycline (0.5 and 1 μM) for 72 hours. For each experimental group, values are normalized against the qPCR data of untreated spheres (UT=1).

Collectively, these data demonstrate that inhibition of Myc in mammary epithelial cells leads to an impairment of the sphere forming ability of CSCs, thus highlighting its fundamental role in the maintenance of cell growth and viability. However, this approach did not allow asking the question as to whether Myc constitutive expression alone is sufficient to maintain the increased self-renewal in the ErbB2-tumor CSCs.

4.4.2 Uncoupling the p53:Myc axis

As a complementary approach, we tried to uncouple the p53:Myc axis, in order to investigate the effects of myc on CSCs independently of the loss of function of p53.

Restoration of p53 signaling in ErbB2 mammospheres has the effect of re-establishing the balance between SC asymmetric and symmetric divisions, thus leading to the gradual

functional exhaustion of mammosphere initiating cells in culture and, more generally, depletion of the content in CSCs, as demonstrated by limiting dilution transplantations *in vivo* (Cicalese, Bonizzi et al. 2009). We now know that this effect happens concomitantly with the down regulation of Myc protein and mRNA levels upon Nutlin treatment (see section 4.1.2). To uncouple the p53 and Myc pathways, we first enforced the Myc expression in the ErbB2-tumor mammospheres, by transducing them with the MycER lentiviral vector. Then, we restored levels of p53 in the MycER-expressing tumor mammospheres by treating them with Nutlin-3, as described in section 4.1.2. In this scenario, we can analyze the effect of constitutive Myc expression on CSCs in the presence of functional p53.

Strikingly, results show that, while the treatment with one dose of Nutlin has the effect of slowing down the growth of tumor mammospheres transduced with the empty vector, as expected (GR=76%), the presence of MycER renders the restoration of p53 ineffective and leads to a complete rescue of the CSC phenotype, as indicated by the fact that the spheres show typical CSC unlimited exponential growth (GR=196%) in culture (**Figure 4-36**). In line with this, the cumulative number of cells in culture (replicative potential) also remains unaffected by Nutlin administration when Myc is constitutively expressed (**Figure 4-37)**.

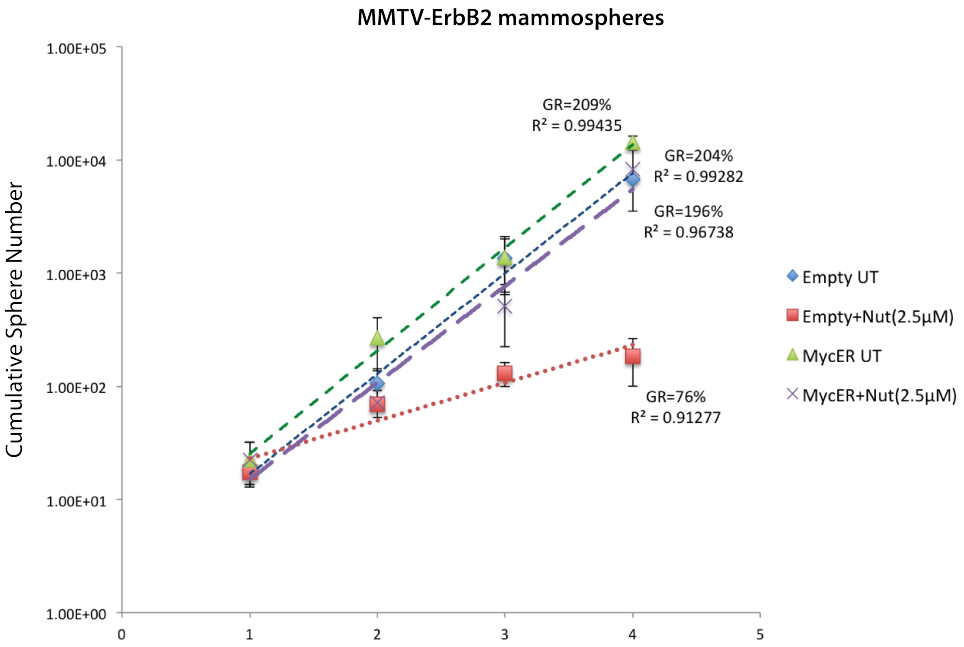

Figure 4-36: ErbB2 mammospheres transduced with MycER are rescued from the Nutlin effect.

Semi-logarithmic plot of Cumulative Sphere numbers. Numbers were obtained from serial replating of MMTV-ErbB2 mammospheres, transduced with empty or MycER vector, in the absence or continuous presence of Nutlin-3 (2.5µM). Each dot in the curve represents the mean of three independent curves; error bars indicate the standard deviation. Regression analysis was performed to obtain trend lines (dashed lines) that best approximate the curves. Growth rates (GR) and coefficients of determination (R^2) for each trend line are reported inside the graph.

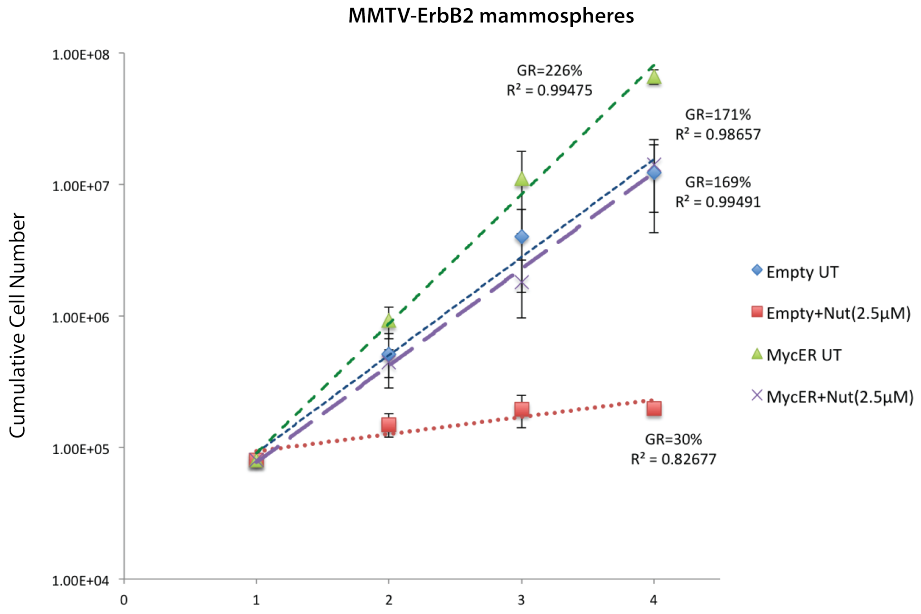

Figure 4-37: Cumulative cell number of ErbB2 mammospheres transduced with MycER and rescued from the Nutlin effect.

Semi-logarithmic plot of Cumulative Cell number. Numbers were obtained from disaggregation to single cells of MMTV-ErbB2 mammospheres, transduced with empty or MycER vector, in the absence or continuous presence of Nutlin-3 (2.5μM). Each dot in the curve represents the mean of three independent curves; error bars indicate the standard deviation. Regression analysis was performed to obtain trend lines (dashed lines) that best approximate the curves. Growth rates (GR) and coefficients of determination (R^2) for each trend line are reported inside the graph.

Thus, in the context of the enforced expression of Myc, restoration of p53 function in tumor mammospheres is not sufficient, by itself, to prevent CSC expansion, suggesting that: 1) Myc acts downstream of p53 and 2) Myc is the critical key effector of CSC maintenance.

To validate these findings *in vivo*, we transplanted ErbB2 tumor cells, infected with either MycER or its corresponding empty vector, in a total of 25 recipient mice; then, when the tumors were palpable (tumor volume ≈ 100 mm^3), we divided the cohort of mice in two further groups: those to be treated with Nutlin-3 (20 mg/kg of body weight) and those to be treated with the treatment vehicle (DMSO). The treatment consisted of seven IP injections every other day for a total period of 14 days. At the end of it, we measured the volume of the resulting tumors: while for the Empty vector-transplanted cohort the Nutlin treatment effectively led to a reduction in tumor size, as compared to the vehicle treated cohort, the same was not true for the MycER-transplanted cohort. In this experimental group, in fact, all the tumors grew at the same rate, regardless of the administration of Nutlin (**Figure 4-38**). Therefore, the *in vivo* data mirror the growth behavior we observed in the mammosphere cultures, with MycER expression being able, by itself, to maintain cancer expansion, independently of p53 functionality.

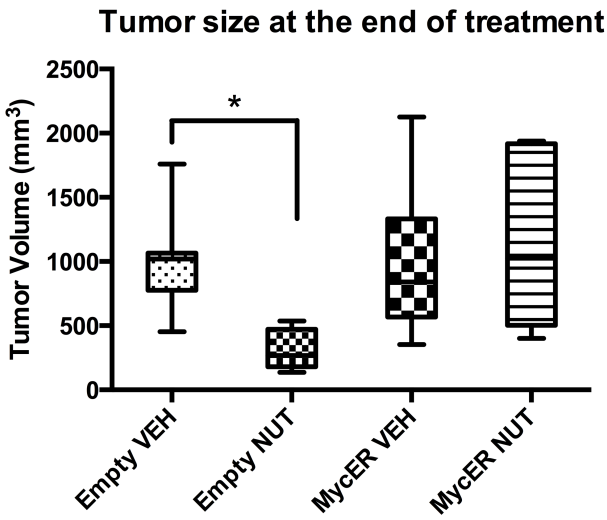

Figure 4-38: Nutlin treatment does not affect the growth of MycER expressing tumors.

Mice were transplanted with ErbB2 cells transduced with the Empty (n=13) or the MycER (n=12) vector. At the time of palpability (tumor volume ≤ 100mm^3) the mice of each group were treated with DMSO (VEH; n=7 for Empty and n=6 for MycER) or with Nutlin-3 (NUT: 20 mg/Kg, n=6 for both Empty and MycER). Tumor volume was measured at the end of the 2 weeks of treatment.

All together these data suggest that attenuated p53 function, which is a common event in many types of tumors, including breast cancer, has profound effects on a cancer population that has the features of CSCs by acting through the de-regulation of its downstream effector Myc. De-regulated Myc is able by itself to fuel the maintenance of the cancer clone, most likely by the rewiring of SC-like mechanisms that ultimately sustain cancer development and progression.

4.5 Downstream of the p53:Myc axis

A further question we have been trying to answer with this thesis work is which intracellular pathway is directly instructed by the p53:Myc axis and is responsible of the biological processes we have described. To address this issue we took advantage of the genome-wide expression data derived from the previously described RNAseq datasets (see section 4.1.4).

In summary, we have generated 4 relevant datasets of differentially expressed genes (DEGs): *i)* genes that are deregulated by oncogene expression in mammary tumor cells (obtained by comparing RNAseq data from ErbB2-tumor vs. WT mammospheres); *ii)* genes that are regulated by p53 expression in mammary normal cells (obtained by comparing RNAseq data from p53-/- vs. WT mammospheres); *iii)* genes that are de-regulated by constitutive Myc expression in mammary cells (obtained by comparing RNAseq data from Myc-ER-expressing and control WT mammospheres); and *iv)* genes that are deregulated in tumor cells as a consequence of p53-loss (obtained by comparing RNAseq data from non-treated ErbB2-tumor *vs.* Nutlin-treated tumor mammospheres). For all these dataset, we applied stringent conditions of comparative analyses, setting a cut-off on the q-value (≤ 0.05) and on the log2fold change (log2FC = |1|) (**Table 4-5**).

	Total	UP	DOWN
ErbB2 *vs.* WT	2062	788	1274
P53-/- *vs.* WT	3428	1363	2065
MycER *vs.* WT	2237	999	1238
ErbB2 *vs.* ErbB2+Nut	260	191	69
TOTAL non-Redundant genes	5236	2248	2988

Table 4-5: Differentially expressed genes (DEGs) in selected RNAseq datasets.

Number of DEGs in each of the indicated comparisons among cell types that satisfy the following thresholds: q value equal or lower than 0.05; Log2FC = |1|. Total: total number of DEGs per group; UP: up-regulated genes; DOWN: down-regulated genes. The last row indicates the total number of non-redundant genes among all the experimental groups.

To identify p53:Myc dependent genes in the erbB2 tumors, we searched for genes in common among the four datasets. Strikingly, from a total of 5,236 non-redundant DEGs present in the 4 datasets, comparative analyses revealed 140 DEGs, including 136 up-regulated genes and 4 down-regulated genes (**Figure 4-39**). Thus, the ErbB2 tumors are characterized by 140 genes whose de-regulated expression depends on ErbB2, p53-loss and constitutive Myc expression, which should represent the downstream effectors of the deregulated p53:Myc axis in mammary cancer cells.

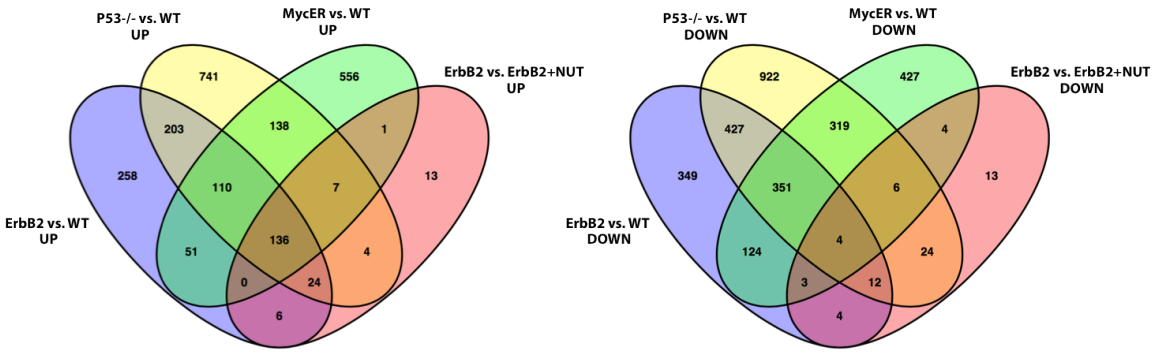

Figure 4-39: Intercrosses among the four datasets generated by RNAseq.

Venn diagrams show the overlap among the UP regulated and DOWN regulated genes in each of the four datasets under analysis (ErbB2 vs. WT; p53-/- vs. WT; MycER vs. WT; ErbB2 vs ErbB2+NUT)

To investigate which cellular processes might be affected by the identified 140 DEGs, we then performed a pathway analysis and gene ontology (GO) search, taking advantage of the molecular signature database (MSigDB) available on the GSEA website (www.broadinstitute.org/gsea). In details, we computed the overlap between our gene-set and curated gene datasets (C2) which consist of a collection of various databases, such as online pathway databases, including KEGG, BIOCARTA and REACTOME, and knowledge of domain experts. In **Table 4-6** the top 20 pathways are listed together with the number of genes, among the 140, in overlap with a given dataset. Remarkably, all the pathways we found are cell cycle related, with a particular focus on mitotic processes. As a visual aid, the Kyoto Encyclopedia of Genes and Genomes (KEGG) pathway named "Cell-Cycle" is shown in **Figure 4-40**, and the genes present in our list are highlighted with a red star. As it is clear from the figures, most of these genes are key component of the G2/M and mitotic processes.

Gene Set Name	# Genes in Gene Set (K)	Description	# Genes in Overlap (k)	k/K	p-value	FDR q-value
REACTOME_CELL_CYCLE	421	Genes involved in Cell Cycle	53	0.1259	3.07E-73	4.08E-70
REACTOME_CELL_CYCLE_MITOTIC	325	Genes involved in Cell Cycle, Mitotic	48	0.1477	1.68E-69	1.12E-66
REACTOME_DNA_REPLICATION	192	Genes involved in DNA Replication	37	0.1927	9.73E-58	4.31E-55
REACTOME_MITOTIC_M_M_G1_PHASES	172	Genes involved in Mitotic M-M/G1 phases	34	0.1977	2.12E-53	7.05E-51
REACTOME_MITOTIC_PROMETAPHASE	87	Genes involved in Mitotic Prometaphase	24	0.2759	1.31E-41	3.49E-39
PID_PLK1_PATHWAY	46	PLK1 signaling events	17	0.3696	3.00E-32	6.65E-30
PID_AURORA_B_PATHWAY	39	Aurora B signaling	15	0.3846	6.90E-29	1.31E-26
KEGG_CELL_CYCLE	128	Cell cycle	18	0.1406	1.34E-25	2.22E-23
REACTOME_CELL_CYCLE_CHECKPOINTS	124	Genes involved in Cell Cycle Checkpoints	16	0.129	3.09E-22	4.57E-20
REACTOME_G2_M_CHECKPOINTS	45	Genes involved in G2/M Checkpoints	11	0.2444	6.14E-19	8.17E-17
REACTOME_MITOTIC_G1_G1_S_PHASES	137	Genes involved in Mitotic G1-G1/S phases	14	0.1022	4.03E-18	4.87E-16
REACTOME_KINESINS	24	Genes involved in Kinesins	9	0.375	1.18E-17	1.22E-15
REACTOME_G1_S_TRANSITION	112	Genes involved in G1/S Transition	13	0.1161	1.19E-17	1.22E-15
PID_FOXM1_PATHWAY	40	FOXM1 transcription factor network	10	0.25	1.97E-17	1.87E-15
REACTOME_CHROMOSOME_MAINTENANCE	122	Genes involved in Chromosome Maintenance	13	0.1066	3.76E-17	3.33E-15
KEGG_OOCYTE_MEIOSIS	114	Oocyte meiosis	12	0.1053	7.42E-16	6.17E-14
REACTOME_S_PHASE	109	Genes involved in S Phase	11	0.1009	1.99E-14	1.56E-12
PID_AURORA_A_PATHWAY	31	Aurora A signaling	8	0.2581	2.62E-14	1.83E-12
REACTOME_ACTIVATION_OF_THE_PRE_REPLICATIVE_COMPLEX	31	Genes involved in Activation of the pre-replicative complex	8	0.2581	2.62E-14	1.83E-12
REACTOME_REGULATION_OF_MITOTIC_CELL_CYCLE	85	Genes involved in Regulation of mitotic cell cycle	10	0.1176	6.52E-14	4.33E-12

Table 4-6: Pathway analysis of the 140 genes in our signature.

Computed overlap between our signature and curated gene signatures performed through the C2 tool (www.broadinstitute.org/gsea). The top 20 pathways are shown under the Gene set name. # Genes in the gene set (K): total number of genes in the called dataset; # Genes in overlap (k): number of genes of our signature that overlap with those of the called dataset; k/K: ratio of the genes in overlap with the total number of genes of the called dataset.

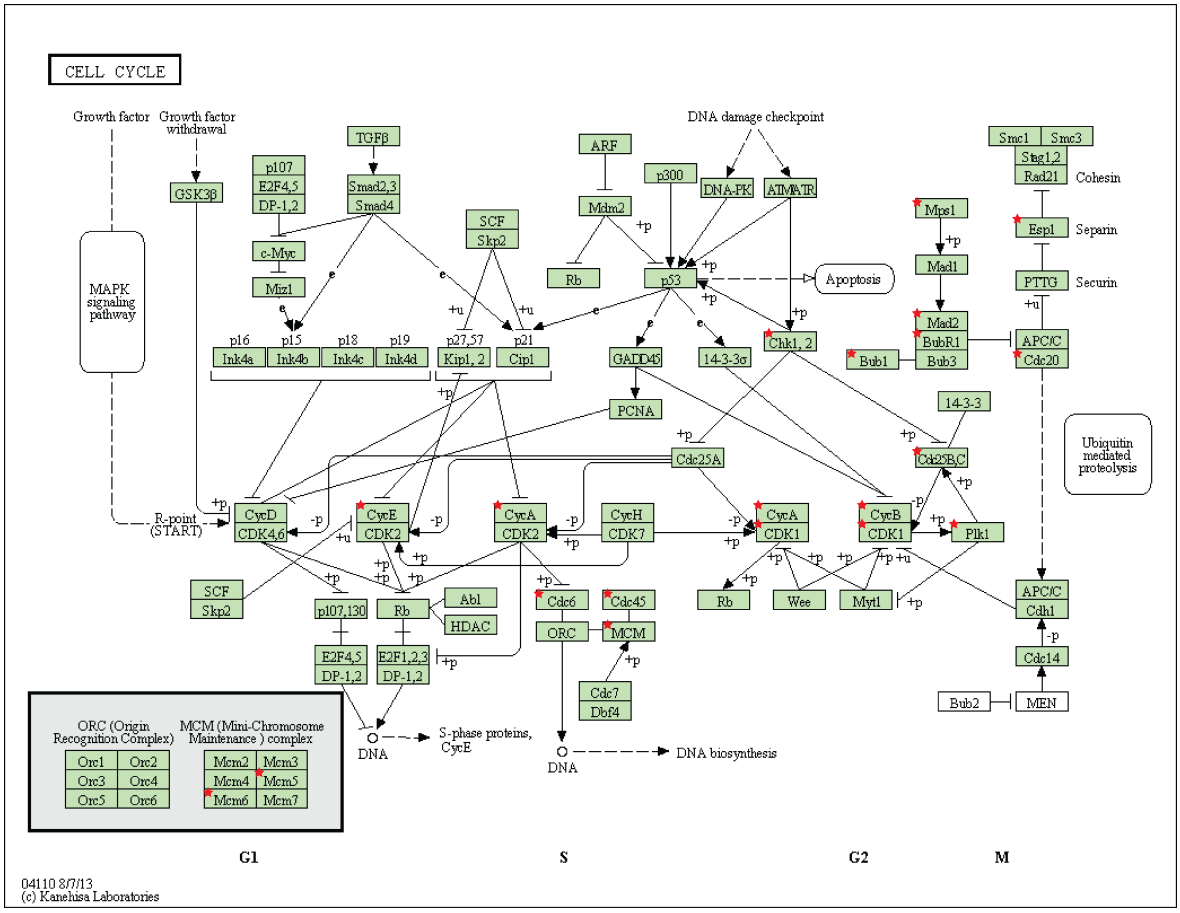

Figure 4-40: KEGG pathway: cell cycle.

Representative image of the KEGG cell cycle pathway as depicted by DAVID (the Database for Annotation, Visualization and Integrated Discovery) bioinformatics tool. Red stars indicate the genes present in our signature

Furthermore, when we performed a GO analysis (C5), in which the overlap between our dataset and annotated genes based on their ontology (biological processes, cellular component, molecular function), we could again observe an enrichment of cell cycle and mitosis-specifically-related terms (listed in **Table 4-7**).

Gene Set Name	# Genes in Gene Set (K)	Description	# Genes in Overlap (k)	k/K	p-value	FDR q-value
CELL_CYCLE_PROCESS	193	GO term GO:0022402	36	0.1865	1.36E-55	1.98E-52
CELL_CYCLE_GO_0007049	315	GO term GO:0007049	39	0.1238	6.80E-53	4.94E-50
CELL_CYCLE_PHASE	170	GO term GO:0022403	31	0.1824	1.84E-47	8.92E-45
MITOTIC_CELL_CYCLE	153	GO term GO:0000278	30	0.1961	5.86E-47	2.13E-44
M_PHASE	114	GO term GO:0000279	27	0.2368	9.94E-45	2.89E-42
INTRACELLULAR_NON_MEMBRANE_BOUND_ORGANELLE	631	GO term GO:0043232	41	0.065	6.52E-44	1.35E-41
NON_MEMBRANE_BOUND_ORGANELLE	631	GO term GO:0043228	41	0.065	6.52E-44	1.35E-41
M_PHASE_OF_MITOTIC_CELL_CYCLE	85	GO term GO:0000087	24	0.2824	6.89E-42	1.25E-39
MITOSIS	82	GO term GO:0007067	23	0.2805	4.36E-40	7.04E-38
INTRACELLULAR_ORGANELLE_PART	1192	GO term GO:0044446	43	0.0361	2.55E-35	3.71E-33
ORGANELLE_PART	1197	GO term GO:0044422	43	0.0359	3.03E-35	4.01E-33
MICROTUBULE_CYTOSKELETON	152	GO term GO:0015630	24	0.1579	3.63E-35	4.40E-33
CYTOSKELETAL_PART	235	GO term GO:0044430	25	0.1064	4.18E-32	4.68E-30
CYTOSKELETON	367	GO term GO:0005856	26	0.0708	1.07E-28	1.11E-26
CHROMOSOME	124	GO term GO:0005694	19	0.1532	1.01E-27	9.75E-26
NUCLEUS	1430	GO term GO:0005634	39	0.0273	2.15E-27	1.95E-25
SPINDLE	39	GO term GO:0005819	14	0.359	1.62E-26	1.39E-24
CHROMOSOMAL_PART	96	GO term GO:0044427	15	0.1562	3.14E-22	2.53E-20
REGULATION_OF_MITOSIS	41	GO term GO:0007088	11	0.2683	1.93E-19	1.48E-17
CELL_CYCLE_CHECKPOINT_GO_0000075	48	GO term GO:0000075	11	0.2292	1.36E-18	9.87E-17

Table 4-7: Gene Ontology analysis of our gene signature.

Computed overlap between our signature and genes annotated by their ontology, performed through the C5 tool (www.broadinstitute.org/gsea). The top 20 GO terms are shown under the Gene set name. # Genes in the gene set (K): total number of genes in the called GO term; # Genes in overlap (k): number of genes of our signature that overlap with those of the called GO term; k/K: ratio of the genes in overlap with the total number of genes of the called GO term.

More in details, the list enrolls a total of 82 genes related to mitosis. Functionally, expression of all these genes is required for: the APC/C mediated mitotic spindle checkpoint (Bub1, Bub1B, Mad2l1, cdc20) that is activated by mis-attachment of microtubules and sister-chromatids to kinetochores, and delays mitosis until all kinetochores are properly attached; the G2/M checkpoint (Cdc45, Cdc25c, Mcm5/6/8/10, Chek1); mitosis-entry or progression (Cdk1, cyclinA and B1, CDC25A/B, Plk1,

AuroraA/B, Nek2, Plk1/4); spindle assembly at metaphase (AurkA, AurkB, Plk1, Nek2); association to kinetochore complexes (CenpH/I/Q/M/N, Nls1, Nuf2, Kntc1). Furthermore the list includes the M-phase promoting factor Cdk1-Ccnb1 and many genes involved in the assembly and motility of the spindle microtubules, like Kif2c, Kif18a, Kif20a, Racgap1.

Taken together, it emerges from these data that our p53-Myc dependent signature in tumors is enriched for genes involved in the process of mitosis and cytokinesis, suggesting that the p53:Myc axis could exert its tumor suppressive role by tightly regulating cell division mechanisms, in terms of organization of the mitotic spindle, regulation of cytoskeleton changes, and distribution of the organelles.

5 Discussion

5.1 Epistatic relationship between p53 and Myc in mammary SCs and CSCs

The CSC population is defined as the rare population of cells which maintain the cancer clone and sustain its progression and its recurrence after chemotherapy. CSCs share many properties with normal SCs, including the ability to regenerate (self-renewal) and the capacity to form differentially specialized progeny. These two properties can be accomplished at the same time by a peculiar type of mitosis, the asymmetric cell division, whereby one SC gives rise to two daughter cells: one committed toward differentiation, the other maintaining SC identity. In situations requiring tissue regeneration, SCs can also divide symmetrically, generating two identical daughter cells endowed with the same self-renewal potential of the mother.

These two modalities of division, symmetric and asymmetric, are tightly regulated in normal tissues and allow maintenance of constant numbers of SCs under homeostatic conditions. SCs mode of division is one of the cellular processes that are altered in CSCs and that promote their transformation. Our group demonstrated that a switch from asymmetric to symmetric SC division is the underlying force determining CSC unlimited expansion in a model of breast tumorigenesis. The growth and self-renewal properties of CSCs were modeled with *in vitro* (*i.e.*, *via* the ability of SCs and CSCs to form mammospheres that could be propagated in culture) and *in vivo* (*i.e.*, *via* the ability to repopulate the cleared fat-pad of a mouse and develop into normal tissues or tumors with the same complexity of the tissues of origin) assays. They led to the observation that CSCs constantly expand, both *in vitro* and *in vivo*, and thus have increased replicative potential.

The tumor suppressor gene p53 was found to be the master regulator governing the choice between symmetry and asymmetry at SC mitosis, and its absence or functional impairment was demonstrated to be the leading cause of CSC extended self-renewal. Moreover, restoration of p53 signaling by Nutlin-3 administration in tumors was shown to re-assess the balance between symmetric and asymmetric divisions and, consequently, set a brake on the geometric growth of CSCs and reduce their total number, as demonstrated by transplantation experiments (Cicalese, Bonizzi et al. 2009).

Being p53 at the center of a plethora of regulatory networks that go from DNA damage response to cell cycle arrest, we wanted to understand which one is the relevant downstream pathway in the described biological phenotype.

To this end, we used a candidate gene approach and investigated Myc as the putative downstream effector of p53. Myc is frequently de-regulated in cancer and is also a key player in SC biology. Its transcriptional program has been linked to SC-like signatures and is found enriched in the more aggressive, metastatic and poorly differentiated breast cancers (Kim, Woo et al. 2010); furthermore, Myc is a known key gene in the maintenance of the pluripotent state in ESCs. Of note, Myc expression is repressed by p53 (Ho, Ma et al. 2005, Sachdeva, Zhu et al. 2009, Li, He et al. 2012).

In line with our hypothesis, we found that both Myc levels and Myc transcriptional activity are up-regulated and de-regulated in our ErbB2 driven tumor model of mammary gland carcinogenesis. In this model, a constitutively active ErbB2 affects the regulation of Mdm2, an E3 ubiquitin-ligase which targets p53 for degradation, by activating the Akt pathway that, in turn, enhances Mdm2 phosphorylation and therefore inhibits p53 functions (Zhou, Liao et al. 2001). We have shown that the treatment of MMTV-ErbB2 mammospheres with the Mdm-2 inhibitor Nutlin-3 and the consequent disruption of the p53-degrading pathway result in the down-regulation of Myc both at the mRNA and at the

protein level. Our data, derived from p53-/- and p53+/- models and from acute activation of p53, suggest that p53 and Myc are epistatically related, with the first molecule actively repressing the second. These results contribute to add complexity to the intricate network involving these two master regulators of transcription in the cell. It is also very well known, in fact, that over-expression of Myc leads to p53-dependent induction of apoptosis (Hermeking and Eick 1994). This notion found confirmation in previous data from our group showing that high levels of Myc lead to p53 mediated apoptotic death (Pasi, Dereli-Oz et al. 2011). Together these findings suggest that a tight regulation of the interaction between p53 and Myc in a cell is essential to determine its destiny and that any change in the levels of these two molecules could lead to important, and different, biological outputs.

In this thesis, we envision a model in which the loss of function of p53 impacts on the fine regulation of Myc, which, once de-regulated, is the key effector of the biological processes that alter SC functions. Whether this regulation is direct or indirect remains still unknown, although we have indication that a transcriptional mechanism could be involved. Indeed, we have shown that Myc mRNA abundance is strongly dependent on the levels of p53. When we examined Myc expression in non-transformed mammospheres harboring the homozygous or hemizygous knock-out of the p53 allele, the levels of Myc transcript were varying coherently; furthermore, the acute activation of p53 upon Adriamycin treatment of WT cells profoundly down-regulated Myc at the transcriptional level. Preliminary data based on ChIP-qPCR experiments on a murine immortalized mammary cell line, confirmed that high levels of p53 lead to its recruitment on the Myc promoter. Nevertheless, considering also that there are many controversies around the mechanisms of trans-repression by p53, we cannot exclude that additional post-transcriptional regulation is taking place in the peculiar phenotype we describe. Indeed, in the context of somatic cell reprogramming to ESCs and tissue de-differentiation, it is known that p53 can “put a

brake" on SCs through the activation of specific families of miRNAs, such as miR-34, miR-145, and miR146, which are involved in numerous inhibitory activities of SC self-renewal (Bieging, Mello et al. 2014). In particular, the miR-145 family has been shown to negatively regulate Myc (Sachdeva, Zhu et al. 2009), while miR-34 is predicted to bind Myc 3'-UTR sequence (our unpublished observations). Both transcriptional and post-transcriptional mechanisms of regulation are concordant with the fact that exogenous MycER expression is not controlled by p53 in our system, as this human coding sequence does not possess the Myc-3'UTR. Therefore, it seems plausible that p53 exerts its control on Myc through multiple mechanisms, according to the complex upstream signaling network that carefully regulates the levels of Myc in the cell.

5.2 The p53:Myc axis in the self-renewal of mammary SCs

The tight regulation of Myc expression is a key tumor suppressive mechanism. Indeed, it is evident from both our data and published studies that too little or too much Myc is harmful to a cell; this is why its levels and its activity are so stringently controlled by multiple mechanisms and restrained by feedback loops. Our results show that the over-expression of Myc leads to very different outcomes, depending on the extent of its activation: in our studies, both mammary SCs and progenitor cells composing the mammospheres responded either by activating an apoptotic response (high level up-regulation) or by intensifying their self-renewal (low level increase). Conversely, too little Myc was shown to be extremely deleterious for mammary SCs, as infection with a Myc-targeting shRNA was not compatible with cell survival. Only when we impaired Myc functions through the exogenous expression of low levels of a Myc dominant-negative mutant (Omomyc), we managed to observe a reduction in the CSCs' sphere-forming ability. Notably, preliminary

observations suggest that Omomyc expression does not induce toxicity to WT mammosphere cultures. All together, these observations indicate that a precise regulation of the amount of the Myc protein and its concomitant signaling are important factors in the control of mammary stem and progenitor cell fate decisions. Clearly, in cancer, these regulatory networks are altered and Myc is found de-regulated in a very high fraction of human tumors.

In line with this, Myc is found over-expressed and de-regulated in our model of breast tumorigenesis. Indeed we have shown both *ex vivo* and *in vitro* that ErbB2 tumors display higher levels of the Myc protein and Myc mRNA than WT mammary glands. Furthermore, these levels remain constantly high during mammosphere formation, while WT cells stop proliferating and down-regulate Myc expression. Remarkably, Myc transcriptional activity mirrors this behavior, thus showing that a Myc-dependent gene signature is active in our ErbB2-driven tumors.

In our system, over-expression of Myc did not transform normal SCs, as transplantation of cells transduced with the MycER vector into recipient mice resulted in the formation of normal tissues two months after engraftment, and in the absence of palpable masses up to one year after the injection. This is in accordance with what is known in the literature: Myc alone can initiate tumorigenesis but needs cooperating events to induce a full-blown transformed phenotype (Gabay, Li et al. 2014). Therefore, it is reasonable to hypothesize that tumor formation in low Myc-expressing cells does not occur, even after a very long latency, until these cells undergo a second oncogenic hit.

5.2.1 Dissecting the p53:Myc axis in stem and progenitor cells

We have shown that precise de-regulation of the levels of Myc induces profound changes in the balance between self-renewal and differentiation. Indeed, the number of SCs within a mammosphere culture appears to increase upon enforced expression of Myc, as demonstrated by mammosphere assays and by transplantation in the cleared fat pad. We showed that this effect can be explained by two mechanisms: on the SCs' side, low-Myc promotes switching of the modality of division of purified SCs, from mainly asymmetric to mainly symmetric; on the progenitors' side, it induces phenotypic changes that bestow them a new identity, with properties and functions that usually define SCs. To be able to dissect the two mechanisms, we purified a population enriched in SCs (Cicalese, Bonizzi et al. 2009), which was slowly proliferating and therefore retaining the PKH-26 dye, as opposed to the putative progenitor population (PKHneg).

PKHneg cells in fact do not contain cells with SC properties as they *i)* are not able to form clonal mammospheres in culture, but only small and irregular aggregates that cannot be passaged; *ii)* can only form mono-lineage colonies in matrigel assays, and, most importantly, *iii)* do not reconstitute the mammary gland structure upon transplantation in pre-pubertal mice. However, we have demonstrated that PKHneg cells expressing low levels of Myc possess increased self-renewal ability in culture. Strikingly, they fully recapitulate the mammary gland morphogenesis and function when transplanted in the cleared fat pad (as demonstrated by the presence of myoepithelial and luminal cytokeratins and by the ability to produce milk during pregnancy), and possess high self-renewal potential (as suggested by serial transplantation), thus proving that they contain multipotent SCs. These acquired regenerative potential and self-renewing abilities suggest therefore

that progenitor cells can undergo a cellular reprogramming that leads to the formation of SCs.

The reprogramming event driven by Myc happens at a very low frequency (1:100,000 progenitors), indicating that only a few cells within this heterogeneous population of PKHneg cells respond to low-Myc levels and de-differentiate. This could be interpreted in two ways: *i)* the reprogramming phenomenon is completely stochastic and randomly targets only few cells that have a permissive genetic or epigenetic state; or *ii)* there exist preferential target populations, sharing a particular replicative history or degree of differentiation, which are more prone to the "low-Myc" effect. Both scenarios are plausible as it was demonstrated that enforced expression of Myc can have profoundly diverse effects depending on the differentiation stage of a cell (Wilson, Murphy et al. 2004, Watt, Frye et al. 2008, Reavie, Della Gatta et al. 2010), and that the epigenetic state of a cell influences the degree of availability of the target genes to the binding by Myc. Recent findings that assign to Myc a role as a general amplifier of previously activated gene expression programs could provide the mechanistic basis for the described heterogeneous responses (Lin, Lovén et al. 2012, Nie, Hu et al. 2012).

Despite being very infrequent, this reprogramming effect is likely to have dramatic effects *in vivo* if one considers the large quantity of progenitors, at different differentiation stages, which reside in a tissue.

Finally, as regards the effects of Myc on the SC population, we showed that while normal SCs mainly divide asymmetrically, cells with enforced expression of Myc switch to the symmetric mode of division. Indeed, purified PKH positive (PKHpos) cells infected with the MycER vector preferentially underwent symmetric divisions, generating two cells with analogous proliferating capacities. This was also confirmed by staining the dividing SCs with an antibody that recognizes the fate determinant Numb and finding that it was

asymmetrically distributed in WT SCs, while uniformly localized on the membrane of dividing SCs that expressed low levels of Myc (unpublished data). Interestingly, Numb was reported to be regulating the activity of p53 (Colaluca, Tosoni et al. 2008), therefore acting as a potential upstream link to the p53:Myc axis in the regulation of SC mitosis. Notably, the effect of Myc on symmetric/asymmetric divisions is undistinguishable from that previously described for p53-loss (Cicalese, Bonizzi et al. 2009).

Regardless of their relative impact, the different effects of Myc on SCs and progenitors may contribute to the maintenance, *in vivo*, of the expanding pool of CSCs. We have shown, indeed, that Myc constitutive expression in ErbB2 tumors renders cells resistant to the effect of Nutlin treatment, thus demonstrating that Myc, by itself, is sufficient to maintain the pool of CSCs *in vitro* and *in vivo*, even when p53 is reactivated.

In conclusion, by contributing to the continuous generation of new CSCs, both the above-mentioned biological effects of Myc constitutive expression appear to participate in the process leading to tumor sustainment.

5.2.2 Implications for the process of tumorigenesis

P53 and Myc have been implicated in the pathogenesis of different tumors, and their relevance for CSC specific mechanisms further confirms their criticality for the transformation process.

Somatic mutations and/or deletion of the *tp53* gene are found in almost every type of cancer at various rates (up to nearly 100% in high-grade serous carcinoma of the ovary) (Rivlin, Brosh et al. 2011). In tumors with low mutation rates, p53 is found in their germline configuration and it is often inactivated by genetic alterations of genes involved in the regulation of p53 functions. For example, many tumors, most frequently

hematological malignancies, exhibit amplification of the E3-ligase Mdm2, which leads to Mdm2 overexpression and p53 degradation, in the presence of WT p53 alleles (Kruse and Gu 2009). In breast cancer, p53 loss correlates with aggressiveness and un-differentiated subtypes (Mizuno, Spike et al. 2010).

We have shown in this thesis that a functional p53 targets the expression of Myc, as its downstream effector for the regulation of SC self-renewal. *Myc* is one of the most studied proto-oncogenes. Mutations affecting the *myc* gene are found infrequently, and their effect on Myc function is not clear. *Myc* is translocated in Burkitt's lymphomas, where it forms a fusion gene with the regulatory regions of the constant region of the genes coding for the immunoglobulin heavy or light chains (Boxer and Dang 2001). In breast cancer, genetic amplification of *myc* is reported for 22% of the cases collected by the TCGA consortium (Cancer Genome Atlas 2012). Nevertheless, Myc expression is elevated or de-regulated in a much higher fraction of breast tumors and is particularly associated with the most aggressive triple negative subtype (Cancer Genome Atlas 2012, Horiuchi, Kusdra et al. 2012). A number of studies have demonstrated that the gene signature dictated by Myc does not only characterize ESCs but is also predictive of poor prognostic parameters, mainly defining the most un-differentiated, highly metastatic types of cancer (Ben-Porath, Thomson et al. 2008, Kim, Woo et al. 2010).

Therefore, p53 loss and Myc activation appear to be integral processes that sustain tumor "stemness" in the vast majority of tumors. The continuous generation of cells with the properties of CSCs might represent an invariable property of many tumor types, likely the most aggressive ones, and the manipulation of the p53:Myc axis seems to constitute a potential tool to modulate tumor development.

5.3 A mitotic gene-signature fuels the expansion of the CSC pool

Analysis of the p53:Myc downstream pathway might provide novel insights in the mechanisms of regulation of SCs in normal and transformed tissues. We have shown that the activity of the p53:Myc axis in CSCs might converge towards a small cluster of 140 genes. Gene-ontology analysis of p53:Myc-regulated genes revealed enrichment of 82 genes that are involved in the regulation of the G2 or mitotic phases of the cell cycle, namely mitosis-entry or progression and execution of the mitotic spindle checkpoint. Strikingly, all of them were down regulated by p53 and up regulated by Myc in normal mammary epithelial cells, while, in the ErbB2 tumor cells, they were all up-regulated. Most notably, expression of these genes in the tumor cells was strictly dependent on p53-loss and Myc-activation (as inferred by the ErbB2-Nutlin dataset).

Transcription from all these genes is usually repressed in G1 and activated in S-phase to progress to G2 and M. Our list enrolls many players of the mitotic spindle checkpoint which are important regulators of the cell replicative fate. Indeed, it is known that reduced levels of several components of the spindle checkpoint, including Bub3 and BubR1, induce cellular senescence (Stark and Taylor 2004). Thus, down-regulation of these genes in normal cells, following p53 activation (and down-regulation of Myc), would unequivocally lead to inhibition of cell proliferation, through a block of the G2-M transition or the mitotic process, or by acceleration of senescence. Vice versa, in cancer cells, loss of p53 function (and Myc activation) would favor mitotic entry and execution of the mitotic processes.

Predicting the effects of the de-regulation of these genes in SCs and CSCs is much more challenging, as very little is known about their specific role in SCs. We know that de-regulation of mitotic kinase activity, of regulators of the spindle assembly, and of cytokinesis has profound effect on the correct execution of SC asymmetric division. For

example, in *Drosophila* neuroblasts, mutations in mitotic kinases like Cdk1, Aurora A, Aurora B and Plk1 result in mis-localization of asymmetric markers and cell fate determinants, including Numb and Prospero, thus influencing the correct execution of mitosis and differently modulating cell polarity and the balance between asymmetric and symmetric cell divisions (Malumbres 2011). Furthermore, in *Drosophila*, mutagenesis of different centrosomal proteins causes impaired ACD of neural SCs and is tumorigenic in larval brain tissue; also, loss of astral microtubules can lead to inefficient spindle orientation and mis-segregation of cell-fate determinants (Castellanos, Dominguez et al. 2008).

With regard to reprogramming, it is known that differentiated cells are required to be cycling in order to better respond to the action of the four "reprogramming factors", Myc, Oct4, Sox2 and Klf4, and turn into iPSCs. Indeed, pluripotent SCs have a peculiar cell cycle structure and spend relatively short time in G1 and most of the time in the S/G2/M phases of the cell cycle, a pre-requisite for inhibition of differentiation and for preservation of an epigenetic state with open chromatin (Singh and Dalton 2009).

Regardless of how de-regulation of these mitotic genes might influence SC properties, a role for Myc and p53 in mitosis has been clearly demonstrated.

P53 is known to be at the center of a regulatory network with several mitotic kinases, like Plk1, BubR1 and Aurora (Ha and Breuer 2012), which are all included in our signature. Several lines of evidence have demonstrated that, in mammalian cells, p53 takes part in pathways that maintain G2 arrest in response to DNA damage. In particular, it has been shown that activation of p53 induces transcriptional repression of many mitotic genes, including Cdc2, cyclin B2 and Cdc25C (Stark and Taylor 2004), which are all included in our list. P53 loss has been shown to favor reprogramming (Hong, Takahashi et al. 2009),

and p53 regulation of mitotic players could have a role in this process. The continuous proliferative state typical of ESCs halts the onset of replicative senescence, thus the concomitant loss of p53 does constitute an important pre-condition for reprogramming. It is known that upon mitotic-entry, all the transcriptional regulators dissociate from the genome and re-associate with chromatin only after cell division, thus establishing new gene expression patterns, as it happens during reprogramming (Egli, Birkhoff et al. 2008).

The involvement of Myc in the regulation of mitotic progression is less well understood. It is known that Myc transcriptionally regulates Aurora kinases A and B, which are included in our list of mitotic genes, and whose role in tumorigenesis is an intense area of study also at the clinical level (Kollareddy, Zheleva et al. 2012). Furthermore, very recent works studying Myc inhibition point towards Myc involvement in cell mitotic proficiency. Annibali and colleagues describe defective mitosis and induction of mitotic catastrophe upon suppression of Myc activity through Omomyc, an effect that is mediated by Sae1, a protein involved in the SUMO pathway and implicated in the control of the mitotic chromosome structure, cell cycle progression, kinetochore function and cytokinesis (Annibali, Whitfield et al. 2014). These data demonstrate a central role of Myc in the regulation of mitotic programs, even though the precise molecular mechanisms through which it works are still only partially delineated, and could possibly vary among cell types and cell-cycle states. Additionally, enforced Myc expression might be relevant for keeping cells in a high rate of cycling, thus favoring the reprogramming process (Singh and Dalton 2009). Therefore, we could speculate that by enforcing the transit through G2/M, Myc and the loss of p53 establish the conditions that allow the association of transcriptional regulators and chromatin remodelers to the genome, determining the fate of a cell at the onset of the new G1.

The molecular mechanism through which the p53:Myc axis regulates mitotic genes is unknown. A number of indirect data suggests that a subset of them, including those that came out of our analysis, shares common regulatory motifs in their promoter region that allow p53-mediated trans-repression. Indeed, several mitotic genes are characterized by the presence, in their promoters, of tandem repressor-elements (CDE/CHR) responsible for G1-specific silencing, namely the cell cycle-dependent element (CDE) and the cell cycle genes homology region (CHR).

Many CDE/CHR genes, such as Cdc2, Cyclin B1, Cyclin B2 and Cdc25C, are down-regulated by the tumor suppressor p53. The mechanisms of p53 recruitment to promoters of repressed target genes are not definitively ascertained. It was reported that, upon DNA damage, p53 binding to these promoters does not require canonical p53 binding-sites and depends on intact CDE/CHR/ elements (Muller and Engeland 2010).

How Myc interacts and activates these promoters is less clear. Usually the CDE/CHR promoters also contain a site for transcriptional activation; indeed, they are frequently found in conjunction with two or three CCAAT-box elements through which NF-Y transcription factors activate the promoters. Thus, it is tempting to speculate that Myc is recruited to the CAAT-box elements at the G1-S transition, thus allowing their transcriptional activation during G2 and M. This would lead to envision a model in which these mitotic genes are directly repressed by p53 and activated by Myc by alternative binding to their promoters, and where p53 and Myc are epistatically related, thus providing coordinated repressing or activating signals in G0/G1 (by p53) and in S-G2-M (by Myc).

5.4 Clinical relevance

The p53:Myc axis might represent a critical target for anti cancer therapeutic strategies. Patients with tumors carrying WT p53 can be treated with drugs that reactivate p53 function. Nutlin-3 is a small molecule that inhibits the binding between Mdm2 and p53 and it is currently being tested in phase I of clinical trials, together with other compounds that exploit the inhibition of the same catalytic pocket. Clearly, to be effective, these p53 activators require the existence of a WT p53 as mutations in the p53 gene mainly disrupt its ability to bind Mdm2 (Moll and Petrenko 2003). The possibility of re-expressing p53 in tumors is a very promising area of therapeutics, not only because it results in an apoptotic or senescent response and enhancement of immune-mediated activity (Suzuki and Matsubara 2011), but also because it reduces the tumor mass by acting on CSCs (Cicalese, Bonizzi et al. 2009).

Our experiments, both *in vitro* and *in vivo*, show that the impossibility to restore p53 functions, due, for example, to the presence of a mutated p53, makes the tumor dependent on the levels of the de-regulated Myc. In line with this, it was shown that a mutant p53 (p53-143A) binds Myc and activates its transcription, leading to Myc de-regulation (Frazier, He et al. 1998). “Addiction” to the “correct” levels of Myc is a common feature of cancer, especially of cancers driven by oncogenes other than Myc (Gabay, Li et al. 2014), exactly like in our ErbB2 model of breast tumorigenesis. This provides relevant opportunities for therapy, as the suppression of Myc would efficiently promote tumor regression and, eventually, eradication. Currently, several strategies have been developed for the inhibition of Myc activity; they are either focused on inhibiting Myc expression or Myc ability to interact with its DNA-binding partner Max (as Omomyc does), or they interfere with Myc target genes. BET-bromodomain inhibitors fall in the first category

(Filippakopoulos, Qi et al. 2010). It has been shown that these domains are potent regulators of *myc* transcription in different tumors and the use of these inhibitors led to regression of multiple myeloma (Delmore, Issa et al. 2011) and acute myeloid leukemia (Zuber, Shi et al. 2011) in murine models.

Omomyc was shown to be able to revert KRas-induced lung cancers and human gliomas without apparent toxic effects to the normal tissues (Soucek, Whitfield et al. 2013, Annibali, Whitfield et al. 2014). Indeed, in the *in vitro* testing of the efficiency of Omomyc in the inhibition of the CSC expansion of our tumor cells, we have observed the same finding as our preliminary data suggest that the mutant has no effect on the survival of WT cells. It would be very useful to discover whether the Myc dependency of our tumor model might be exploited *in vivo* as a CSC specific therapy, and to elucidate how it could cooperate with p53 restoration strategies.

Notably, Omomyc, by disrupting the interaction between Myc and Max, functionally impairs only the trans-activating activity of Myc and not the trans-repressing. Thus, its action would affect the downstream pathways of Myc that we have characterized and that mainly concern cell cycle promotion and mitotic proficiency.

Finally, our findings have clinical implications with respect to the issue of biological heterogeneity and tumor targeting. They suggest that the elimination of CSCs might not be enough for effective cancer eradication, and that targeting those cellular mechanisms that induce reprogramming of tumor cells into cells with CSC properties is also required.

6 References

Al-Hajj, M., M. S. Wicha, A. Benito-Hernandez, S. J. Morrison and M. F. Clarke (2003). "Prospective identification of tumorigenic breast cancer cells." Proc Natl Acad Sci U S A **100**(7): 3983-3988.

Amati, B., S. R. Frank, D. Donjerkovic and S. Taubert (2001). "Function of the c-Myc oncoprotein in chromatin remodeling and transcription." Biochimica et Biophysica Acta (BBA) - Reviews on Cancer **1471**(3): M135-M145.

Anders, S. and W. Huber (2010). "Differential expression analysis for sequence count data." Genome Biol **11**(10): R106.

Anders, S., P. T. Pyl and W. Huber (2015). "HTSeq—a Python framework to work with high-throughput sequencing data." Bioinformatics **31**(2): 166-169.

Annibali, D., J. R. Whitfield, E. Favuzzi, T. Jauset, E. Serrano, I. Cuartas, S. Redondo-Campos, G. Folch, A. Gonzalez-Junca, N. M. Sodir, D. Masso-Valles, M. E. Beaulieu, L. B. Swigart, M. M. Mc Gee, M. P. Somma, S. Nasi, J. Seoane, G. I. Evan and L. Soucek (2014). "Myc inhibition is effective against glioma and reveals a role for Myc in proficient mitosis." Nat Commun **5**: 4632.

Ben-Porath, I., M. W. Thomson, V. J. Carey, R. Ge, G. W. Bell, A. Regev and R. A. Weinberg (2008). "An embryonic stem cell-like gene expression signature in poorly differentiated aggressive human tumors." Nat Genet **40**(5): 499-507.

Betschinger, J., K. Mechtler and J. A. Knoblich (2006). "Asymmetric Segregation of the Tumor Suppressor Brat Regulates Self-Renewal in Drosophila Neural Stem Cells." Cell **124**(6): 1241-1253.

Bieging, K. T., S. S. Mello and L. D. Attardi (2014). "Unravelling mechanisms of p53-mediated tumour suppression." Nat Rev Cancer **14**(5): 359-370.

Bonizzi, G., A. Cicalese, A. Insinga and P. G. Pelicci (2012). "The emerging role of p53 in stem cells." Trends in Molecular Medicine **18**(1): 6-12.

Bonnet, D. and J. E. Dick (1997). "Human acute myeloid leukemia is organized as a hierarchy that originates from a primitive hematopoietic cell." Nat Med **3**(7): 730-737.

Boxer, L. M. and C. V. Dang (2001). "Translocations involving c-myc and c-myc function." Oncogene **20**(40): 5595-5610.

Bu, P., K. Y. Chen, J. H. Chen, L. Wang, J. Walters, Y. J. Shin, J. P. Goerger, J. Sun, M. Witherspoon, N. Rakhilin, J. Li, H. Yang, J. Milsom, S. Lee, W. Zipfel, M. M. Jin, Z. H. Gumus, S. M. Lipkin and X. Shen (2013). "A microRNA miR-34a-regulated bimodal switch targets Notch in colon cancer stem cells." Cell Stem Cell **12**(5): 602-615.

Buganim, Y., D. A. Faddah and R. Jaenisch (2013). "Mechanisms and models of somatic cell reprogramming." Nature reviews. Genetics **14**(6): 427-439.

Cancer Genome Atlas, N. (2012). "Comprehensive molecular portraits of human breast tumours." Nature **490**(7418): 61-70.

Cartwright, P., C. McLean, A. Sheppard, D. Rivett, K. Jones and S. Dalton (2005). "LIF/STAT3 controls ES cell self-renewal and pluripotency by a Myc-dependent mechanism." Development **132**(5): 885-896.

Castellanos, E., P. Dominguez and C. Gonzalez (2008). "Centrosome Dysfunction in Drosophila Neural Stem Cells Causes Tumors that Are Not Due to Genome Instability." Current Biology **18**(16): 1209-1214.

Charafe-Jauffret, E., C. Ginestier, F. Iovino F, C. Tarpin, M. Diebel, B. Esterni, G. Houvenaeghel, J.-M. Extra, F. Bertucci, J. Jacquemier, L. Xerri, G. Dontu, G. Stassi, Y. Xiao, S. H. Barsky, D. Birnbaum, P. Viens and M. S. Wicha (2010). "ALDH1-positive cancer stem cells mediate metastasis and poor clinical outcome in inflammatory breast cancer." Clinical cancer research : an official journal of the American Association for Cancer Research **16**(1): 45-55.

Chen, K., Y.-h. Huang and J.-l. Chen (2013). "Understanding and targeting cancer stem cells: therapeutic implications and challenges." Acta Pharmacol Sin **34**(6): 732-740.

Cho, K. B., M. K. Cho, W. Y. Lee and K. W. Kang (2010). "Overexpression of c-myc induces epithelial mesenchymal transition in mammary epithelial cells." Cancer Letters **293**(2): 230-239.

Cho, R. W., X. Wang, M. Diehn, K. Shedden, G. Y. Chen, G. Sherlock, A. Gurney, J. Lewicki and M. F. Clarke (2008). "Isolation and molecular characterization of cancer stem cells in MMTV-Wnt-1 murine breast tumors." Stem Cells **26**(2): 364-371.

Cicalese, A., G. Bonizzi, C. E. Pasi, M. Faretta, S. Ronzoni, B. Giulini, C. Brisken, S. Minucci, P. P. Di Fiore and P. G. Pelicci (2009). "The tumor suppressor p53 regulates polarity of self-renewing divisions in mammary stem cells." Cell **138**(6): 1083-1095.

Colaluca, I. N., D. Tosoni, P. Nuciforo, F. Senic-Matuglia, V. Galimberti, G. Viale, S. Pece and P. P. Di Fiore (2008). "NUMB controls p53 tumour suppressor activity." Nature **451**(7174): 76-80.

Corbin, A. S., A. Agarwal, M. Loriaux, J. Cortes, M. W. Deininger and B. J. Druker (2011). "Human chronic myeloid leukemia stem cells are insensitive to imatinib despite inhibition of BCR-ABL activity." J Clin Invest **121**(1): 396-409.

Curtis, C., S. P. Shah, S.-F. Chin, G. Turashvili, O. M. Rueda, M. J. Dunning, D. Speed, A. G. Lynch, S. Samarajiwa, Y. Yuan, S. Graf, G. Ha, G. Haffari, A. Bashashati, R. Russell, S. McKinney, A. Langerod, A. Green, E. Provenzano, G. Wishart, S. Pinder, P. Watson, F. Markowetz, L. Murphy, I. Ellis, A. Purushotham, A.-L. Borresen-Dale, J. D. Brenton, S. Tavare, C. Caldas and S. Aparicio (2012). "The genomic and transcriptomic architecture of 2,000 breast tumours reveals novel subgroups." Nature **486**(7403): 346-352.

Dang, Chi V. (2012). "MYC on the Path to Cancer." Cell **149**(1): 22-35.

Delmore, J. E., G. C. Issa, M. E. Lemieux, P. B. Rahl, J. Shi, H. M. Jacobs, E. Kastritis, T. Gilpatrick, R. M. Paranal, J. Qi, M. Chesi, A. C. Schinzel, M. R. McKeown, T. P. Heffernan, C. R. Vakoc, P. L. Bergsagel, I. M. Ghobrial, P. G. Richardson, R. A. Young, W. C. Hahn, K. C. Anderson, A. L. Kung, J. E. Bradner and C. S. Mitsiades (2011). "BET bromodomain inhibition as a therapeutic strategy to target c-Myc." Cell **146**(6): 904-917.

DeOme, K. B., L. J. Faulkin, H. A. Bern and P. B. Blair (1959). "Development of Mammary Tumors from Hyperplastic Alveolar Nodules Transplanted into Gland-free Mammary Fat Pads of Female C3H Mice." Cancer Research **19**(5): 515.

Diehn, M., R. W. Cho, N. A. Lobo, T. Kalisky, M. J. Dorie, A. N. Kulp, D. Qian, J. S. Lam, L. E. Ailles, M. Wong, B. Joshua, M. J. Kaplan, I. Wapnir, F. M. Dirbas, G. Somlo, C. Garberoglio, B. Paz, J. Shen, S. K. Lau, S. R. Quake, J. M. Brown, I. L. Weissman and M. F. Clarke (2009). "Association of reactive oxygen species levels and radioresistance in cancer stem cells." Nature **458**(7239): 780-783.

Dontu, G., W. M. Abdallah, J. M. Foley, K. W. Jackson, M. F. Clarke, M. J. Kawamura and M. S. Wicha (2003). "In vitro propagation and transcriptional profiling of human mammary stem/progenitor cells." Genes Dev **17**(10): 1253-1270.

Egli, D., G. Birkhoff and K. Eggan (2008). "Mediators of reprogramming: transcription factors and transitions through mitosis." Nat Rev Mol Cell Biol **9**(7): 505-516.

Eppert, K., K. Takenaka, E. R. Lechman, L. Waldron, B. Nilsson, P. van Galen, K. H. Metzeler, A. Poeppl, V. Ling, J. Beyene, A. J. Canty, J. S. Danska, S. K. Bohlander, C. Buske, M. D. Minden, T. R. Golub, I. Jurisica, B. L. Ebert and J. E. Dick (2011). "Stem cell gene expression programs influence clinical outcome in human leukemia." Nat Med **17**(9): 1086-1093.

Eramo, A., F. Lotti, G. Sette, E. Pilozzi, M. Biffoni, A. Di Virgilio, C. Conticello, L. Ruco, C. Peschle and R. De Maria (2008). "Identification and expansion of the tumorigenic lung cancer stem cell population." Cell Death Differ **15**(3): 504-514.

Filippakopoulos, P., J. Qi, S. Picaud, Y. Shen, W. B. Smith, O. Fedorov, E. M. Morse, T. Keates, T. T. Hickman, I. Felletar, M. Philpott, S. Munro, M. R. McKeown, Y. Wang, A. L. Christie, N. West, M. J. Cameron, B. Schwartz, T. D. Heightman, N. La Thangue, C. A. French, O. Wiest, A. L. Kung, S. Knapp and J. E. Bradner (2010). "Selective inhibition of BET bromodomains." Nature **468**(7327): 1067-1073.

Frazier, M. W., X. He, J. L. Wang, Z. Gu, J. L. Cleveland and G. P. Zambetti (1998). "Activation of c-myc Gene Expression by Tumor-Derived p53 Mutants Requires a Discrete C-Terminal Domain." Mol Cell Biol **18**(7): 3735-3743.

Gabay, M., Y. Li and D. W. Felsher (2014). "MYC activation is a hallmark of cancer initiation and maintenance." Cold Spring Harb Perspect Med **4**(6).

Ginestier, C., M. H. Hur, E. Charafe-Jauffret, F. Monville, J. Dutcher, M. Brown, J. Jacquemier, P. Viens, C. Kleer, S. Liu, A. Schott, D. Hayes, D. Birnbaum, M. S. Wicha and G. Dontu (2007). "ALDH1 is a marker of normal and malignant human mammary stem cells and a predictor of poor clinical outcome." Cell stem cell **1**(5): 555-567.

Grange, C., S. Lanzardo, F. Cavallo, G. Camussi and B. Bussolati (2008). "Sca-1 identifies the tumor-initiating cells in mammary tumors of BALB-neuT transgenic mice." Neoplasia **10**(12): 1433-1443.

Guo, W., Z. Keckesova, J. L. Donaher, T. Shibue, V. Tischler, F. Reinhardt, S. Itzkovitz, A. Noske, U. Zurrer-Hardi, G. Bell, W. L. Tam, S. A. Mani, A. van Oudenaarden and R. A. Weinberg (2012). "Slug and Sox9 cooperatively determine the mammary stem cell state." Cell **148**(5): 1015-1028.

Ha, G.-H. and E.-K. Y. Breuer (2012). "Mitotic Kinases and p53 Signaling." Biochemistry Research International **2012**: 14.

Hadjantonakis, A. K., M. Gertsenstein, M. Ikawa, M. Okabe and A. Nagy (1998). "Generating green fluorescent mice by germline transmission of green fluorescent ES cells." Mech Dev **76**(1-2): 79-90.

Hanahan, D. and R. A. Weinberg (2011). "Hallmarks of cancer: the next generation." Cell **144**(5): 646-674.

Hermann, P. C., S. L. Huber, T. Herrler, A. Aicher, J. W. Ellwart, M. Guba, C. J. Bruns and C. Heeschen (2007). "Distinct populations of cancer stem cells determine tumor growth and metastatic activity in human pancreatic cancer." Cell Stem Cell **1**(3): 313-323.

Hermeking, H. and D. Eick (1994). "Mediation of c-Myc-induced apoptosis by p53." Science **265**(5181): 2091-2093.

Ho, J. S., W. Ma, D. Y. Mao and S. Benchimol (2005). "p53-Dependent transcriptional repression of c-myc is required for G1 cell cycle arrest." Mol Cell Biol **25**(17): 7423-7431.

Hong, H., K. Takahashi, T. Ichisaka, T. Aoi, O. Kanagawa, M. Nakagawa, K. Okita and S. Yamanaka (2009). "Suppression of induced pluripotent stem cell generation by the p53–p21 pathway." Nature **460**(7259): 1132-1135.

Horiuchi, D., L. Kusdra, N. E. Huskey, S. Chandriani, M. E. Lenburg, A. M. Gonzalez-Angulo, K. J. Creasman, A. V. Bazarov, J. W. Smyth, S. E. Davis, P. Yaswen, G. B. Mills, L. J. Esserman and A. Goga (2012). "MYC pathway activation in triple-negative breast cancer is synthetic lethal with CDK inhibition." The Journal of Experimental Medicine **209**(4): 679-696.

Hu, C., A. Dievart, M. Lupien, E. Calvo, G. Tremblay and P. Jolicoeur (2006). "Overexpression of activated murine Notch1 and Notch3 in transgenic mice blocks mammary gland development and induces mammary tumors." Am J Pathol **168**(3): 973-990.

Hu, Y. and G. K. Smyth (2009). "ELDA: extreme limiting dilution analysis for comparing depleted and enriched populations in stem cell and other assays." J Immunol Methods **347**(1-2): 70-78.

Ishizawa, K., Z. A. Rasheed, R. Karisch, Q. Wang, J. Kowalski, E. Susky, K. Pereira, C. Karamboulas, N. Moghal, N. Rajeshkumar, M. Hidalgo, M. Tsao, L. Ailles, T. Waddell, A. Maitra, B. G. Neel and W. Matsui (2010). "Tumor-initiating cells are rare in many human tumors." Cell Stem Cell **7**(3): 279-282.

Izumi, H. and Y. Kaneko (2014). "Trim32 facilitates degradation of MYCN on spindle poles and induces asymmetric cell division in human neuroblastoma cells." Cancer Res **74**(19): 5620-5630.

Jin, L., K. J. Hope, Q. Zhai, F. Smadja-Joffe and J. E. Dick (2006). "Targeting of CD44 eradicates human acute myeloid leukemic stem cells." Nat Med **12**(10): 1167-1174.

Junttila, M. R. and F. J. de Sauvage (2013). "Influence of tumour micro-environment heterogeneity on therapeutic response." Nature **501**(7467): 346-354.

Karlsson, A., S. Giuriato, F. Tang, J. Fung-Weier, G. Levan and D. W. Felsher (2003). "Genomically complex lymphomas undergo sustained tumor regression upon MYC inactivation unless they acquire novel chromosomal translocations." Blood **101**(7): 2797-2803.

Kerosuo, L., K. Piltti, H. Fox, A. Angers-Loustau, V. Hayry, M. Eilers, H. Sariola and K. Wartiovaara (2008). "Myc increases self-renewal in neural progenitor cells through Miz-1." J Cell Sci **121**(Pt 23): 3941-3950.

Kim, J., J. Chu, X. Shen, J. Wang and S. H. Orkin (2008). "An extended transcriptional network for pluripotency of embryonic stem cells." Cell **132**(6): 1049-1061.

Kim, J., A. J. Woo, J. Chu, J. W. Snow, Y. Fujiwara, C. G. Kim, A. B. Cantor and S. H. Orkin (2010). "A Myc network accounts for similarities between embryonic stem and cancer cell transcription programs." Cell **143**(2): 313-324.

Kollareddy, M., D. Zheleva, P. Dzubak, P. S. Brahmkshatriya, M. Lepsik and M. Hajduch (2012). "Aurora kinase inhibitors: progress towards the clinic." Invest New Drugs **30**(6): 2411-2432.

Kreso, A. and John E. Dick (2014). "Evolution of the Cancer Stem Cell Model." Cell Stem Cell **14**(3): 275-291.

Kreso, A., C. A. O'Brien, P. van Galen, O. I. Gan, F. Notta, A. M. K. Brown, K. Ng, J. Ma, E. Wienholds, C. Dunant, A. Pollett, S. Gallinger, J. McPherson, C. G. Mullighan, D. Shibata and J. E. Dick (2013). "Variable Clonal Repopulation Dynamics Influence Chemotherapy Response in Colorectal Cancer." Science **339**(6119): 543-548.

Kruse, J.-P. and W. Gu (2009). "Modes of p53 Regulation." Cell **137**(4): 609-622.

Lanzkron, S. M., M. I. Collector and S. J. Sharkis (1999). "Hematopoietic stem cell tracking in vivo: a comparison of short-term and long-term repopulating cells." Blood **93**(6): 1916-1921.

Lapidot, T., C. Sirard, J. Vormoor, B. Murdoch, T. Hoang, J. Caceres-Cortes, M. Minden, B. Paterson, M. A. Caligiuri and J. E. Dick (1994). "A cell initiating human acute myeloid leukaemia after transplantation into SCID mice." Nature **367**(6464): 645-648.

Laurenti, E., B. Varnum-Finney, A. Wilson, I. Ferrero, W. E. Blanco-Bose, A. Ehninger, P. S. Knoepfler, P. F. Cheng, H. R. MacDonald, R. N. Eisenman, I. D. Bernstein and A. Trumpp (2008). "Hematopoietic stem cell function and survival depend on c-Myc and N-Myc activity." Cell Stem Cell **3**(6): 611-624.

Levens, D. (2010). "“You Don’t Muck with MYC”." Genes & Cancer **1**(6): 547-554.

Li, M., Y. He, W. Dubois, X. Wu, J. Shi and J. Huang (2012). "Distinct regulatory mechanisms and functions for p53-activated and p53-repressed DNA damage response genes in embryonic stem cells." Mol Cell **46**(1): 30-42.

Li, X., M. T. Lewis, J. Huang, C. Gutierrez, C. K. Osborne, M.-F. Wu, S. G. Hilsenbeck, A. Pavlick, X. Zhang, G. C. Chamness, H. Wong, J. Rosen and J. C. Chang (2008). "Intrinsic Resistance of Tumorigenic Breast Cancer Cells to Chemotherapy." Journal of the National Cancer Institute **100**(9): 672-679.

Li, Y., W. P. Hively and H. E. Varmus (2000). "Use of MMTV-Wnt-1 transgenic mice for studying the genetic basis of breast cancer." Oncogene **19**(8): 1002-1009.

Liao, M. J., C. C. Zhang, B. Zhou, D. B. Zimonjic, S. A. Mani, M. Kaba, A. Gifford, F. Reinhardt, N. C. Popescu, W. Guo, E. N. Eaton, H. F. Lodish and R. A. Weinberg (2007). "Enrichment of a population of mammary gland cells that form mammospheres and have in vivo repopulating activity." Cancer Res **67**(17): 8131-8138.

Lim, E., D. Wu, B. Pal, T. Bouras, M.-L. Asselin-Labat, F. Vaillant, H. Yagita, G. Lindeman, G. Smyth and J. Visvader (2010). "Transcriptome analyses of mouse and human mammary cell subpopulations reveal multiple conserved genes and pathways." Breast Cancer Research **12**(2): R21.

Lin, Charles Y., J. Lovén, Peter B. Rahl, Ronald M. Paranal, Christopher B. Burge, James E. Bradner, Tong I. Lee and Richard A. Young (2012). "Transcriptional Amplification in Tumor Cells with Elevated c-Myc." Cell **151**(1): 56-67.

Littlewood, T. D., D. C. Hancock, P. S. Danielian, M. G. Parker and G. I. Evan (1995). "A modified oestrogen receptor ligand-binding domain as an improved switch for the regulation of heterologous proteins." Nucleic Acids Research **23**(10): 1686-1690.

Littlewood, Trevor D., P. Kreuzaler and Gerard I. Evan (2012). "All Things to All People." Cell **151**(1): 11-13.

Liu, S., G. Dontu and M. S. Wicha (2005). "Mammary stem cells, self-renewal pathways, and carcinogenesis." Breast Cancer Res **7**(3): 86-95.

Liu, Y., S. E. Elf, Y. Miyata, G. Sashida, Y. Liu, G. Huang, S. Di Giandomenico, J. M. Lee, A. Deblasio, S. Menendez, J. Antipin, B. Reva, A. Koff and S. D. Nimer (2009). "p53 regulates hematopoietic stem cell quiescence." Cell Stem Cell **4**(1): 37-48.

Malumbres, M. (2011). Physiological Relevance of Cell Cycle Kinases.

Mani, S. A., W. Guo, M. J. Liao, E. N. Eaton, A. Ayyanan, A. Y. Zhou, M. Brooks, F. Reinhard, C. C. Zhang, M. Shipitsin, L. L. Campbell, K. Polyak, C. Brisken, J. Yang and R. A. Weinberg (2008). "The epithelial-mesenchymal transition generates cells with properties of stem cells." Cell **133**(4): 704-715.

Meacham, C. E. and S. J. Morrison (2013). "Tumour heterogeneity and cancer cell plasticity." Nature **501**(7467): 328-337.

Merlos-Suárez, A., Francisco M. Barriga, P. Jung, M. Iglesias, María V. Céspedes, D. Rossell, M. Sevillano, X. Hernando-Momblona, V. da Silva-Diz, P. Muñoz, H. Clevers, E. Sancho, R. Mangues and E. Batlle (2011). "The Intestinal Stem Cell Signature Identifies Colorectal Cancer Stem Cells and Predicts Disease Relapse." Cell Stem Cell **8**(5): 511-524.

Miller, L. D., J. Smeds, J. George, V. B. Vega, L. Vergara, A. Ploner, Y. Pawitan, P. Hall, S. Klaar, E. T. Liu and J. Bergh (2005). "An expression signature for p53 status in human breast cancer predicts mutation status, transcriptional effects, and patient survival." Proceedings of the National Academy of Sciences of the United States of America **102**(38): 13550-13555.

Mizuno, H., B. T. Spike, G. M. Wahl and A. J. Levine (2010). "Inactivation of p53 in breast cancers correlates with stem cell transcriptional signatures." Proc Natl Acad Sci U S A **107**(52): 22745-22750.

Moll, U. M. and O. Petrenko (2003). "The MDM2-p53 Interaction." Molecular Cancer Research **1**(14): 1001-1008.

Morrison, S. J. and J. Kimble (2006). "Asymmetric and symmetric stem-cell divisions in development and cancer." Nature **441**(7097): 1068-1074.

Moumen, M., A. Chiche, M. A. Deugnier, V. Petit, A. Gandarillas, M. A. Glukhova and M. M. Faraldo (2012). "The proto-oncogene Myc is essential for mammary stem cell function." Stem Cells **30**(6): 1246-1254.

Mouridsen, H., T. Palshof, J. Patterson and L. Battersby (1978). "Tamoxifen in advanced breast cancer." Cancer Treat Rev **5**(3): 131-141.

Muller, G. A. and K. Engeland (2010). "The central role of CDE/CHR promoter elements in the regulation of cell cycle-dependent gene transcription." Febs j **277**(4): 877-893.

Muller, W. J., E. Sinn, P. K. Pattengale, R. Wallace and P. Leder (1988). "Single-step induction of mammary adenocarcinoma in transgenic mice bearing the activated c-neu oncogene." Cell **54**(1): 105-115.

Murphy, D. J., M. R. Junttila, L. Pouyet, A. Karnezis, K. Shchors, D. A. Bui, L. Brown-Swigart, L. Johnson and G. I. Evan (2008). "Distinct thresholds govern Myc's biological output in vivo." Cancer Cell **14**(6): 447-457.

Nie, Z., G. Hu, G. Wei, K. Cui, A. Yamane, W. Resch, R. Wang, D. R. Green, L. Tessarollo, R. Casellas, K. Zhao and D. Levens (2012). "c-Myc is a universal amplifier of expressed genes in lymphocytes and embryonic stem cells." Cell **151**(1): 68-79.

O'Brien, C. A., A. Pollett, S. Gallinger and J. E. Dick (2007). "A human colon cancer cell capable of initiating tumour growth in immunodeficient mice." Nature **445**(7123): 106-110.

Pasi, C. E., A. Dereli-Oz, S. Negrini, M. Friedli, G. Fragola, A. Lombardo, G. Van Houwe, L. Naldini, S. Casola, G. Testa, D. Trono, P. G. Pelicci and T. D. Halazonetis (2011). "Genomic instability in induced stem cells." Cell Death Differ **18**(5): 745-753.

Patrawala, L., T. Calhoun, R. Schneider-Broussard, H. Li, B. Bhatia, S. Tang, J. G. Reilly, D. Chandra, J. Zhou, K. Claypool, L. Coghlan and D. G. Tang (2006). "Highly purified CD44+ prostate cancer cells from xenograft human tumors are enriched in tumorigenic and metastatic progenitor cells." Oncogene **25**(12): 1696-1708.

Pece, S., D. Tosoni, S. Confalonieri, G. Mazzarol, M. Vecchi, S. Ronzoni, L. Bernard, G. Viale, P. G. Pelicci and P. P. Di Fiore (2010). "Biological and molecular heterogeneity of breast cancers correlates with their cancer stem cell content." Cell **140**(1): 62-73.

Ponti, D., A. Costa, N. Zaffaroni, G. Pratesi, G. Petrangolini, D. Coradini, S. Pilotti, M. A. Pierotti and M. G. Daidone (2005). "Isolation and in vitro propagation of tumorigenic breast cancer cells with stem/progenitor cell properties." Cancer Res **65**(13): 5506-5511.

Quintana, E., M. Shackleton, M. S. Sabel, D. R. Fullen, T. M. Johnson and S. J. Morrison (2008). "Efficient tumor formation by single human melanoma cells." Nature **456**(7222): 593-598.

Reavie, L., G. Della Gatta, K. Crusio, B. Aranda-Orgilles, S. M. Buckley, B. Thompson, E. Lee, J. Gao, A. L. Bredemeyer, B. A. Helmink, J. Zavadil, B. P. Sleckman, T. Palomero, A. Ferrando and I. Aifantis (2010). "Regulation of hematopoietic stem cell differentiation by a single ubiquitin ligase-substrate complex." Nat Immunol **11**(3): 207-215.

Reedijk, M., S. Odorcic, L. Chang, H. Zhang, N. Miller, D. R. McCready, G. Lockwood and S. E. Egan (2005). "High-level Coexpression of JAG1 and NOTCH1 Is Observed in Human Breast Cancer and Is Associated with Poor Overall Survival." Cancer Research **65**(18): 8530-8537.

Reis-Filho, J. S. and L. Pusztai (2011). "Gene expression profiling in breast cancer: classification, prognostication, and prediction." Lancet **378**(9805): 1812-1823.

Rios, A. C., N. Y. Fu, G. J. Lindeman and J. E. Visvader (2014). "In situ identification of bipotent stem cells in the mammary gland." Nature **506**(7488): 322-327.

Rivlin, N., R. Brosh, M. Oren and V. Rotter (2011). "Mutations in the p53 Tumor Suppressor Gene: Important Milestones at the Various Steps of Tumorigenesis." Genes & Cancer **2**(4): 466-474.

Sachdeva, M., S. Zhu, F. Wu, H. Wu, V. Walia, S. Kumar, R. Elble, K. Watabe and Y. Y. Mo (2009). "p53 represses c-Myc through induction of the tumor suppressor miR-145." Proc Natl Acad Sci U S A **106**(9): 3207-3212.

Schwamborn, J. C., E. Berezikov and J. A. Knoblich (2009). "The TRIM-NHL Protein TRIM32 Activates MicroRNAs and Prevents Self-Renewal in Mouse Neural Progenitors." Cell **136**(5): 913-925.

Shachaf, C. M., A. M. Kopelman, C. Arvanitis, A. Karlsson, S. Beer, S. Mandl, M. H. Bachmann, A. D. Borowsky, B. Ruebner, R. D. Cardiff, Q. Yang, J. M. Bishop, C. H. Contag and D. W. Felsher (2004). "MYC inactivation uncovers pluripotent differentiation and tumour dormancy in hepatocellular cancer." Nature **431**(7012): 1112-1117.

Shackleton, M., F. Vaillant, K. J. Simpson, J. Stingl, G. K. Smyth, M.-L. Asselin-Labat, L. Wu, G. J. Lindeman and J. E. Visvader (2006). "Generation of a functional mammary gland from a single stem cell." Nature **439**(7072): 84-88.

Shehata, M., R. van Amerongen, A. Zeeman, R. Giraddi and J. Stingl (2014). "The influence of tamoxifen on normal mouse mammary gland homeostasis." Breast Cancer Research **16**(4): 411.

Singh, A. M. and S. Dalton (2009). "The cell cycle and Myc intersect with mechanisms that regulate pluripotency and reprogramming." Cell Stem Cell **5**(2): 141-149.

Singh, S. K., C. Hawkins, I. D. Clarke, J. A. Squire, J. Bayani, T. Hide, R. M. Henkelman, M. D. Cusimano and P. B. Dirks (2004). "Identification of human brain tumour initiating cells." Nature **432**(7015): 396-401.

Soady, K., H. Kendrick, Q. Gao, A. Tutt, M. Zvelebil, L. Ordonez, J. Quist, D. Tan, C. Isacke, A. Grigoriadis and M. Smalley (2015). "Mouse mammary stem cells express prognostic markers for triple-negative breast cancer." Breast Cancer Research **17**(1): 31.

Sotiriou, C., S. Y. Neo, L. M. McShane, E. L. Korn, P. M. Long, A. Jazaeri, P. Martiat, S. B. Fox, A. L. Harris and E. T. Liu (2003). "Breast cancer classification and prognosis based on gene expression profiles from a population-based study." Proc Natl Acad Sci U S A **100**(18): 10393-10398.

Soucek, L., J. Whitfield, C. P. Martins, A. J. Finch, D. J. Murphy, N. M. Sodir, A. N. Karnezis, L. B. Swigart, S. Nasi and G. I. Evan (2008). "Modelling Myc inhibition as a cancer therapy." Nature **455**(7213): 679-683.

Soucek, L., J. R. Whitfield, N. M. Sodir, D. Massó-Vallés, E. Serrano, A. N. Karnezis, L. B. Swigart and G. I. Evan (2013). "Inhibition of Myc family proteins eradicates KRas-driven lung cancer in mice." Genes & Development **27**(5): 504-513.

Soufi, A., G. Donahue and K. S. Zaret (2012). "Facilitators and impediments of the pluripotency reprogramming factors' initial engagement with the genome." Cell **151**(5): 994-1004.

Spike, B. T. and G. M. Wahl (2011). "p53, Stem Cells, and Reprogramming: Tumor Suppression beyond Guarding the Genome." Genes & Cancer **2**(4): 404-419.

Stark, G. R. and W. R. Taylor (2004). "Analyzing the G2/M checkpoint." Methods Mol Biol **280**: 51-82.

Stingl, J., P. Eirew, I. Ricketson, M. Shackleton, F. Vaillant, D. Choi, H. I. Li and C. J. Eaves (2006). "Purification and unique properties of mammary epithelial stem cells." Nature **439**(7079): 993-997.

Subramanian, A., P. Tamayo, V. K. Mootha, S. Mukherjee, B. L. Ebert, M. A. Gillette, A. Paulovich, S. L. Pomeroy, T. R. Golub, E. S. Lander and J. P. Mesirov (2005). "Gene set enrichment analysis: a knowledge-based approach for interpreting genome-wide expression profiles." Proc Natl Acad Sci U S A **102**(43): 15545-15550.

Sugiarto, S., A. I. Persson, E. G. Munoz, M. Waldhuber, C. Lamagna, N. Andor, P. Hanecker, J. Ayers-Ringler, J. Phillips, J. Siu, D. A. Lim, S. Vandenberg, W. Stallcup, M. S. Berger, G. Bergers, W. A. Weiss and C. Petritsch (2011). "Asymmetry-defective oligodendrocyte progenitors are glioma precursors." Cancer Cell **20**(3): 328-340.

Suzuki, K. and H. Matsubara (2011). "Recent Advances in p53 Research and Cancer Treatment." Journal of Biomedicine and Biotechnology **2011**: 7.

Takahashi, K. and S. Yamanaka (2006). "Induction of pluripotent stem cells from mouse embryonic and adult fibroblast cultures by defined factors." Cell **126**(4): 663-676.

Tansey, W. P. (2014). "Mammalian MYC Proteins and Cancer." New Journal of Science **2014**: 27.

Templeton, A. K., S. Miyamoto, A. Babu, A. Munshi and R. Ramesh (2014). "Cancer stem cells: progress and challenges in lung cancer." Stem Cell Investigation **1**(4).

Tschaharganeh, D. F., W. Xue, D. F. Calvisi, M. Evert, T. V. Michurina, L. E. Dow, A. Banito, S. F. Katz, E. R. Kastenhuber, S. Weissmueller, C. H. Huang, A. Lechel, J. B. Andersen, D. Capper, L. Zender, T. Longerich, G. Enikolopov and S. W. Lowe (2014). "p53-dependent Nestin regulation links tumor suppression to cellular plasticity in liver cancer." Cell **158**(3): 579-592.

Uyttendaele, H., G. Marazzi, G. Wu, Q. Yan, D. Sassoon and J. Kitajewski (1996). "Notch4/int-3, a mammary proto-oncogene, is an endothelial cell-specific mammalian Notch gene." Development **122**(7): 2251-2259.

Vaillant, F., M. L. Asselin-Labat, M. Shackleton, N. C. Forrest, G. J. Lindeman and J. E. Visvader (2008). "The mammary progenitor marker CD61/beta3 integrin identifies cancer stem cells in mouse models of mammary tumorigenesis." Cancer Res **68**(19): 7711-7717.

van Amerongen, R., A. N. Bowman and R. Nusse (2012). "Developmental stage and time dictate the fate of Wnt/beta-catenin-responsive stem cells in the mammary gland." Cell Stem Cell **11**(3): 387-400.

Van Keymeulen, A., A. S. Rocha, M. Ousset, B. Beck, G. Bouvencourt, J. Rock, N. Sharma, S. Dekoninck and C. Blanpain (2011). "Distinct stem cells contribute to mammary gland development and maintenance." Nature **479**(7372): 189-193.

Varlakhanova, N. V., R. F. Cotterman, W. N. deVries, J. Morgan, L. R. Donahue, S. Murray, B. B. Knowles and P. S. Knoepfler (2010). "myc maintains embryonic stem cell pluripotency and self-renewal." Differentiation **80**(1): 9-19.

Vassilev, L. T. (2004). "In vivo activation of the p53 pathway by small-molecule antagonists of MDM2." Science **303**: 844-848.

Vater, C. A., L. M. Bartle, C. A. Dionne, T. D. Littlewood and V. S. Goldmacher (1996). "Induction of apoptosis by tamoxifen-activation of a p53-estrogen receptor fusion protein expressed in E1A and T24 H-ras transformed p53-/- mouse embryo fibroblasts." Oncogene **13**(4): 739-748.

Visvader, J. E. (2009). "Keeping abreast of the mammary epithelial hierarchy and breast tumorigenesis." Genes & Development **23**(22): 2563-2577.

Visvader, J. E. and G. J. Lindeman (2008). "Cancer stem cells in solid tumours: accumulating evidence and unresolved questions." Nat Rev Cancer **8**(10): 755-768.

Visvader, J. E. and J. Stingl (2014). "Mammary stem cells and the differentiation hierarchy: current status and perspectives." Genes & Development **28**(11): 1143-1158.

Vousden, K. H. and C. Prives (2009). "Blinded by the Light: The Growing Complexity of p53." Cell **137**(3): 413-431.

Wang, D., C. Cai, X. Dong, Q. C. Yu, X. O. Zhang, L. Yang and Y. A. Zeng (2015). "Identification of multipotent mammary stem cells by protein C receptor expression." Nature **517**(7532): 81-84.

Wang, S., E. A. Konorev, S. Kotamraju, J. Joseph, S. Kalivendi and B. Kalyanaraman (2004). "Doxorubicin Induces Apoptosis in Normal and Tumor Cells via Distinctly Different Mechanisms: INTERMEDIACY OF H2O2- AND p53-DEPENDENT PATHWAYS." Journal of Biological Chemistry **279**(24): 25535-25543.

Watt, F. M., M. Frye and S. A. Benitah (2008). "MYC in mammalian epidermis: how can an oncogene stimulate differentiation?" Nat Rev Cancer **8**(3): 234-242.

Welcker, M. and B. E. Clurman (2008). "FBW7 ubiquitin ligase: a tumour suppressor at the crossroads of cell division, growth and differentiation." Nat Rev Cancer **8**(2): 83-93.

Wierstra, I. and J. Alves (2008). "The c-myc promoter: still MysterY and challenge." Adv Cancer Res **99**: 113-333.

Wilson, A., M. J. Murphy, T. Oskarsson, K. Kaloulis, M. D. Bettess, G. M. Oser, A. C. Pasche, C. Knabenhans, H. R. Macdonald and A. Trumpp (2004). "c-Myc controls the balance between hematopoietic stem cell self-renewal and differentiation." Genes Dev **18**(22): 2747-2763.

Xu, J., Y. Chen and O. I. Olopade (2010). "MYC and Breast Cancer." Genes & cancer **1**(6): 629-640.

Yilmaz, O. H., R. Valdez, B. K. Theisen, W. Guo, D. O. Ferguson, H. Wu and S. J. Morrison (2006). "Pten dependence distinguishes haematopoietic stem cells from leukaemia-initiating cells." Nature **441**(7092): 475-482.

Zeng, Y. A. and R. Nusse (2010). "Wnt proteins are self-renewing factors for mammary stem cells and promote their long-term expansion in culture." Cell stem cell **6**(6): 568-577.

Zhang, M., F. Behbod, R. L. Atkinson, M. D. Landis, F. Kittrell, D. Edwards, D. Medina, A. Tsimelzon, S. Hilsenbeck, J. E. Green, A. M. Michalowska and J. M. Rosen (2008). "Identification of tumor-initiating cells in a p53-null mouse model of breast cancer." Cancer Res **68**(12): 4674-4682.

Zhao, Z., J. Zuber, E. Diaz-Flores, L. Lintault, S. C. Kogan, K. Shannon and S. W. Lowe (2010). "p53 loss promotes acute myeloid leukemia by enabling aberrant self-renewal." Genes & Development **24**(13): 1389-1402.

Zheng, H., H. Ying, H. Yan, A. C. Kimmelman, D. J. Hiller, A. J. Chen, S. R. Perry, G. Tonon, G. C. Chu, Z. Ding, J. M. Stommel, K. L. Dunn, R. Wiedemeyer, M. J. You, C. Brennan, Y. A. Wang, K. L. Ligon, W. H. Wong, L. Chin and R. A. DePinho (2008). "p53 and Pten control neural and glioma stem/progenitor cell renewal and differentiation." Nature **455**(7216): 1129-1133.

Zhou, B. P., Y. Liao, W. Xia, Y. Zou, B. Spohn and M.-C. Hung (2001). "HER-2/neu induces p53 ubiquitination via Akt-mediated MDM2 phosphorylation." Nat Cell Biol **3**(11): 973-982.

Zuber, J., J. Shi, E. Wang, A. R. Rappaport, H. Herrmann, E. A. Sison, D. Magoon, J. Qi, K. Blatt, M. Wunderlich, M. J. Taylor, C. Johns, A. Chicas, J. C. Mulloy, S. C. Kogan, P. Brown, P. Valent, J. E. Bradner, S. W. Lowe and C. R. Vakoc (2011). "RNAi screen identifies Brd4 as a therapeutic target in acute myeloid leukaemia." Nature **478**(7370): 524-528.

7 Acknowledgements

Thanks to Thalia Vlachou who helped me in all the possible aspects that have concerned this project, from the experiments to the long discussions and over-night work: this thesis would not have gotten this shape without her support.

Thanks to Giorgio Melloni for his precious work on the bioinformatics data. Thanks to Dr. Cristina Pasi and to Dr. Linsey Reavie for their amazing contribution to the groundwork of this thesis, for having introduced me into this topic and for the very helpful scientific discussions. Thanks to Dr. Angelo Cicalese for the setting up and characterization of the mammosphere system. Thanks to Dr. Cristina Moroni and Errico D'Elia for their help with the pregnancy experiment and to Dr. Camilla Recordati for the histopathological evaluation of mammary outgrowths. Thanks to Dr. Paola Bonetti for providing the p53-ER expressing vector and for useful scientific inputs and to Dr. Matteo Marzi for the help with GSEA analysis. Thanks to Dr. Bruno Amati's group for kindly providing the Rosa26-MycER murine model.

Thanks to Dr. Paola Dalton for her untiring efforts in reviewing this thesis.

I deeply thank my supervisor Prof. Pier Giuseppe Pelicci who always strongly believed in the project, for having been an amazing guide throughout this path despite all the difficulties and the time-constrains.

Also, I would like to thank all the friends and colleagues I met over the last years that added an extra-value to this work experience. Finally, a huge thanks goes to my family for their constant support and trust and to Lorenzo for his priceless patience and love.